SANDIA REPORT

SAND95–2643 • UC–705
Unlimited Release
Printed December 1995

Molecular Engineering of Polymer Alloys – A Final Report of Results Obtained on CRADA #1078

John G. Curro, Kenneth S. Schweizer, J. Dana Honeycutt

Prepared by
Sandia National Laboratories
Albuquerque, New Mexico 87185 and Livermore, California 94550
for the United States Department of Energy
under Contract DE-AC04-94AL85000

Approved for public release; distribution is unlimited.

SF2900Q(8-81)

Issued by Sandia National Laboratories, operated for the United States Department of Energy by Sandia Corporation.

Available to DOE and DOE contractors from
Office of Scientific and Technical Information
PO Box 62
Oak Ridge, TN 37831

Prices available from (615) 576-8401, FTS 626-8401

Available to the public from
National Technical Information Service
US Department of Commerce
5285 Port Royal Rd
Springfield, VA 22161

NTIS price codes
Printed copy: A03
Microfiche copy: A01

SAND-2643
Unlimited Release
Printed December, 1995

Distribution
Category UC-705

Molecular Engineering of Polymer Alloys - A Final Report of Results Obtained on CRADA # 1078

John G. Curro
Molecular Research of Polymers Department
Sandia National Laboratories
Albuquerque, NM 87185-0335

Kenneth S. Schweizer
Department of Materials Science and Engineering
University of Illinois
Urbana, Illinois 61801

J. Dana Honeycutt
BIOSYM Technologies
San Diego, California 92121-3752

Abstract

This report summarizes the technical progress made in the past three years on CRADA #1078, *Molecular Engineering of Polymer Alloys*. The thrust of this CRADA was to start with the basic ideas of PRISM theory and develop it to the point where it could be applied to modeling of polymer alloys. In this program, BIOSYM, Sandia and the University of Illinois worked jointly to develop the theoretical techniques and numerical formalisms necessary to implement the theoretical ideas into commercial software aimed at molecular engineering of polymer alloys. This CRADA focused on developing the techniques required to make the transition from theory to practice. These techniques were then used by BIOSYM to incorporate PRISM theory and other new developments into their commercial software.

TABLE OF CONTENTS

I. INTRODUCTION

Condensed polymeric fluids exhibit a rich and complex set of experimental phenomena associated with the combined influences of local, system-specific monomer structure and global connectivity and flexibility. Such behavior is of both fundamental and practical interest. Early pioneering theoretical work focused largely on simple lattice models which invoked severe simplifications of both molecular structure and statistical mechanics[1,13]. More recently, remarkable progress has been made in describing relatively long wavelength structure and properties by employing scaling and renormalization-group approaches inspired by analogies with critical phenomena, as well as self-consistent field methods[2-4]. However, these modern continuous space approaches have restricted ranges of applicability(e.g., long chains, low and moderate densities) , and generally address only the generic qualitative behavior of macromolecular systems from a polymer physics point of view. System-specific chemical structure features are lumped into fitting constants or "prefactors", and local fluid structure is not addressed. Thus, the *a priori* chemical predictive capacity of such approaches is generally modest or nonexistent. In contrast, for simple atomic(and colloidal) and small molecule fluids much theoretical progress for both structural and thermodynamic properties has been made over the past two-to-three decades based on continuous space "integral equation" methods[5]. Such approaches are nonperturbative in interaction potentials and density(though generally "uncontrolled"), microscopic in nature, and can treat the physical consequences of the local molecular structure and intermolecular forces over a wide range of thermodynamic state conditions.

We shall focus on one particular integral equation approach, the "Polymer Reference Interaction Site Model" (PRISM) theory[6,9,10] which was first proposed by us in 1987. PRISM is a macromolecular extension of the pioneering RISM theory of Chandler, Andersen and co-workers[7,8,11,12]. The purpose of this report is to summarize the technical progress made in the past three years on CRADA #1078, *Molecular Engineering of Polymer Alloys*.. The thrust of this CRADA was to start with the basic ideas of PRISM theory and develop it to the point where it could be applied to modeling of polymer alloys. In this program, BIOSYM,

Sandia and the University of Illinois worked jointly to develop the theoretical techniques and numerical formalisms necessary to implement the theoretical ideas into commercial software aimed at molecular engineering of polymer alloys. This CRADA focused on developing the techniques required to make the transition from theory to practice. These techniques were then used by BIOSYM to incorporate PRISM theory and other new developments into their commercial software.

II. PRISM THEORY : BASIC ASPECTS

The integral equation approach to simple classical liquids was pioneered by Kirkwood and many others[5,14]. Considerable progress was made initially in the application of integral equation theory to simple monatomic liquids[5,15]. The most accurate theories for simple liquids are based on the well-known Ornstein-Zernike equation which defines the direct correlation function C(r) in terms of fluid density and the radial distribution function g(r) = 1 + h(r). Pioneering work was done in the 1960's and early 1970's.[5] For *dense* simple liquids with strongly repulsive and weak attractive interactions, the Percus-Yevick (PY) approximation[5,16] gives remarkably accurate results when compared to computer simulation and x-ray scattering experiments on monatomic liquids. The PY approximation can be viewed as a closure which approximately relates the direct correlation function to the radial distribution function, interatomic potential, and temperature. This closure, together with the Ornstein-Zernike equation, leads to a nonlinear integral equation for the radial distribution function g(r) of a monatomic liquid. Theoretical treatment of the structural consequences of attractive forces at moderate and low densities is far more difficult even for simple fluids[5]. This area remains active in order to get better quantitative and thermodynamically consistent theories[5,17], a better description of nonclassical critical phenomena[18], and also to correctly treat situations where the intermolecular interactions are complex such as in colloidal suspensions[19].

In the 1970's Chandler,Andersen, and coworkers initiated the pioneering extension and applications of atomic integral equation concepts to molecular liquids based on the Reference Interaction Site Model or RISM theory[7,8]. This work, and other theoretical approaches based on interaction

site models, has been reviewed in several places[8,20]. In RISM theory each molecule is subdivided into bonded spherically symmetric "interaction sites". For small molecules(e.g., nitrogen, benzene, carbon tetrachloride) the definition of such sites is essentially obvious based on the chemical view of a molecule as a bonded collection of elementary units or functional groups. The liquid structure can be characterized by a matrix of site-site intermolecular pair correlation or radial distribution functions $g_{\alpha\gamma}(r)$ defined according to[7,8]

$$\tilde{\rho}^2 g_{\alpha\gamma}(r) = \left\langle \sum_{i\neq j=1}^{M} \delta(\vec{r}_i^{\,\alpha})\delta(\vec{r}-\vec{r}_j^{\,\gamma}) \right\rangle \tag{2.1}$$

for a fluid of M molecules. In Eq. (2.1) $\tilde{\rho}$ is the number density of molecules and $\vec{r}_i^{\,\alpha}$ specifies the position of site α on molecule i. In RISM theory Chandler and Andersen generalized the Ornstein-Zernike equation of monatomic liquids to molecular liquids in a manner which includes intramolecular, as well as, intermolecular correlations[7]. Physically, the key idea is that intramolecular chemical bonding constraints, which describe molecular shape of rigid molecules, strongly influence *inter*molecular packing. Based on heuristic arguments, Chandler and Andersen then employed a PY type closure for the direct correlation functions in analogy with the monatomic case[7,8]. The resulting set of nonlinear integral equations can be solved numerically for the intermolecular pair correlation functions[8,21].

Chandler and coworkers successfully applied this RISM formalism to describe the structure of rigid diatomic and polyatomic molecular liquids[8,21]. The generalization of the RISM theory to treat flexible molecules was initiated by Chandler and Pratt[12] in the late 1970's, and extensively applied to short alkane liquids[12] and the hydrophobic effect[22]. By combining the RISM methodology for a single flexible "ring molecule" (in imaginary time) with the Feynman path integral formulation of quantum mechanics, Chandler and coworkers have recently developed microscopic theories of quantum processes in fluids focusing particularly on the solvated electron problem[23,24].

Beginning in 1987, we and our coworkers have extended and widely

applied the RISM concepts to the case of flexible polymer solutions and melts[6,25,26], polymer mixtures or blends[27-32], and block copolymers[33]. We generically refer to this work as polymer-RISM or PRISM theory[10]. The connection of the elementary aspects of PRISM theory with the quantum electron work has been discussed[34].

The earliest version of PRISM theory rests on two very simple ideas which allow the circumvention of difficult computational and conceptual problems inherent to flexible macromolecular systems : points (1) and (2) enumerated in the Introduction. The first technical simplification applies to linear polymers when the degree of polymerization N is large. In this case one can, to a good approximation, take each of the monomers along the chain backbone as equivalent. At the most fundamental level, this corresponds to assuming the site-site direct correlation functions are independent of where monomers are located along the chain. This "pre-averaging of end effects" approximation results in a reduced theory for "chain averaged" site-site pair correlation functions[6] such as $g(r) = N^{-2} \Sigma_{\alpha\gamma} g_{\alpha\gamma}(r)$. Such a simplification, $g_{\alpha\gamma}(r) = g(r)$, would be exact for cyclic ring polymers. Of course, this approach represents a loss of detailed structural information, and interesting questions such as the packing of chain ends cannot be addressed. Tractable schemes to go beyond the equivalent monomer approximation have been proposed[6], but to our knowledge not implemented. Numerical RISM studies on short linear molecules(propane, butane) suggest the "pre-averaging" approximation is very accurate for the chain averaged pair correlations[35] even when N= 3 or 4.

Within the equivalent monomer approximation scheme, each monomer in the linear chain is constructed from one or more spherically symmetric interaction sites A, B, C, etc. The generalized Ornstein-Zernike-like equations of Chandler and Andersen[7] can be conveniently written in Fourier transform space in the general form

$$\underset{\sim}{\hat{H}}(k) = \underset{\sim}{\hat{\Omega}}(k).\underset{\sim}{\hat{C}}(k).\left[\underset{\sim}{\hat{\Omega}}(k) + \underset{\sim}{\hat{H}}(k)\right] \qquad (2.2a)$$

where the caret denotes Fourier transformation with wave vector k. In real space one obtains

$$\underset{\sim}{H}(r) = \int d\vec{r}' \int d\vec{r}'' \underset{\sim}{\Omega}(|\vec{r} - \vec{r}'|) \cdot \underset{\sim}{C}(|\vec{r}' - \vec{r}''|) \cdot \left[\underset{\sim}{\Omega}(\vec{r}'') + \underset{\sim}{H}(\vec{r}'') \right] \tag{2.2b}$$

The first set of terms on the right hand side of Eq(2.2) describes all possible site-site correlation pathways *between a pair of tagged molecules.* In the low molecular density limit only these contributions survive. The second set of terms describe all correlation pathways between two sites on different molecules which are mediated by one or more *different* molecules. The matrix multiplications in Eqs. (2.2) run over ν independent sites A, B, C, etc., and $C_{\alpha\gamma}(r)$ is the ν x ν matrix of direct correlation functions. Because of symmetry there are $\nu(\nu+1)/2$ independent Ornstein-Zernike equations for the total correlation functions $H_{\alpha\beta}(r)$

$$H_{\alpha\gamma}(r) = \rho_\alpha \rho_\gamma h_{\alpha\gamma}(r) = \rho_\alpha \rho_\gamma [g_{\alpha\gamma}(r) - 1] \tag{2.3}$$

where $\rho_\alpha \equiv \tilde{\rho} N_\alpha$ is the density of sites of type α, and N_α is the number of sites of type α per chain.

When the generalized Ornstein-Zernike-like or PRISM Eq. (2.2) is applied to flexible macromolecules a *conformational preaveraging* assumption is employed by replacing the instantaneous, N-body intramolecular structure of the flexible chain by its ensemble-averaged pair correlation function description[6,8,12,24]. Thus, all information concerning the intramolecular structure of the polymer chains is contained in the functions $\Omega_{\alpha\gamma}(r)$ defined as

$$\Omega_{\alpha\gamma}(r) = \tilde{\rho} \sum_{i \in \alpha, j \in \gamma} \omega_{ij}(r) \tag{2.4}$$

where $\omega_{ij}(r)$ is the normalized probability density between two sites i and j on the *same* molecule. In Fourier transform space $\hat{\Omega}_{\alpha\gamma}(k)$ can be identified as the single-chain partial structure factors.

The generalized Ornstein-Zernike-like equations in Eq. (2.2) define $\nu(\nu+1)/2$ independent direct correlation functions. In order to have a solvable system of equations additional approximate "closure relations" are required. This is the critical step, since the RISM or PRISM equations are

really just defining relations for the site-site direct correlation functions. The most accurate closure is system-specific, and is a question of enduring interest. In our original work on *dense one-component repulsive force* liquids, we followed Chandler and Andersen by adopting the approximate site-site PY closure[7,8]

$$C_{\alpha\gamma}(r) \cong \left\{1-\exp[\beta v_{\alpha\gamma}(r)]\right\} g_{\alpha\gamma}(r) \qquad (2.5a)$$

where $v_{\alpha\gamma}(r)$ is a spherically symmetric, *repulsive* interaction potential between sites α and γ, and $\beta = 1/k_B T$ at temperature T where k_B is Boltzmann's constant. For hard sphere interactions between sites, the PY closure reduces to the particularly simple form

$$\begin{aligned} g_{\alpha\gamma}(r) &= 0 \qquad & r < d_{\alpha\gamma} \\ C_{\alpha\gamma}(r) &\cong 0 \qquad & r > d_{\alpha\gamma} \end{aligned} \qquad (2.5b)$$

which is equivalent to the so-called "Mean Spherical Approximation" (MSA)[5,8,11]. The condition inside the distance of closest approach $d_{\alpha\gamma}$ is an exact statement reflecting the impenetrability of hard spheres. The second condition, in which the direct correlation functions are approximated as zero outside the hard core, exploits the standard idea of Ornstein and Zernike that the direct correlation function is spatially short range. For atomic fluids, Eq(2.5b) can be derived by established graph theoretical partial summations and other functional methods.[5] However, for interaction site molecular fluids the PY closure is argued to be useful based on analoies with atomic fluids and hueristic physical concepts.[7,8] The lack of a rigorous interaction site cluster series basis for Eq(2.5b) has lead to RISM theory being described as a "diagramatically improper" theory.[8]

Eqs. (2.3) - (2.5) lead to $\nu(\nu+1)/2$ coupled integral equations which make up the polymer RISM theory in its simplest form appropriate for dense, repulsive force polymer fluids. The integral equations can be solved numerically using a variety of standard techniques[5,8].

Alternative closure approximations for the repulsive force fluid have been investigated and will be briefly commented on in subsequent sections.

Based on the idea that the atomic-like closures are useful by analogy for molecular fluids , there are several alternatives to the PY or MSA approximation for hard core fluids. These include the Hypernetted Chain (HNC) approximation[5,20,36]

$$c_{\alpha\gamma}(r) = h_{\alpha\gamma}(r) - \ln\left(1+h_{\alpha\gamma}(r)\right) \quad , \quad r > d_{\alpha\delta} \tag{2.6}$$

and the Martytnov-Sarkisov (MS) closure[5,37]

$$c_{\alpha\gamma}(r) = h_{\alpha\gamma}(r) - (1/2)[\{1+\ln\left(1+h_{\alpha\gamma}(r)\right)\}^2 - 1] \quad , \quad r > d_{\alpha\delta} \tag{2.7}$$

Numerical studies of chain molecule fluids have also been carried out by Yethiraj[38] using the considerably more complicated "diagramatically proper" formulation of RISM theory due to Chandler, Silbey and Ladanyi[39,40]. Novel, even more complicated closures have been recently proposed by several workers[41,42] but numerical predictions for polymer fluids have not been established.

Appropriate closures for describing the influence of attractive forces on polymer liquid structure is a much more subtle and difficult problem than the repulsive force or hard core fluid case. We defer discussing this aspect until Section VI.

In our application of PRISM theory to flexible polymer systems one expects that the *intra*molecular structure, represented by Eq. (2.4), depends on the *inter*molecular structure specified in Eq. (2.3) and vice versa[6,8,12]. Thus, in a rigorous calculation the intramolecular and intermolecular structure must be determined in a *self-consistent* manner leading to problem (2) mentioned in the Introduction. This problem represents a major conceptual difficulty and might be thought to be especially formidable for large macromolecules. The self-consistent issue for flexible molecules was originally addressed by Chandler and Pratt in both a formal diagrammatic manner, and in the context of tractable approximation schemes formulated for short chain molecules[8,12]. For macromolecules, several new theories for performing such self-consistent structural calculations have been formulated and applied [43-47] which will be discussed in Sections VIII and IX.

A simple, zeroth approximation to the self-consistent problem *for dense one-component polymer melts* can be invoked as suggested by our earliest PRISM work[6]. Subsequent structurally self-consistent calculations(see section VII), as well as computer simulations and experiments, suggest that to a good approximation one can avoid (*under appropriate conditions*) the self-consistency complication by exploiting Flory's "ideality hypothesis". Flory[1,48] argued many years ago that in a high density melt of strongly interpenetrating chains at high density, the "long range" *intra*molecular excluded volume interactions that lead to chain expansion in a dilute solution in a good solvent are "screened out" or "canceled" by the *compressive* intermolecular interactions between chains embedded in a nearly incompressible fluid. *At the level of a single chain,* the net result is a cancellation of repulsive bare intrachain interactions by the attractive, "solvent-mediated" interactions. Thus, in a dense, one-component melt the chains act as a "theta or ideal solvent" for themselves in the sense that the chain radius-of-gyration obeys the maximum entropy ideal random walk scaling law : $R_g \propto N^{1/2}$. The "prefactor" in this scaling relation can be computed based on an atomistic single chain model[13] which *ignores* interactions among monomers beyond close neighbors. Neutron scattering experiments[49] and computer simulations[50,51] on polymer melts have demonstrated the accuracy of Flory's conjecture. This approximation provides an enormous simplification because the intramolecular correlations in Eq. (2.4) can then be calculated from a separate single chain computation in which long range (in chemical sequence) interactions along the chain backbone are set to zero. A wide variety of single chain models are available[13], and thus the connection between polymer structural features and bulk properties and phenomena can be systematically investigated.

It is important to note that in calculation of the intramolecular structure factors for input into PRISM theory, one can include as much(or as little) chemical detail regarding the molecular architecture as desired. For questions regarding intermolecular packing on relatively long length scales (eg. the so-called "correlation hole" regime[2] corresponding to intermolecular separations of several monomer diameters and larger), the local monomeric structure is not important and one can use a coarse grained description of the polymer chain structure[2-4,13]. In this case a

Gaussian, freely-jointed, or semiflexible chain model for $\hat{\Omega}_{\alpha\beta}(k)$ would suffice. Such coarse-grained models are also useful for investigating general trends which transcend the fine details of specific polymer molecules.

On the other extreme, in order to make specific quantitatively accurate predictions for thermodynamic properties and the details of local packing, we anticipate that the local monomeric structure is important. For the often subtle question of macromolecular mixture miscibility and copolymer self-assembly, it is often unclear *a priori* what level of chemical detail is adequate. For such problems, one may employ a model that includes the effects of constant bond lengths, bond angles and rotational potentials such as the rotational isomeric state model[13]. Inclusion of these local details into $\hat{\Omega}_{\alpha\beta}(k)$ is feasible but requires significantly more numerical effort.With modern workstations, a tractable option is to perform a *single-chain* simulation to provide a chemically realistic input to PRISM. Thus PRISM theory is versatile in its ability to make predictions about intermolecular packing on both local (monomeric) and global (radius of gyration) length scales, as a functional of intramolecular architecture. In this article we will describe PRISM applications that include the entire range of local chemical detail.

III. STRUCTURE AND THERMODYNAMICS OF DENSE MELTS

Pure one-component polymer liquids or "melts", are in one sense the simplest case since single chain conformation is nearly "ideal". However, there remains the question of the influence of local chemical architecture on melt structure, thermodynamic properties, and physical phenomena(e.g., wide angle scattering, crystallization). In the context of PRISM theory, the question is on what length scale, or degree of coarse-graining, is an "interaction site" defined ? Since there does not exist a rigorous renormalization group type scheme to "integrate out" degrees of freedom and chemical details, the practical approach is to study families of models of variable levels of realism[52]. Figure 3.1 illustrates this process schematically in the context of an industrially important class of saturated

3.1 Schematic representation of three levels of chain models considered and the coarse-graining procedure. The top level is an atomistic model of polyolefins. The second level shows two intermediate models: site overlapping semiflexible chain(with bending energy e_b) and freely-jointed branched chain. The bottom level is the Gaussian thread chain.

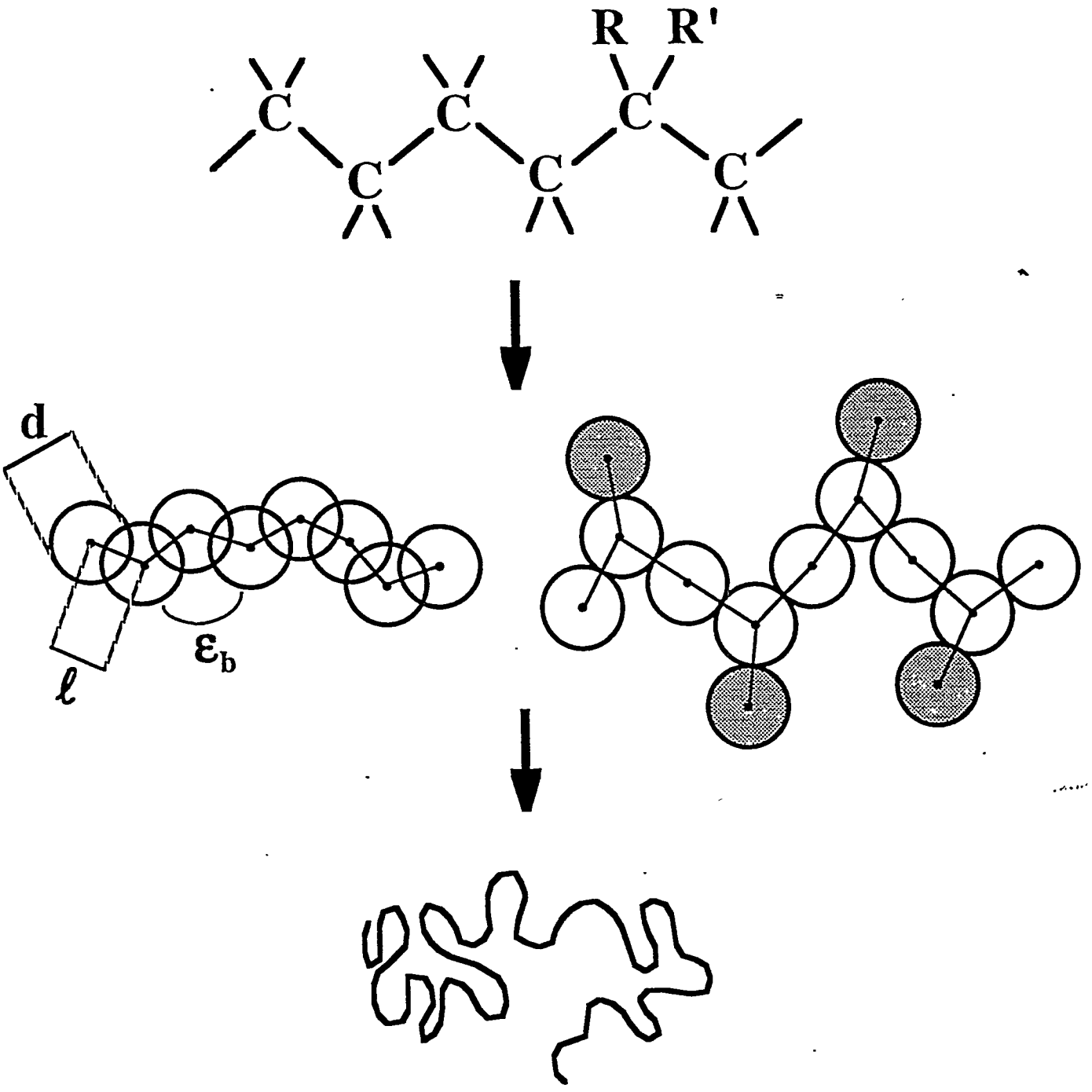

hydrocarbon polymers(polyolefins). Three general levels of chain models are illustrated. (1) An atomistic level where there may be multiple symmetry-inequivalent sites within a monomer repeat unit. For polyolefins, sites may be a methylene, methyl , or methyne group, and Angstrom level structure is explicitly accounted for. (2) A *single site* intermediate level "semi-flexible chain" (SFC) model, or multiple site "freely-jointed" branched chain. Such models correspond to a modest degree of coarse-graining. (3) The extreme, heavily coarse-grained "Gaussian thread model" where the polymer is crudely treated as a thin, fully flexible, ideal random walk space curve. It is at this level that self-consistent field theoretic approaches describe polymer structure[2-4].

In the next two sections we consider melt structure, as embodied in the intermolecular site-site radial distribution functions and the total structure factor describing collective density fluctuations in Fourier space, as a function of degree of coarse-graining. Possible "mappings" which relate the different chain models are briefly mentioned[52]. Purely repulsive(generally hard core) interchain site-site potentials are employed corresponding to an athermal melt situation. At high liquid densities, structure is expected to be dominated by such purely steric packing forces[5,11]. Use of the structural information to compute thermodynamic properties is addressed in section C.

A. Single Site Homopolymers

Consider first linear polymers composed of identical spherical sites which interact intermolecularly via a pair decomposable site-site hard core potential of diameter d. The dimensionless reduced fluid density is $\rho_m d^3$, where $\rho_m = N\rho$ is the site number density.

1. Gaussian Thread Chains

At the most coarse-grained level the polymer is described as an ideal random walk *on all length scales*. The intramolecular structure factor matrix is Gaussian and given by[2-4]: $\hat{\omega}_{\alpha\gamma}(k) = \exp(-k^2\sigma^2|\alpha-\gamma|/6)$ where σ is the so-called "statistical segment length". Physically, it represents a length scale beyond which real chain units are orientationally uncorrelated. The mean square end-to-end distance, R , and radius-of-gyration, R_g, are given by $\langle R^2\rangle = N\sigma^2$, and $R_g = R/\sqrt{6}$, respectively,

where N is the number of statistical segments. The single chain structure factor $\hat{\omega}(k) = N^{-1}\sum_{\alpha,\gamma}^{N}\hat{\omega}_{\alpha\gamma}(k)$, is easily computed in closed form. Numerically-obtained PRISM predictions of g(r) and the dimensionless collective density fluctuation structure factor, $\hat{S}(k) = \hat{\omega}(k) + \rho_m\hat{h}(k)$, for such a model have been presented for a wide range of N and reduced densities[6,25,30]. Gaussian ring polymers have also been studied[6,25]. As expected physically, *for large N* only minor structural differences between ring and chain melts are found *on* macromolecular length scales, and identical behavior is predicted for the local region of g(r) .

A further model simplification, corresponding to taking a type of "continuum limit" (commonly employed in field theoretic approaches[2-4] in the large N regime), can be taken in order to obtain analytic results which capture all the essential physical features of the Gaussain chain model[25,30]. The single chain structure factor is approximated by a Lorentzian[3]

$$\hat{\omega}(k) = \frac{1}{(k^2\sigma^2/12) + N^{-1}} \qquad (3.1)$$

This form neglects the self-scattering term appropriate for the $k\sigma \to \infty$ regime, but which is irrelevant in a continuum-of-sites description. Eq(3.1) very accurately describes the exact Gaussian $\hat{\omega}(k)$ for the $k\sigma<1$ regime of interest in a continuum model. In particular, it exactly reproduces the k=0 value and the "self-similiar" intermediate scaling regime, $\hat{\omega}(k) = 12\,(k\sigma)^{-2}$ for $R_g^{-1} << k << \sigma^{-1}$. In real space, this self-similiar behavior corresponds to power law , or critical-like, correlations, $\omega(r) \propto r^{-1}$. This is a polymeric effect associated with the ideal random walk chain statistics on intermediate length scales, and is widely exploited in the "scaling theory" approach to polymer physics problems[2-4]. The second simplification is to take the "thread" limit, corresponding to $d \to 0$ and $\rho_m \to \infty$ such that the reduced fluid density is finite and nonzero. This simplification reduces the hard core impenetrability constraint to a point condition , g(r=0) = 0. Thus, within the PY closure approximation the site-site direct correlation function reduces to a delta-function form : $C(r) = C_0\delta(\vec{r})$, where

$C_0 = \hat{C}(k=0)$ is a parameter to be determined by application of the PRISM integral equation and the core exclusion condition[25,30].

The resulting PRISM integral equation is analytically solvable for the Gaussian thread model. The structural predictions are[25,30]

$$g(r) - 1 = \frac{3}{\pi \rho_m \sigma^2 r}\left[\exp(-r/\xi_\rho) - \exp(-r/\xi_c)\right] \tag{3.2}$$

$$\begin{aligned} \hat{S}(k) &\equiv \hat{\omega}(k) + \rho_m \hat{h}(k) \\ &= \frac{12(\xi_\rho/\sigma)^2}{1+(k\xi_\rho)^2} \end{aligned} \tag{3.3}$$

The fundamental length scales are the density screening length, ξ_ρ, given by

$$\xi_\rho^{-1} = \frac{\pi \rho_m \sigma^2}{3} + \xi_c^{-1} \tag{3.4}$$

which controls the *local* packing of threads,and the "correlation hole" length scale $\xi_c = R_g/\sqrt{2}$. Eq(3.2) shows the correlated part of g(r) consists of a local and macromolecular contribution. "Negative" correlation is predicted on all length scales, i.e. $g(r) < 1$ for all r, and simple-liquid like solvation shells are entirely absent. Remarkably, these general features survive qualitatively in more chemically realistic, even atomistic, models of polymer structure due to thermal conformational disorder and destructive interference between the packing consequences of multiple local length scales(see section IIB). For the simple thread model the local contribution to g(r) is directly related to $\hat{S}(0) = 12(\xi_\rho/\sigma)^2$ and hence the isothermal compressibilty, κ, via the thermodynamic relation $\hat{S}(0) = \rho_m k_B T \kappa$. The simple Yukawa forms in Eqs(3.2) and (3.3) are a consequence of the technical simplifications invoked by the Gaussian thread model. Hence, the precise details of g(r) in the local region will change as more chemically realistic models are employed.

The depth of the *local* correlation hole is predicted to be controlled by a so-called "packing length" $(\rho_m \sigma^2)^{-1}$. This quantity is invariant to arbitrary re-definition of a coarse-grained segment (or re-grouping of real

monomers). Under melt conditions and for normal temperatures (T=250-500 Kelvin), the packing length falls typically in the range of 1.7 - 5.5 Angstroms for a very wide class of semiflexible polymers[52,53].

The predicted power law relation(for large N) of Eq(3.4) between the density screening length and ρ_m is in excellent agreement with experiments, scaling arguments, and field theories for dense solutions but *not* melts[52,54]. However, under many solution conditions the "ideality" approximation breaks down and the effective statistical segment length, and hence R_g , acquires a polymer concentration dependence. This aspect has been incorporated by using the fully self-consistent version of PRISM(see Sec.VIII), or more simply by combining field theoretic and/or scaling predictions[2,3] for single chain size(e.g., $\sigma \propto \rho^{-1/8}$ in good solvents) with the PRISM analysis of intermolecular packing[54].

The second contribution to g(r) in Eq(3.2) is called the correlation hole effect by deGennes[2], and is associated with the longer wavelength universal aspects of chain connectivity and interchain repulsive forces. On intermediate length scales it has a critical power law form due to chain conformation self-similiarity, and this simple analytic form remains an excellent representation even for chemically realistic models when intersite separations exceed an intrinsic(N-independent) distance of the order of 3-5 site diameters.[25]

The dimensionless collective structucture factor, $\hat{S}(k)$ in Eq(3.3), is of a purely decaying, or "diffusive" , form ; no large angle peaks(which must be present in real dense fluids) are present. Again, this is a consequence of the idealized Gaussian thread model, although the diffusive form is in general accord with experiments(in the $k\sigma<1$ regime) and field theoretic predictions for moderately concentrated ("semidilute") polymer solutions[2,3].

The analytic Gaussian thread model has been generalized to approximately treat nonzero chain thickness ($d\neq0$) in a simple average manner[30]. This generalization is called the "Gaussian string model", and results in a g(r) and $\hat{S}(k)$ of the same form as Eq(3.2) but the density-density screening does not obey Eq(3.4). For long chains all the basic structural and thermodynamic features remain the same as the thread model, although the contact value, g(d), is now nonzero and this has important implications for particular physical problems. The Gaussian string model has been shown to generally be in remarkable agreement with numerical PRISM

predictions for discrete, nonzero thickness Gaussian chains[30]. This agreement suggests that a type of "self-averaging" process occurs in polymer fluids, i.e. the essential part of C(r) is its long wavelength, integrated strength $C_0 = \hat{C}(k = 0)$.

2. Semiflexible Chain Models

The most fundmental aspects of real polymer structure are : (a) nonzero chain thickness, (b) semi-flexibility, i.e. a system-specific and thermodynamic state dependent tendency for chain bending or coiling due to rotational isomerism, and (c) an overall size strongly correlated with the degree of polymerization. As displayed in Figure 3.1, the discrete semiflexible chain(SFC) model includes these features by introducing (a) a site diameter, d ; (b) a local bending energy ε_b which controls the "chain persistence length", defined as $\xi_p = \Sigma_\alpha < l_1 * l_\alpha > / l_b$,which for the large N is given by $\xi_p = l_b/\{1+<\cos(\theta)>\}$ where l_b is the magnitude og the nearest neighbor rigid bond length; and (c) a degree of polymerization, N, which determines the overall size $<R^2> = l_b (2\xi_p - l)N$ (for large N). The ratio l_b/d controls the amount of exposed surface area available for interchain site-site interactions or packing.

Summarizing, the structure of a fluid of *hard core* SFC polymers is characterized by four dimensionless variables which can be chosen to be : $\rho_m d^3$ (reduced density) or total site packing fraction η , $\Gamma = \xi_p/d$ (chain aspect ratio) , l_b/d , and degree of polymerization, N. Novel approximate, but accurate and computationally convenient, numerical procedures have been developed by Honnell et. al.[55] for the calculation of the single chain structure factor, $\hat{\omega}(k)$, of the SFC model. In the polymer field jargon, the SFC model is the discrete, finite thickness generalization of the "worm-like-chain" or "Koyama" model[4,56], which interpolates between the rigid rod and ideal random walk chain models. The approximate calculation of $\hat{\omega}(k)$ is based on a cumulant expansion and rigorous evaluation of the second and fourth moments of $r_{\alpha\gamma}$, or equivalently $<\cos(\theta)>$ and $<\cos^2(\theta)>$. In addition, it is possible to exactly compute the next nearest neighbor correlations[43], $\omega_{\alpha,\alpha+2}(r)$, and this extension is generally adopted and accounts for the most local part of the intramolecular excluded volume interactions.

Details of the rotational potentials, chemical bond lengths, bond angles, and nonspherical monomer structure are ignored in the SFC model and thus can only be mimicked by judicious choice of SFC model parameters. However, it has been recently demonstrated by Schweizer et. al.[52] that by appropriate choice of SFC parameters *both* the single chain and interchain packing of real polymer liquids can be reproduced to surprising accuracy by the SFC model. Although inherently nonunique, specific procedures for "mapping" a real polymer onto the SFC have been formulated and successfully applied. Here we present a few representative results and refer the reader to the original literature for the details[52].

Figure 3.2 shows the predicted g(r) at melt-like density for N=1000 chains , l_b/d = 0.5, and a range of aspect ratios(of order unity) relevant to typical flexible polymers of experimental interest[52]. For these cases g(r) is relatively featureless and slowly varying in rough accord with the simple Gaussian thread model behavior. There is both a local and global correlation hole, and $g(r) < 1$ for all r. These features are in qualitative accord with atomistic calculations. Moreover, the form of g(r) appears to be a remarkably good, coarse-grained representation of the site-averaged correlations predicted by atomistic PRISM theory(see subsection 4 and B below) and atomistic simulations[57-59]. Such agreement is *not* because real polymers are Gaussian on all length scales as assumed by the thread model. Rather, it is the multitude of local chemical lengths, and thermal conformational disorder associated with chains composed of real monomers, which frustrates the development of well-defined solvation shells and positive correlation in g(r)[52].

Another important structural feature in Fig 3.2 is that the local correlation hole is very sensitive to aspect ratio. As expected physically, it deepens as the chain becomes more flexible and less able to efficiently pack with neighboring polymers. This feature has important consequences for thermodynamic properties(e.g.,cohesive energy density)and the miscibility of polymer mixtures[52].

As the chain aspect ratio is significantly increased above $\Gamma \cong 1.4$, and/or the accessible site surface area is enhanced by increasing l_b/d, more well-defined solvation shells develop and "positive correlation" ($g(r) > 1$) occurs. The extreme limit is the rigid rod polymer. The predicted packing of such models(not shown) begins to resemble a smeared version of the g(r) of

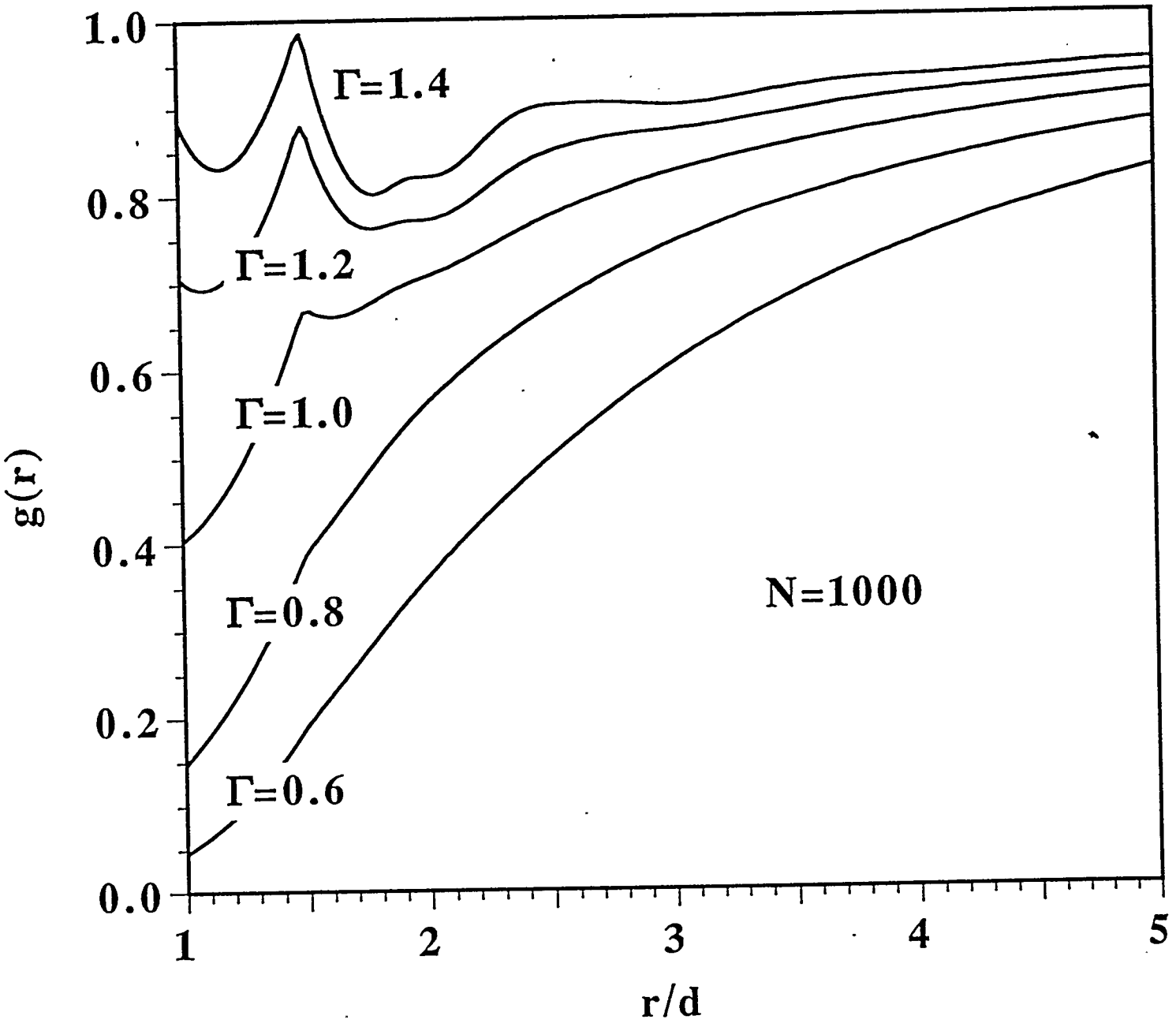

3.2 PRISM results for the site-site g(r) of a N=1000, h =0.5 SFC model liquid and several experimentally relevant choices of chain aspect ratio G.

simple atomic liquids, particularly in the "tangent" SFC limit[55] where l_b=d. Thus, such a tangent model appears to be a *poorer* coarse-grained representation(relative to the l_b/d<1 SFC models) of the g(r) of real polymer fluids.

The "tangent" SFC model with chain aspect ratio of $\Gamma \cong 1.4$ has been studied in recent large scale molecular dynamics and Monte Carlo simulations of dense melts by several groups[51,60]. Comparisons of PRISM theory predictions with these benchmark simulations has shown agreement at roughly the same level obtained for atomic and small molecule(RISM) liquids(e.g. 10-20% errors at contact and much better as r increases). This is significant since it shows that the standard site-site PY closure for hard core fluids suffers no obvious loss of accuracy as the chains become longer. For linear chain solutions and melts interacting via pure hard core potentials the site-site PY closure appears to be the most accurate closure for g(r) as judged by overall comparison with computer simulations[60]. At the highest melt-like densities, Yethiraj and Schweizer[61] have shown that PRISM theory with the PY, HNC and MS closures yield the most similiar results for g(r). However, the PY closure is the most robust since under certain density and chain length conditions the HNC , MS, and diagramatically proper closures[38-40] can fail to converge and/or result in extremely poor descriptions of collective structure and density fluctuations especially on long length scales. Theoretical arguments for this have been suggested[61]. Very recent simulation studies by Yethiraj[62] of hard core fluids composed of rather stiff chains of larger aspect ratios (roughly Γ>2) reveals that PRISM theory predicts the local (near contact) behavior of g(r) very well, but longer range aspects associated with liquid layering and solvation shell structure is not accurately described.

An example of a comparison by Honnell et. al.[55] of PRISM theory with the molecular dynamics simulations of Kremer and Grest[51] are shown in Figure 3.3. Details of the model are given elsewhere[51,55]. Briefly, a melt-like density was studied for N = 50 - 150 unit chains. The linear polymers were modeled as freely-jointed beads with a purely repulsive, shifted Lennard-Jones interaction between all segment pairs. The corresponding chain aspect ratio is $\Gamma \cong 1.4$. PRISM theory with the PY closure(plus a standard correction for repulsive force softness) was applied for two choices of the intramolecular structure factor $\hat{\omega}(k)$: (i) a SFC chain model with

3.3 Intermolecular site-site radial distribution function for soft-core, repulsive Lennard-Jones chain liquids at h = 0.464 and (a) N=50 and (b) N=150. The circles are the molecular dynamics simulation results of Grest and Kremer[51]. Curves are PRISM predictions[55] based on the exact w(k) (solid line for N=50), and the SFC model (dashed curve for N=50 and solid curve for N=150). Distances are scaled by the Lennard-Jones site diameter.

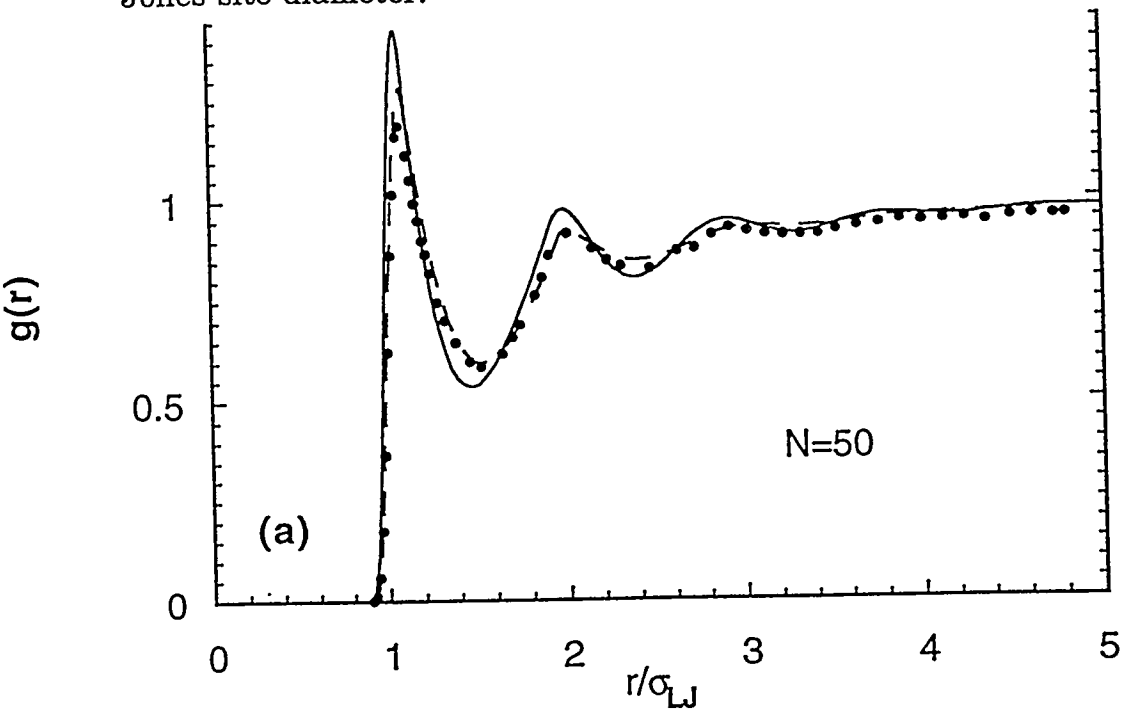

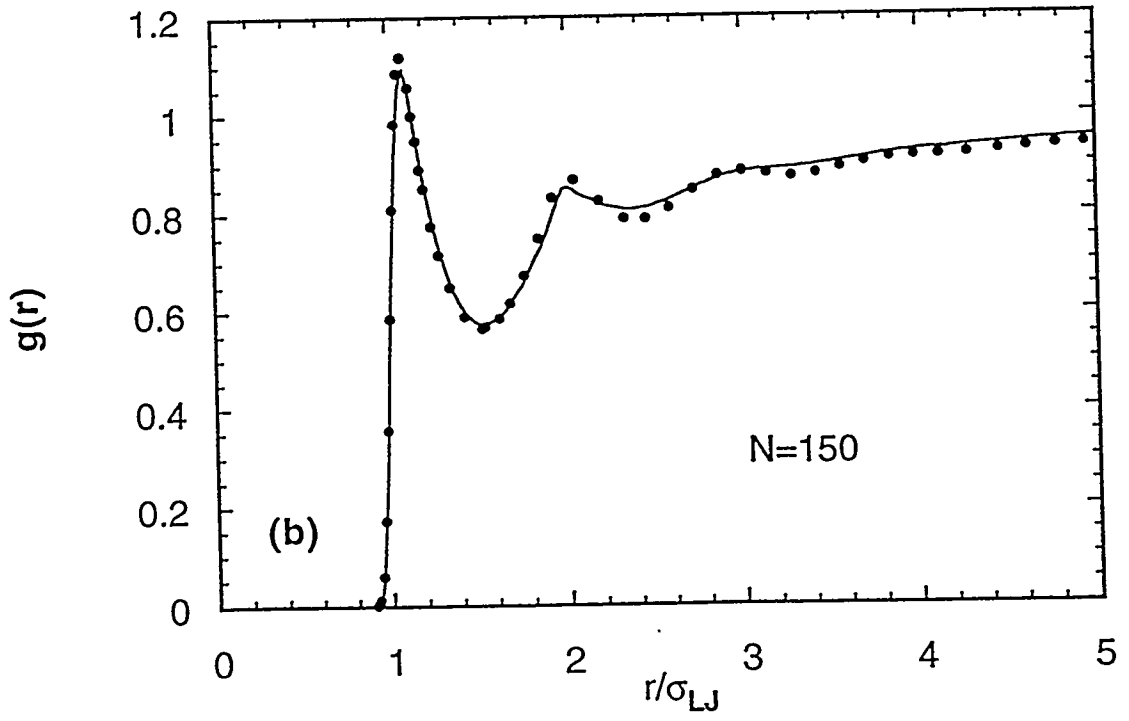

bending energy chosen to reproduce the simulated value of the chain end-to-end distance, and (ii) the exact, simulation result for the *single chain* quantity $\hat{\omega}(k)$. The second approach involves the fewest statistical mechanical approximations, and provides a precise check on the accuracy of the PRISM/PY theory for interchain packing. Errors of the size of 15% are found at small separations, which become much smaller as r increases. Calculation (i) is in the best agreement with the N=50 simulation. This is partially fortuitous, i.e. errors in PRISM theory and errors in the approximate calculation of $\hat{\omega}(k)$ have largely canceled to yield nearly perfect agreement for N=50, 100(not shown) and 150. Calculations for a simpler ideal freely-jointed chain model have also been performed[51,55] (not shown here) , and are in the poorest agreement with simulation since this fully flexible ideal model ignores the very local intrachain excluded volume interactions between monomers separated by two bonds. Thus, chain size is *underestimated* leading to the strong underestimation of g(r) locally.

The trends of g(r) with decreasing fluid density are qualitatively similiar to decreasing aspect ratio at melt density[55]. Single chain conformational entropy becomes increasingly more important relative to interchain packing entropy as the fluid becomes more dilute, resulting in a g(r) which is less structured with a much deeper *local* correlation hole. Many examples have been given in the literature[6,25,55]. However, as true for RISM theory of simple molecules[8], the quantitative accuracy of PRISM theory is reduced as the fluid density is lowered even if the exact, simulated $\hat{\omega}(k)$ is employed[60,61]. Similiarly, at fixed density and aspect ratio, the chains pack more poorly (less solvation shell structure and deeper hole locally in g(r)) as N is increased[6,25,55].However, a stable long chain limit is approached in the local region of g(r), and this occurs more quickly as the density and/or chain aspect ratio is increased.

3. Atomistic Models

The structurally simplest polymer, and one of the most commercially important, is polyethylene. It consists of a linear chain of CH_2 units, which we model as single spherical sites in the *single site* homopolymer spirit. There exist well-developed ideal rotational isomeric state chain models[13] where the bond rotational degrees of freedom are represented as discrete

trans and *gauche* isomers. Numerical calculation of the required single chain structure factor can be achieved via Monte Carlo simulation, or using the recently developed computationally convenient approximate methods of McCoy and coworkers[63].

The predictions of PRISM theory for melts of $(-CH_2-)_N$ chains based on purely hard core intermolecular potentials have been numerically obtained, including a systematic study of the n-alkanes by Honnell et. al. (N=4-20)[64,65]. Detailed comparisons with wide angle x-ray scattering measurements of Narten and Habenschuss have been carried out, and excellent agreement between theory and experiment has been demonstrated[64-66]. This agreement has motivated theoretical extensions which employ PRISM theory of the liquid as input to treat melt thermodynamic properties(PVT equation-of-state, compressibility, thermal expansion coefficient)[67], and the development and application of novel polymeric density functional theories of crystallization[68] and polymer near surfaces and interfaces. For the strongly first order crsytallization transition, it has been found by McCoy et. al. that the atomistically realistic description of polyethylene is required for a proper description of the phase transition[68]. This is not surprising since crystallization is a phenomenon exquisitely sensitive to local molecular structure and packing.

Figure 3.4 shows the predicted melt methylene-methylene g(r) for a range of temperatures[52]. The experimental density and a temperature-dependent hard core diameter associated with the repulsive Lennard-Jones methylene interactions(computed according to the standard Barker-Hendersen procedure)[5,11] has been employed in the calculations. Although there is some fine local structural details for r<20 Angstroms, they are rather weak and g(r) crosses over to the long range correlation hole form for larger separations [$h(r) \propto r^{-1}$]. Random behavior corresponding to g(r) = 1 is attained only when $r > R_g$. As the temperature is raised, the reduction of local packing efficiency occurs due to the lower liquid density and enhanced conformational disorder(more twisted *gauche*± conformers). Comparison of the predicted dimensionless collective structure factor, $\hat{S}(k)$, with wide angle scattering data is shown in Figure (3.5)[64,66]. Excellent agreement is obtained for the chemically sensible value of 3.9 Angstroms for the methylene hard core diameter. Comparable

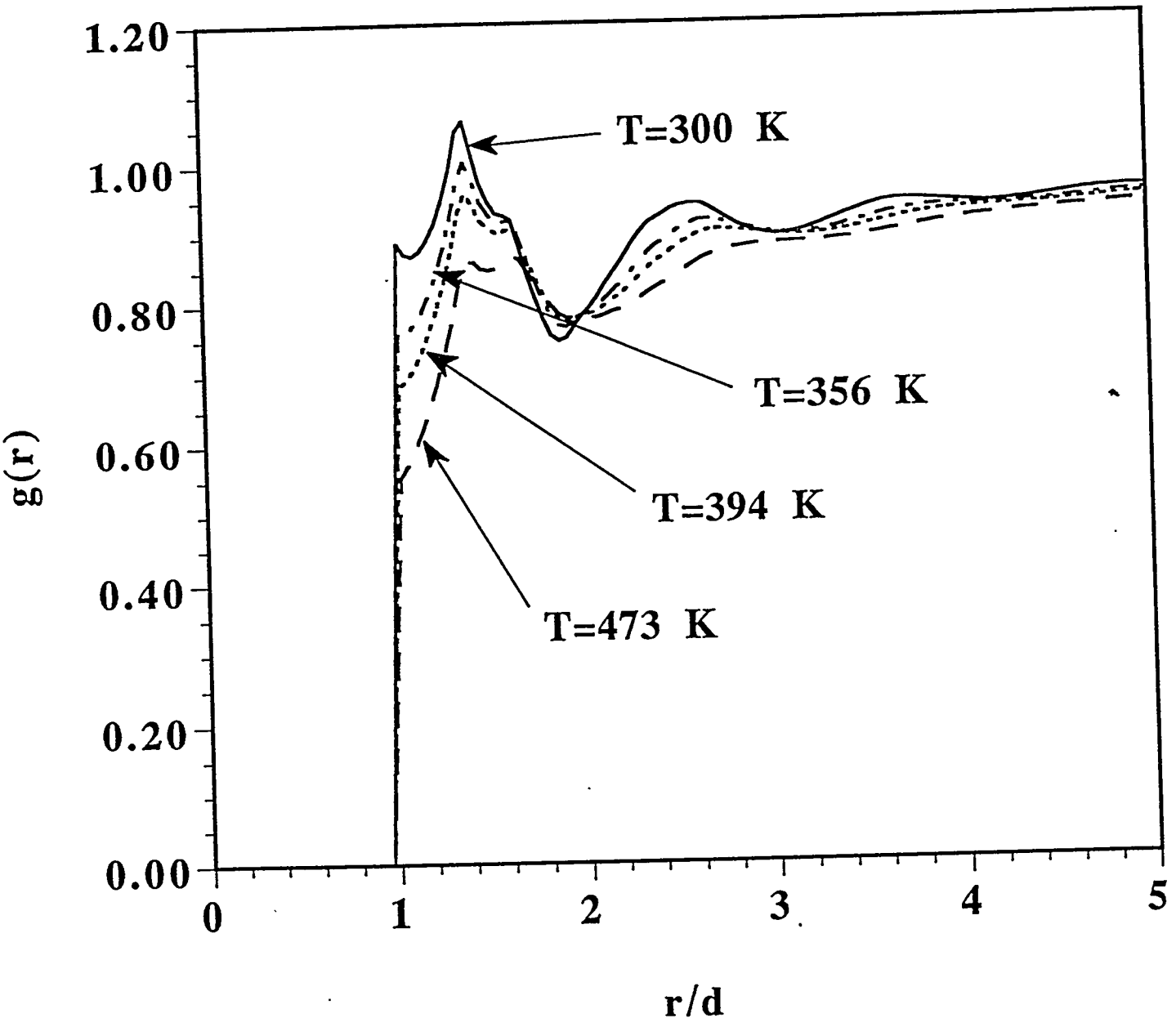

3.4 PRISM predictions for the site-site radial distribution function of an N=1000 RIS model of a hard core polyethylene melt at various temperatures[52]. Distances are scaled by the effective(T-dependent) hard core diameter.

3.5. Dimensionless total structure versus absolute wavevector for a N=6429 polyethylene melt just above its melting temperature.[64,66] The solid circles are the x-ray scattering data, and the line is the PRISM prediction based on a hard core model with d_{CH2} = 3.9 Angstroms. The solid square at k=0 represents the experimental value based on the measured isothermal compressibility and liquid density.

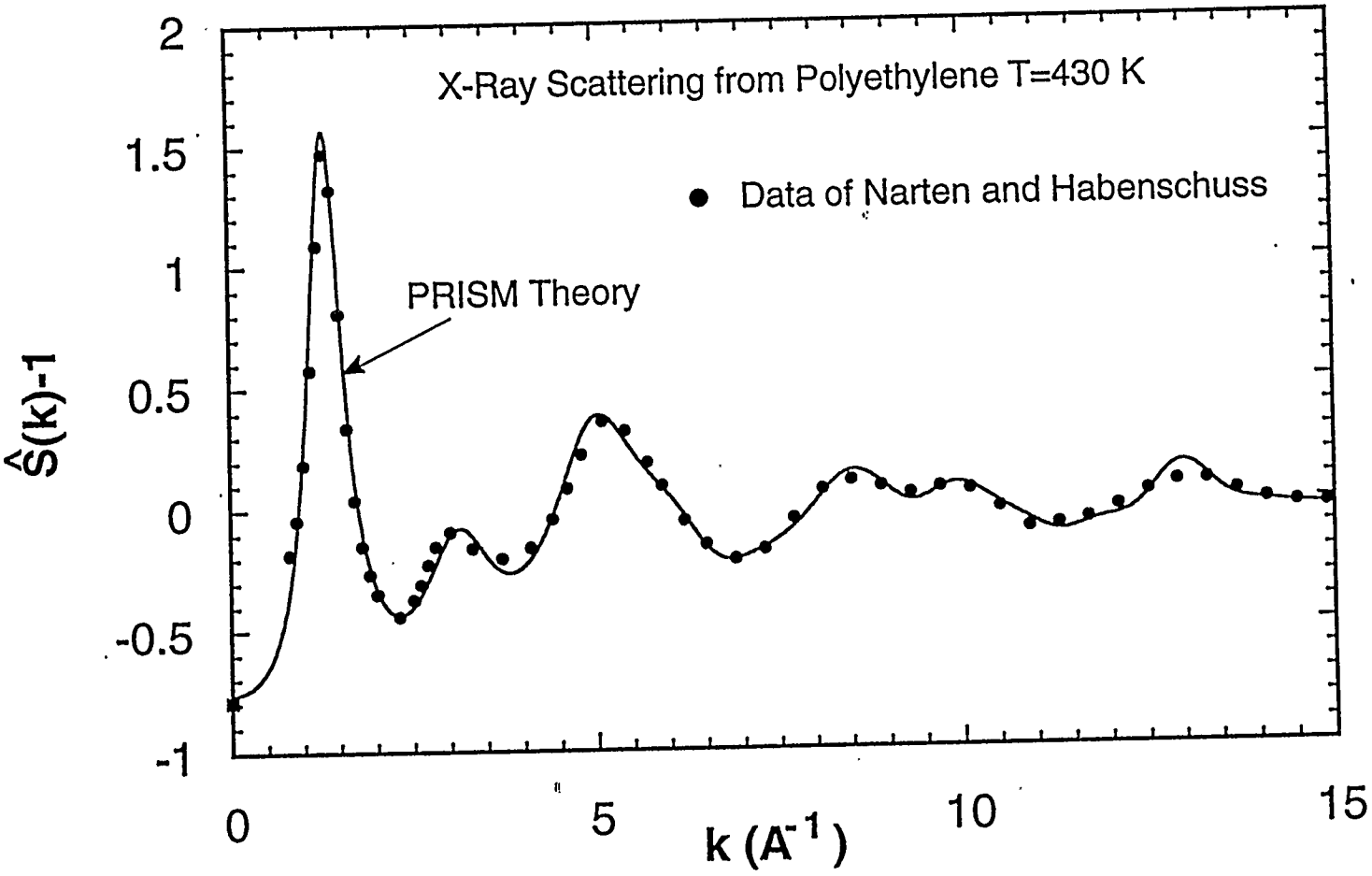

agreement between theory and experiment has been found for the entire alkane series[65].

The most significant feature of Figure 3.5 is the strong first diffraction peak or "amorphous halo" which is influenced by *both* inter- and intra-molecular pair correlations[64-66]. The very large angle scattering reflects single chain correlations which are *input* to the theory. Agreement of the theoretical prediction for the collective structure factor at k=0 with the measured data point is partially fortuitous since the attractive intermolecular interactions present in the real fluid have not been included in the calculation of this thermodynamic property.

The broad message of all the atomistic PRISM studies of linear hydrocarbons is that the theory is capable of an essentially quantitative, *ab initio* description of melt structure for the structurally simplest case of $(-CH_2-)_N$.

4. Coarse-graining and Relationship of Different Chain Models

The collective density fluctuation melt structure factor, $\hat{S}(k)$, has been computed for a wide range of single site models and chain parameters[6,25,55,64-66,68]. There are two primary packing related features of interest: the zero angle scattering $\hat{S}(0)$, and the first strong diffraction peak. These basic density correlation features are *qualitatively* the same for all chain models since they are not intrinsically of polymeric origin. However, clear differences exist with rather well-defined trends. For example, at fixed fluid packing fraction ,chain length, and chain persistence length, both the inverse zero angle scattering amplitude and the amplitude and sharpness of the amorphous halo *increase* as the monomer structural model includes more local structural features[55,64-66]. Within the SFC model[55], these features also increase as the chain aspect ratio increases and/or N decreases since local packing is enhanced, although a saturation behavior occurs for sufficiently large Γ and/or N.

The ability to construct coarse-grained models in such a way as to mimic, or reproduce, selected properties of real polymers or atomistic computations is a goal of both computational and conceptual value. Recently, some progress has been made in this direction using PRISM theory[52]. Briefly, in its minimalist implementation the key ideas employed to *select* the parameters of the coarse-grained model are as follows. (1)

Require an identical aspect ratio as the atomistic model or real experimental polymer ; this parameter has been argued to be the primary one in determining the average interchain packing efficiency. (2) Set N equal to the degree of polymerization on a monomer basis. (3) Choose the reduced density such that $\hat{S}(0)$ is equal to the experimental value; part of the motivation here is the intriguing direct connection between $\hat{S}(0)$ and the *local* g(r) suggested by the Gaussian thread analytic results, and empirically verified for more realistic chain model studies. In the initial studies based on the SFC model, a purely hard core interaction has been employed with a common value of d and $l_b/d=0.5$.

The results of this approach as applied to polyethylene are shown in Figure 3.6. Remarkable agreement between the atomistic model g(r) and the SFC g(r) is found. Moreover, even the Gaussian thread result seems reasonable as an "interpolation" through the atomistic g(r). For integrated thermodynamic quantities, such as the cohesive energy density associated with intermolecular attractive forces, remarkably close agreement is found between all three approaches[52].

Generalization of this mapping scheme to polymers of more complex monomer structure, such as polypropylene, also yield promising results[52] for the *chain-averaged* carbon-carbon radial distribution $g_{av}(r)$. Although there will undoubtably be systems and phenomena where such a "pre-averaging" of chemical structure detail will incur significant(and perhaps fatal) errors, such a mapping scheme allows one to construct and study coarse-grained SFC models for a very large number of materials. Thus, this approach has significant potential for making PRISM theory a "molecular design tool" in the sense that many possible materials systems can be quickly studied based on input of a small amount of conformational and related information. This approach has been recently implemented by Schweizer and coworkers with considerable success for understanding and predicting melt solubility parameters and polyolefin blend miscibility[52,69].

B. Multiple-Site Vinyl Polymers

In order to capture the nonspherical nature of monomers for polymers more complicated than polyethylene, one can use additional independent sites to build the monomer structure. An example is shown in Fig. 3.7 for a vinyl polymer. Note that the sites can be overlapping to maintain the correct

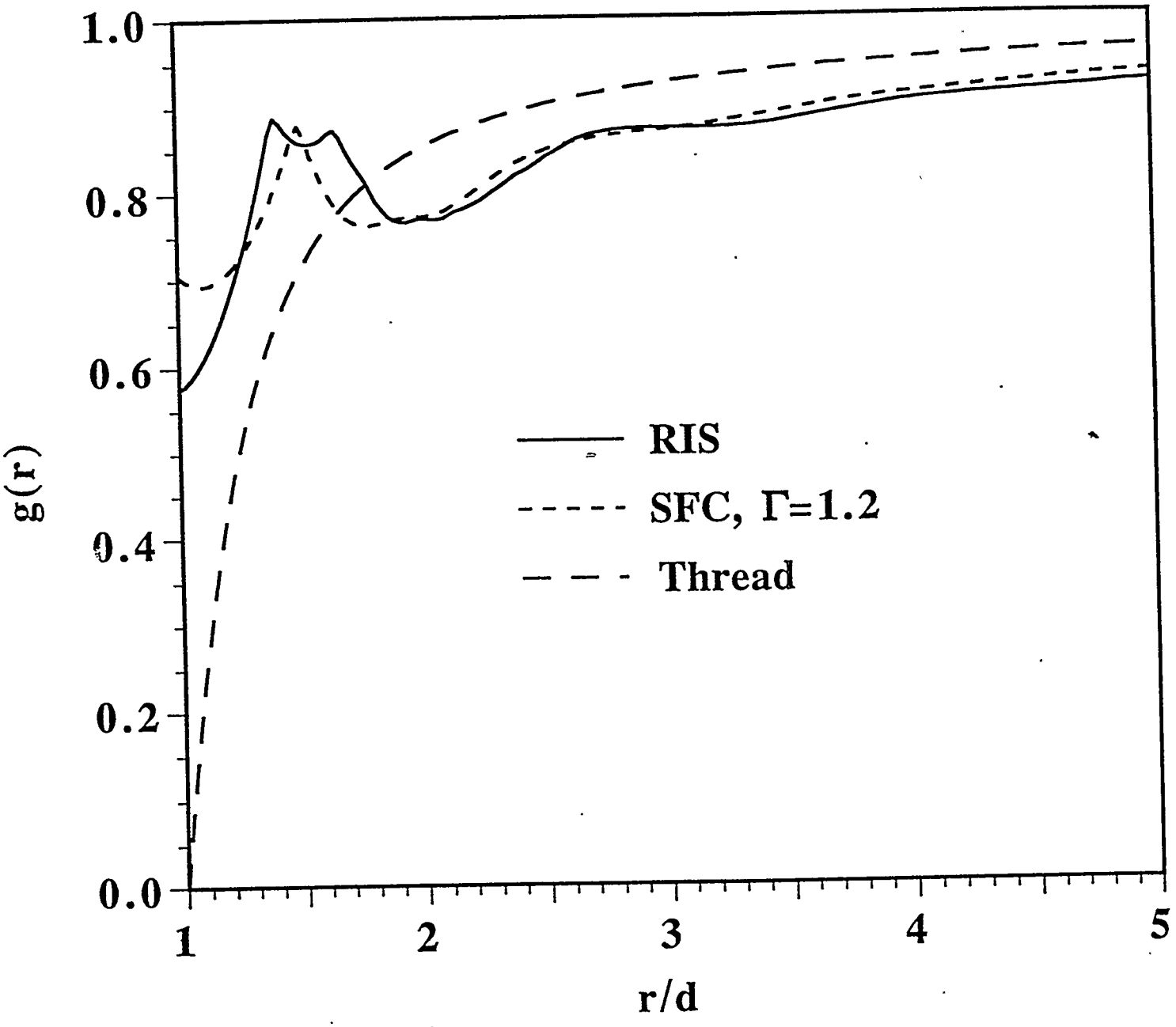

3.6 Predicted interchain radial distribution function for a hard core polyethylene melt described by 3 single chain models : atomistic RIS at 430 Kelvin, overlapping(l/d=0.5) SFC model with appropriately chosen aspect ratio and site number density(see text), and the Gaussian thread model (shifted horizontally to align the hard core diameter with the value of r/d=1).

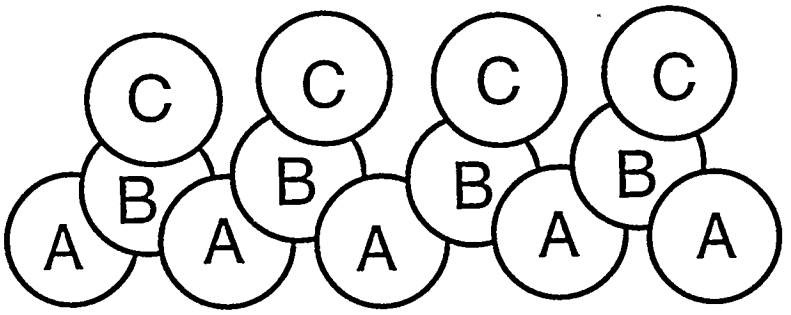

Vinyl Chain

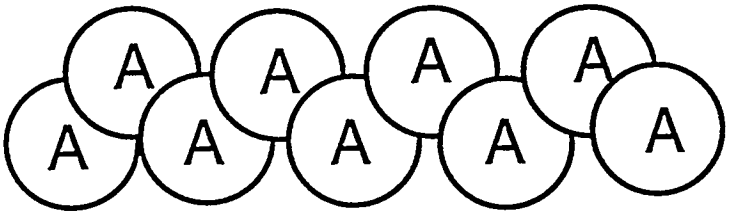

Polyethylene

3.7 Schematic representation of a three site model for describing vinyl polymers contrasted with a one site model for polyethylene.

bond lengths, angles and steric volume of the atoms or groups of atoms making up each site. We use a united atom scheme[26] to construct a vinyl monomer from three independent sites where site A represents a CH_2 group, site B represents a CH group, and site C depicts a side chain substituent. PRISM theory in Eqs. (2.3) - (2.5) now yields six integral equations for the six independent radial distribution functions $g_{AA}(r)$, $g_{BB}(r)$, $g_{CC}(r)$, $g_{AB}(r)$, $g_{AC}(r)$, and $g_{BC}(r)$ which characterize the intermolecular packing.

As a first approximation[26] one can model the vinyl polymer as a freely-jointed, tangent hard sphere chain as depicted on the second line of Figure 3.1. Thus each bond(of fixed length) is completely flexible with each site, including the side group site C, acting as a universal joint. Invoking the Flory ideality hypothesis, the intramolecular structure functions $\hat{\Omega}_{\alpha\gamma}(k)$ in Eq. (2.4) become[26]

$$\hat{\Omega}_{\alpha\gamma}(k) = \tilde{\rho} \sum_{i\in\alpha} \sum_{j\in\gamma} \left[\frac{\sin(kd_{\alpha\gamma})}{kd_{\alpha\gamma}} \right]^{m(i,j)} \tag{3.5}$$

where m(i,j) is the number of bonds between a pair of sites i and j on the same chain. The summations in Eq. (3.5) can be performed in a straightforward manner and are detailed in reference 26.

In reality it is known from computer simulation[51] that the intramolecular excluded volume is not completely screened out in a polymer melt, even at high density. Overall the chains will exhibit ideal scaling with $R_g \sim N^{1/2}$ characteristic of a chain with no long range repulsions, but the chain expands locally due to intramolecular overlaps. This is confirmed in self-consistent calculations[43-47] as discussed in section VIII. In order to quantitatively compare PRISM calculations for the intermolecular structure with computer simulations, it is necessary to compensate for this local chain overlap. This can be accomplished by using the intramolecular structure functions $\hat{\Omega}_{\alpha\gamma}(k)$ obtained from the full many chain simulation. Alternatively one can compute $\hat{\Omega}_{\alpha\gamma}(k)$ from a single chain calculation or simulation in which only local, short range repulsions are included. Figure 3.8 shows selected components of the intramolecular structure factor matrix for vinyl chains of 33 monomers obtained from Monte Carlo simulations of Yethiraj and coworkers[70]. The points are from

3.8 Predictions for two diagonal partial structure factors of vinyl chain melts of 33 monomers. The points are from the multiple chain Monte Carlo simulations of Yethiraj and coworkers[70]. The curves are from single-chain simulations[70] in which repulsive interactions between sites separated more than 2 bonds are screened (set to zero). The BB structure factors are similar to AA and were omitted for clarity.

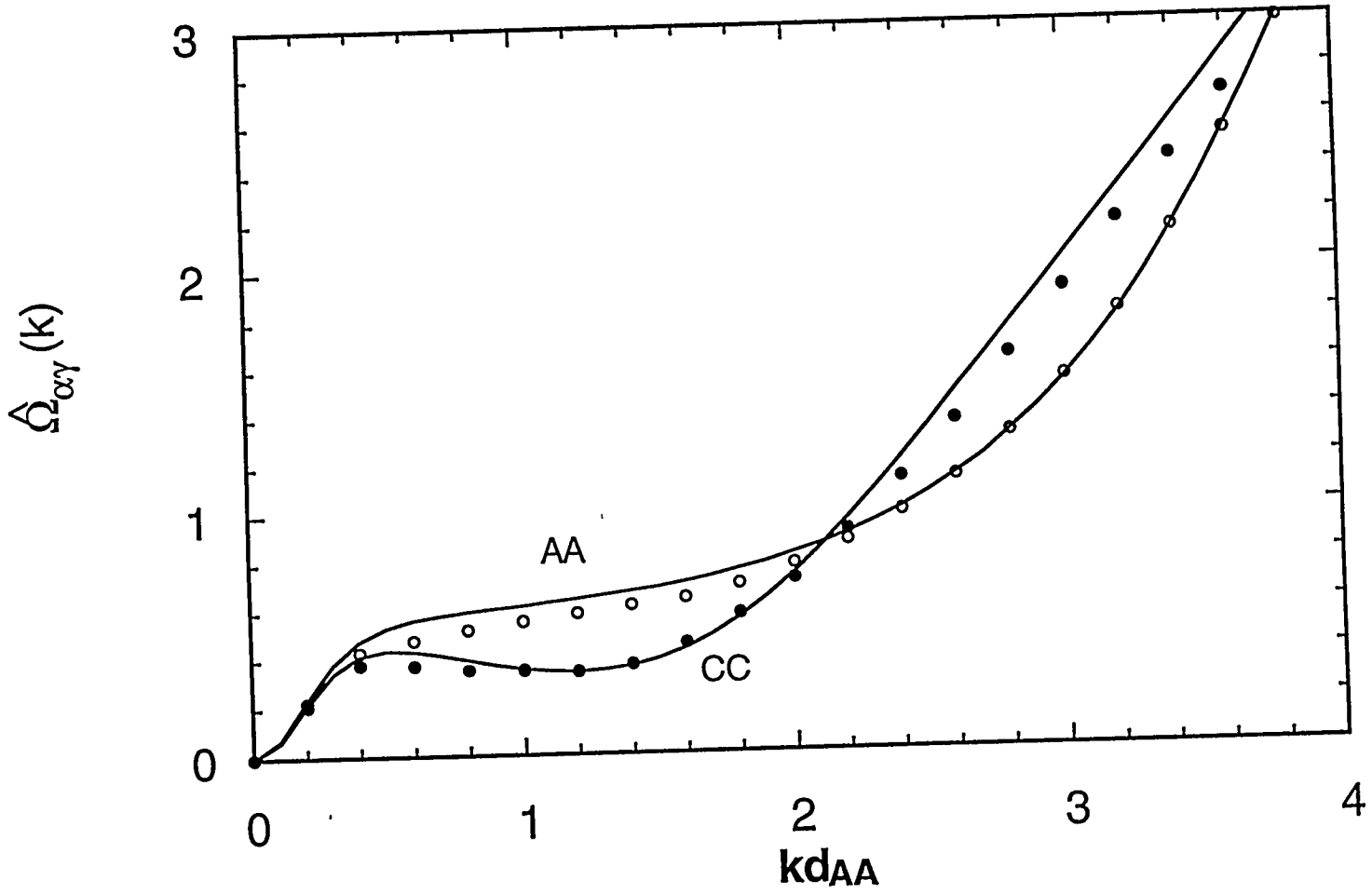

the full, many chain simulation, whereas the curves were obtained from a single chain Monte Carlo simulation in which sites separated by 2 bonds are prohibited from overlapping. Interactions between sites separated by more than two bonds are set to zero based on the physical expectation that long range excluded volume is screened under melt conditions. It can be seen from this figure that the intramolecular structure of a chain, with local repulsions only is an excellent approximation of a chain in a melt.

Using these results for $\hat{\Omega}_{\alpha\gamma}(k)$ as input to PRISM theory, the six coupled equations resulting from Eqs. (2.2) and (2.5) can be solved numerically using a straightforward Picard iteration scheme[26]. The intermolecular packing of vinyl chains of 33 monomers is compared with the simulations of Yethiraj[70] in Figs. 3.9. While the agreement is not quantitative, it can be seen that the PRISM theory certainly captures the essential features of the intermolecular packing. The comparison with simulation in Figs. 3.9 was carried out at a packing fraction characteristic of a concentrated solution(η= 0.35). We anticipate that the agreement between PRISM and theory would improve as the packing fraction increases to η~ 0.5 characteristic of a neat polymer melt.

It is instructive to examine the details of the 6 intermolecular radial distribution functions in Figs. 3.9. Note that on long length scales (R_g~3) all the $g_{\alpha\gamma}(r)$ are essentially identical in the correlation hole regime. This verifies that the local monomer architecture does not affect the packing on intermediate and long length scales. On the other hand, on short length scales near contact, significant local packing differences are seen between the different types of sites making up each monomer. We observe from Fig. 3.9a that $g_{CC}(r)$ is much larger than all the other local correlations. This is a consequence of the fact that the C sites are situated on the outside of the chain and hence can easily approach each other near contact.

By contrast, $g_{BB}(r)$ is small near contact because of screening effects. The B site is located on the chain backbone underneath the C groups and therefore is strongly shielded by the surrounding sites. These qualitative screening ideas[26,70] can be carried further to explain the relative order of all the radial distribution functions near contact: $g_{CC}(d) > g_{AC}(d) > g_{BC}(d) > g_{AA}(d) > g_{AB}(d) > g_{BB}(d)$. Not surprisingly the local packing, characterized by the 6 different $g_{\alpha\gamma}(r)$, is a sensitive function of the detailed monomeric structure. For example $g_{CC}(r)$ is seen[26,70] to

3.9a A comparison of theoretical PRISM predictions (curves) for the radial distribution functions with Monte Carlo simulations (points)[70]. The simulations were performed on vinyl chain melts of N=33 monomers at a packing fraction of 0.35. Note the shielding effects at short distances. The diagonal components AA, BB and CC of the correlation functions are shown.

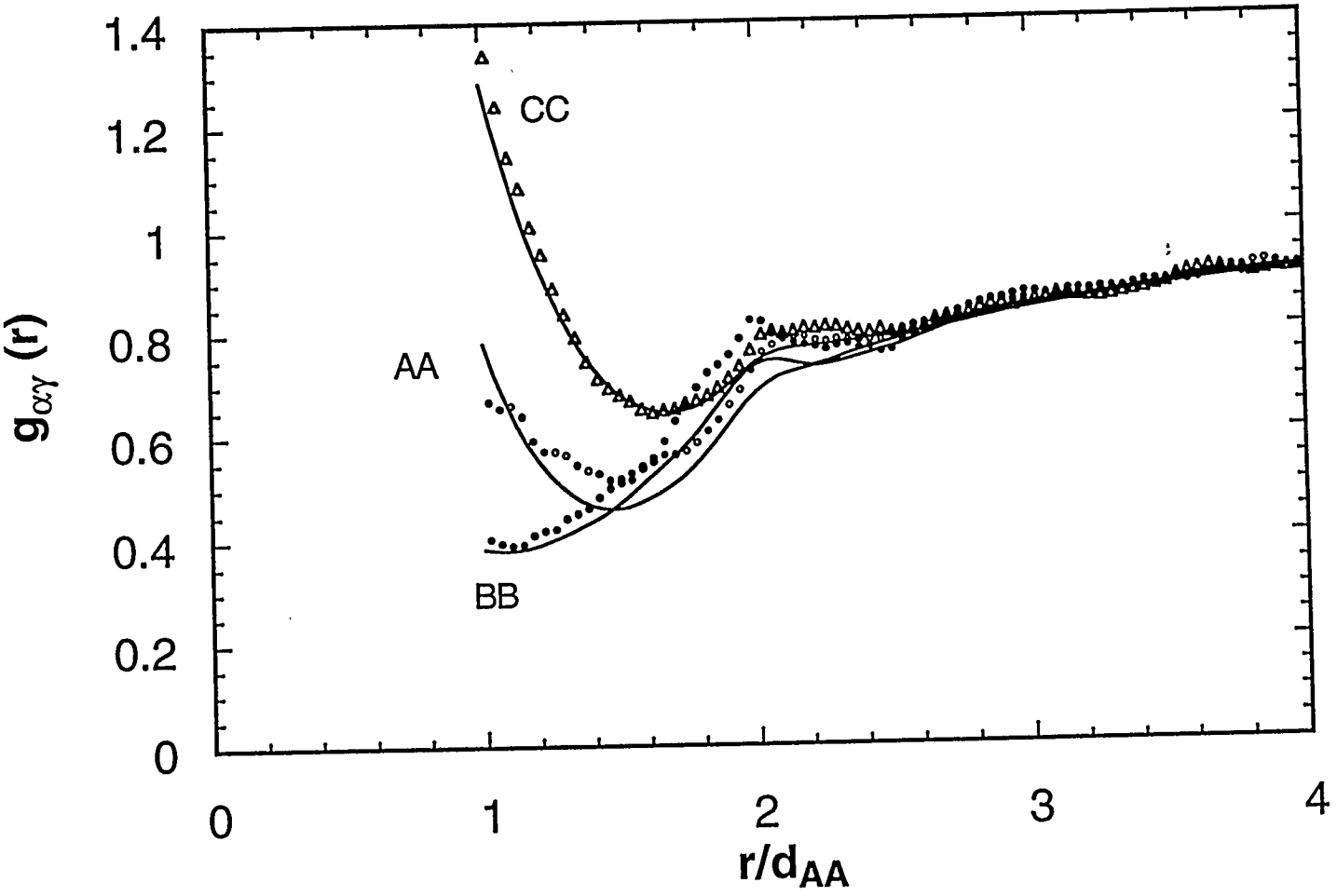

3.9b A comparison of theoretical PRISM predictions (curves) for the radial distribution functions with Monte Carlo simulations (points)[70]. The simulations were performed on vinyl chain melts of N=33 monomers at a packing fraction of 0.35. Note the shielding effects at short distances. The off-diagonal components AB, AC and BC of the correlation functions are shown.

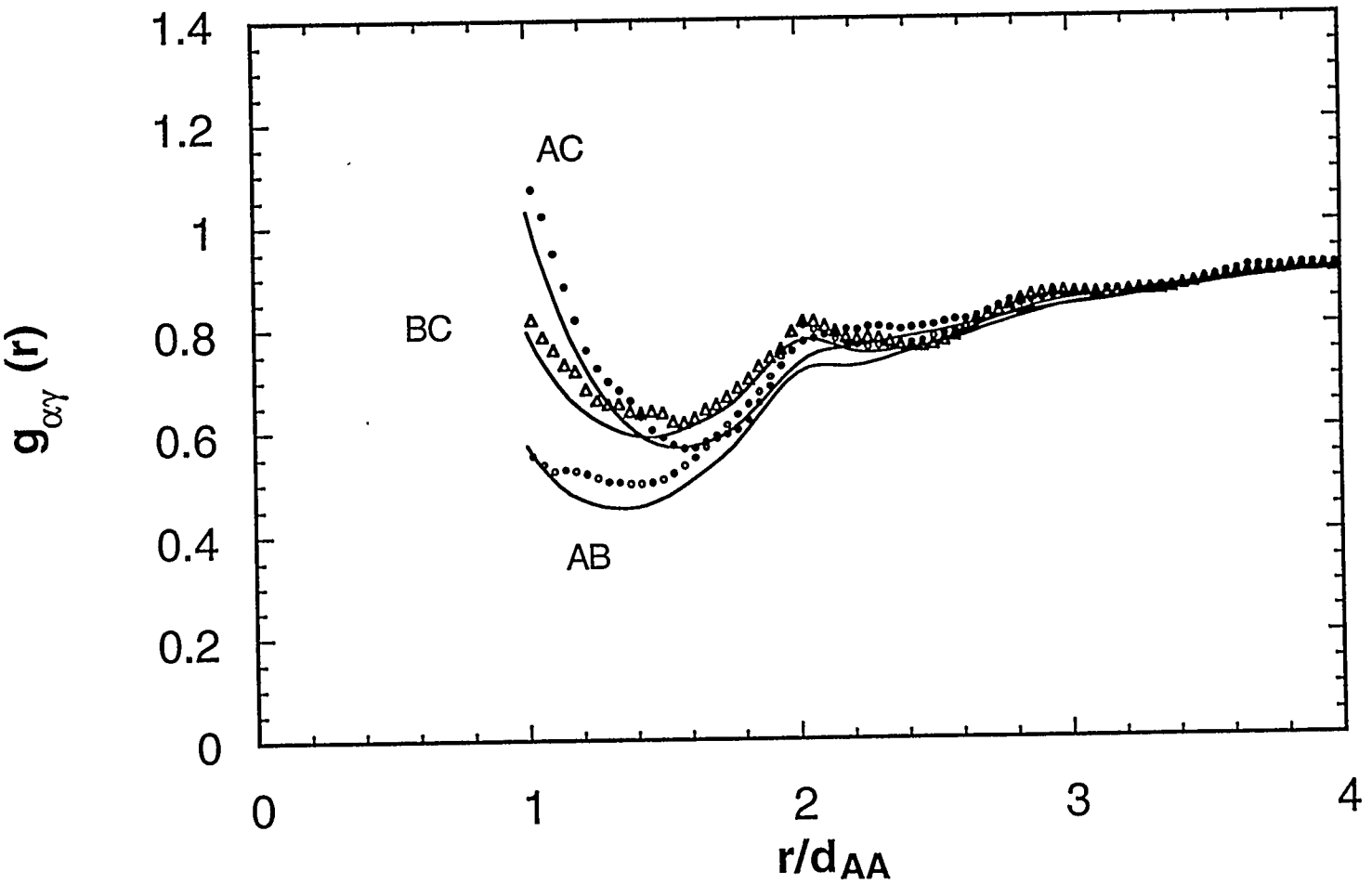

systematically increase near contact when the hard core diameter of the C site is increased. For typical nonpolar van der Waals interactions the attractive interactions between sites are spatially short range. For this reason one expects the local intermolecular packing details are important in determining the thermodynamic properties(e.g., cohesive energy) of the polymer liquid.

The structure of a polymer melt can be probed by x-ray or neutron scattering experiments. The intensity of scattering I(k) is given by

$$I(k) = \sum_{\alpha\gamma} b_\alpha b_\gamma \hat{S}_{\alpha\gamma}(k) \tag{3.6}$$

where b_α is a scattering cross section of species α, and the $\hat{S}_{\alpha\gamma}(k)$ are the partial structure factors making up a structure factor matrix defined analogously to Eq. (3.3)

$$\begin{aligned} \underset{\sim}{\hat{S}}(k) &\equiv \underset{\sim}{\hat{\Omega}}(k) + \underset{\sim}{\hat{H}}(k) \\ &= \left(\underset{\sim}{1} - \underset{\sim}{\hat{\Omega}}(k)\cdot\underset{\sim}{\hat{C}}(k)\right)^{-1} \cdot \underset{\sim}{\hat{\Omega}}(k) \end{aligned} \tag{3.7}$$

The second equality in Eq. (3.7) follows from Eq. (2.2). The summations in Eq. (3.6) run over the ν independent sites making up the monomer. Assuming for the moment that the scattering cross sections of each site are equal, then the scattering intensity of a three site vinyl polymer melt is proportional to the average structure factor defined according to

$$\hat{S}_{av}(k) = \tfrac{1}{9}\sum_{\alpha\gamma} \hat{S}_{\alpha\gamma}(k) \tag{3.8}$$

$\hat{S}_{av}(k)$ is plotted in Fig. 3.10 for a tangent-hard-sphere, freely-jointed chain melt[26] for various diameters d_{CC} of the side group site labeled as C. Note that when there is no side chain group (d_{CC} =0) the vinyl chain reduces to a one site, freely-jointed polyethylene type chain. In this case the main structural feature at low wave vector is seen from Fig. 3.10 to occur at $kd_{AA} \approx 7$ corresponding to the nearest neighbor distance ($\approx 2\pi/k$). When a side group substituent is added, however, a new peak grows in below

3.10 The average total structure factor calculated from PRISM theory for a melt freely-jointed, vinyl chains having N=50 monomers[26]. Each curve was computed for different diameters of the C (side chain) site. The dashed curve (d_C=0.0) refers to a one site, polyethylene-like chain. Note the emergence of a low angle peak at kd_{AA}~1.5-2.0 as the size of the side group is increased.

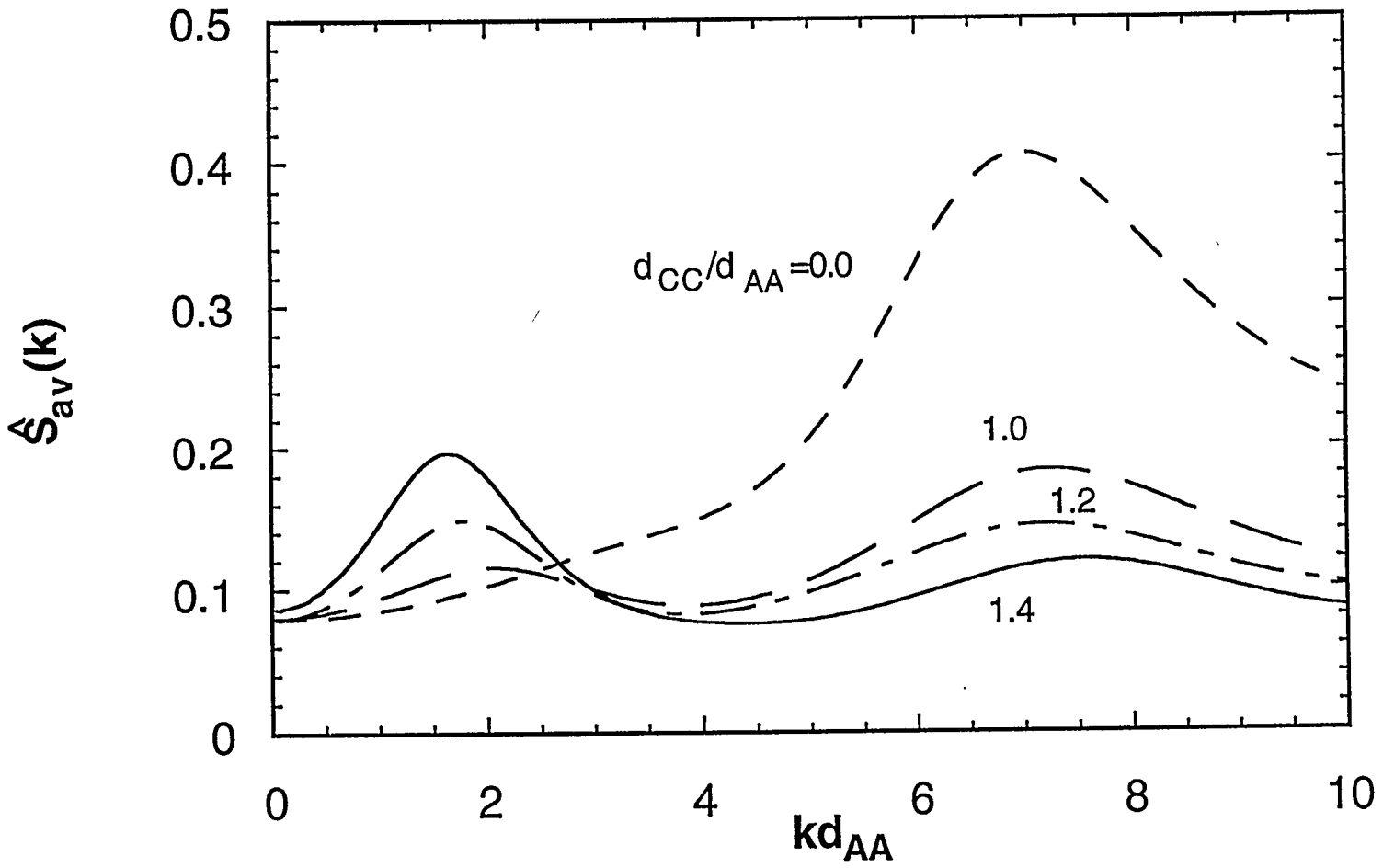

$kd_{AA} \approx 2$. This low angle peak grows in intensity and shifts to smaller wave vectors as the size of the side group increases. Curiously, this low angle feature corresponds to packing distances in real space of approximately 3 hard core diameters. Such a "pre-peak" has been reported for some vinyl polymer melts like polystyrene[71], however, recent x-ray scattering measurements[72] on isotactic polypropylene show no indication of a pre-peak. Examination[26] of the partial structure factors reveals that the pre-peak is arising from relatively long range interchain correlations between backbone carbon centers which are modulated by the presence of the side groups.

It should be emphasized that Fig. 3.10 was calculated for an idealized freely-jointed chain melt in which the site diameter and bond length are the same. In order to make *quantitative* contact with experiments, it is necessary to more faithfully represent the monomer architecture through the intramolecular functions $\hat{\Omega}_{\alpha\gamma}(k)$. A model which captures more of the local chemical structure of real polymer chains is the well known rotational isomeric state model[13]. In order to mimic a chain in a theta solvent or a melt, intramolecular repulsions are included between sites separated by less than or equal to 4 bonds (the "pentane effect")[13].

Detailed PRISM calculations[32] were performed by Rajasekaran, Curro and Honeycutt on the stereochemically regular *isotactic* polypropylene (i-PP) of N=200 monomers employing the rotational isomeric state model of Suter and Flory[73] to compute the required $\hat{\Omega}_{\alpha\gamma}(k)$. The characteristic ratio of a linear chain is defined as $C_\infty = \langle R^2 \rangle / N_b \, l_{cc}^2$, where N_b is the number of backbone carbon-carbon bonds of length l_{cc} . According to the Suter - Flory rotational isomeric state calculation for i-PP, $C_\infty \cong 4.0$ at 473 K. SANS measurements[74], however, indicate that $C_\infty = 6.2$ for i-PP in the melt state. In order to compensate for this discrepency in chain dimensions, the rotational state energies (or equivalently the temperature T=286 K) was rescaled to obtain the experimental C_∞. Although the moments of the distribution can be computed in closed form, the single chain structure functions cannot be computed analytically for the rotational isomeric state model. Thus, a Monte Carlo simulation of a single chain was employed to obtain the six functions $\hat{\Omega}_{\alpha\gamma}(k)$.

The six intermolecular radial distribution functions for i-PP were then deduced from PRISM calculations using the single chain simulation results as input. The diagonal correlation functions are shown in Fig. 3.11a, and the off-diagonal components are given elsewhere[32]. It can be seen that the i-PP correlation functions are qualitatively similar to the idealized chain results in Figs. 3.9. An interesting feature of the BB radial distribution function for the atomistically realistic model is that because of shielding effects, and the added constraints of the local chain architecture, $g_{BB}(r)$ approaches zero at a distance greater than the $d_{BB} = 3.9$ Angstrom hard core diameter. In other words, because of local steric constraints, the CH sites on different chains are restricted from coming into direct contact.

The resulting x-ray scattering pattern of the i-PP melt was found to be in some disagreement with the wide angle scattering measurements of Habenschuss and Londono[72] in the region $k \approx 1\ A^{-1}$. This led Curro and coworkers[75] to introduce further realism into the single chain structure by performing single chain Monte Carlo simulations in which the internal rotational angles ϕ were allowed to vary in a continuous manner. This additional realism in the local chain architecture leads to excellent agreement with scattering measurements on i-PP melts, as discussed elsewhere[75].

A comparison at *fixed* liquid packing fraction of the *chain-averaged* carbon-carbon radial distribution function, $g_{av}(r)$, for polyethylene ($C_\infty \cong 7$), isotactic polypropylene(with 2 values of C_∞), and syndiotactic polypropylene are shown in Figure 3.11b[52]. The polymers i-PP and s-PP are regular multiple site homopolymers of different stereochemistry and significantly different characteristic ratios($C_\infty \cong 10.5$ for s-PP) . The clear differences among all the systems demonstrates the sensitivity of local packing in polymer melts to monomer shape, stereochemistry or tacticity, and backbone stiffness. Finally, as discussed in depth elsewhere, the l_b/d=0.5 SFC model of section B reproduces the structural variations quite well based on the effective aspect ratio mapping idea[52].

C. Thermodynamics

Having determined the structure of the polymer liquid, it is in principle possible to compute most thermodynamic properties of interest[5,8]. Whereas the structure or radial distribution functions at liquid density are

3.11a PRISM predictions for hard core atomistic RIS models of polyolefins. The 3 diagonal radial distribution functions of isotactic polypropylene[32].

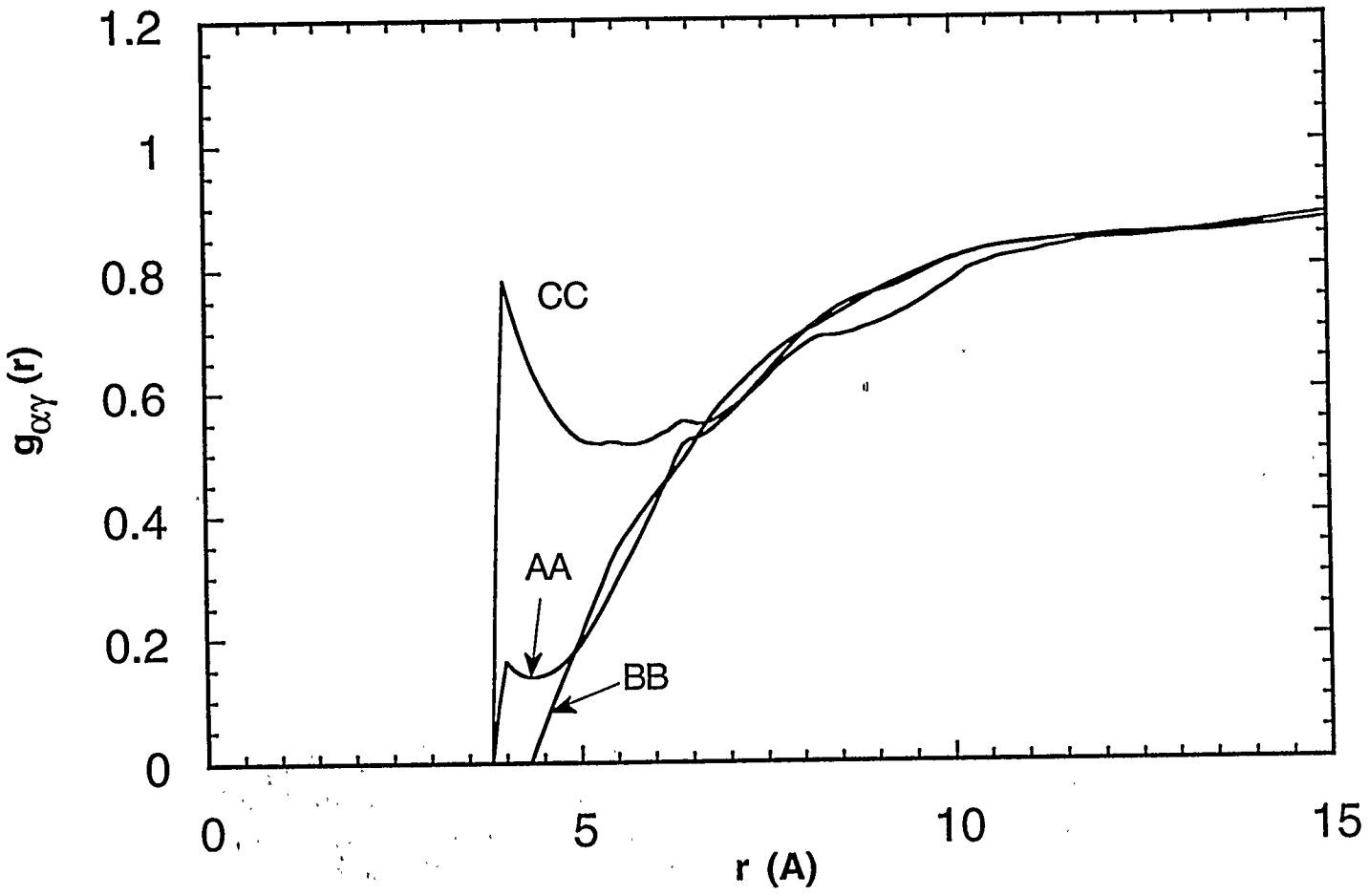

3.11b PRISM predictions for hard core atomistic RIS models of polyolefins. A comparison of chain *averaged* site-site radial distribution functions at 473 Kelvin for N_b =400 models of polyethylene, isotactic polypropylene, and syndiotactic polypropylene[52]. The characteristic ratio of the RIS models employed for PP are shown in parenthesis.

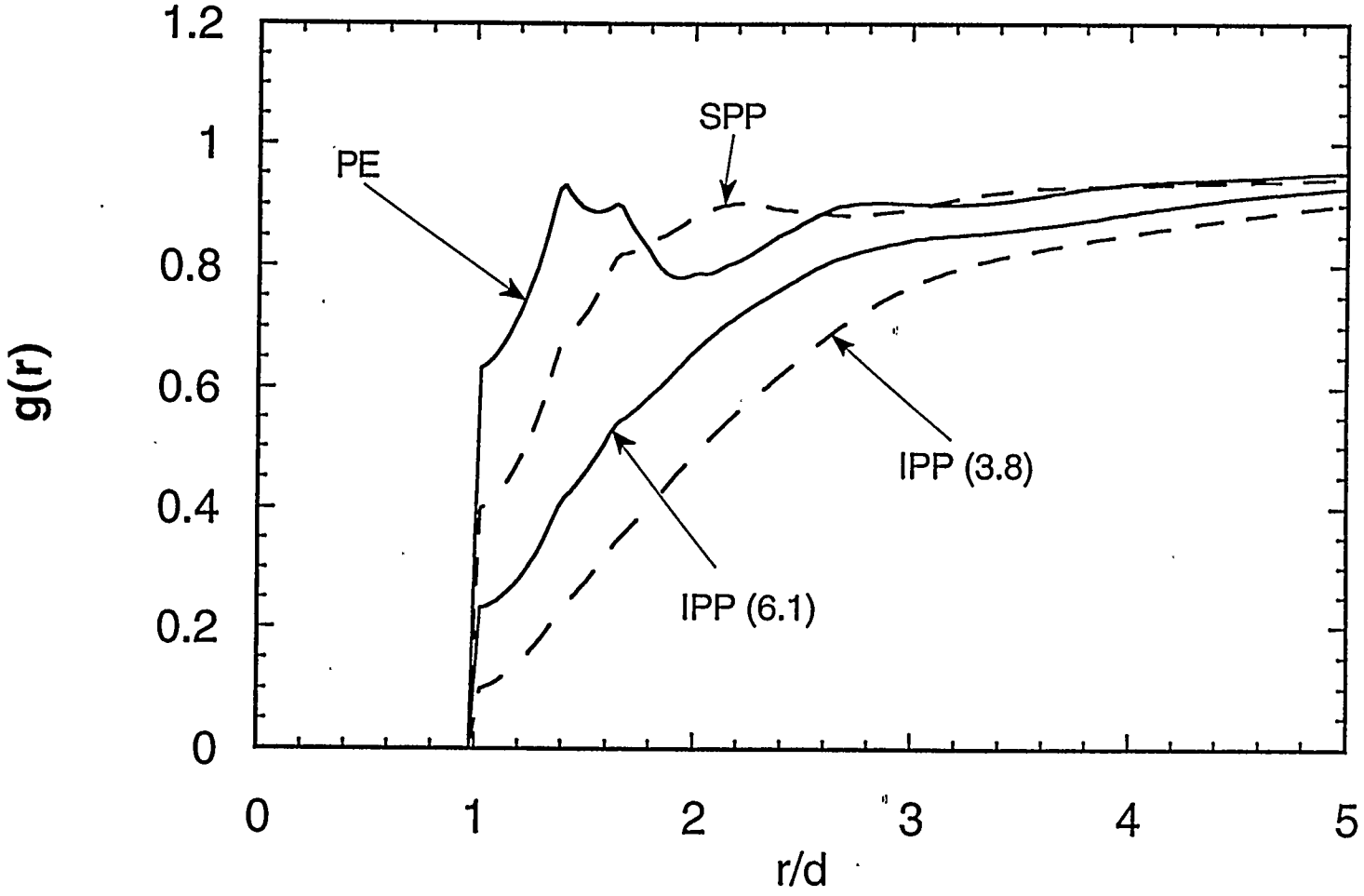

primarily controlled by the repulsive part of the intersite potentials, thermodynamic quantities will also be sensitive to the attractive potentials. In the case of a one component melt, thermodynamic quantities of interest include the pressure P, isothermal compressibility κ, and the internal or cohesive energy U. Since in general one theoretically knows g(r) only approximately, the thermodynamic properties derived from the structure will be approximate. Moreover, integral equation theory leads to *thermodynamically inconsistent* results in the sense that the predictions depend on the particular thermodynamic route used to relate the thermodynamic quantity to the structure[5,8].

1. Equation-of-State

Thermodynamic inconsistency is particularly apparent for the pressure of polymer fluids[67]. There are at least three routes which relate the pressure to the structure. Perhaps the easiest method to implement is the so-called "compressibility route" :

$$\frac{P}{\rho_m k_B T} = \int_0^{\rho_m} \frac{d\rho}{\hat{S}_{av}(0)} \tag{3.9a}$$

where $\rho_m^2 k_B T \kappa = \hat{S}_{av}(0)$. The analog of the virial route of monatomic liquids for the pressure of a molecular liquid is the "free energy charging formula". For hard core potentials one can write[5,8]

$$\frac{F - F_o}{V k_B T} = 2\pi\rho_m^2 \sum_{\alpha\gamma} d_{\alpha\gamma}^3 \int_0^1 g_{\alpha\gamma}^{(\lambda)}(\lambda d_{\alpha\gamma})\lambda^2 d\lambda \tag{3.9b}$$

where $g_{\alpha\gamma}^{(\lambda)}(\lambda d_{\alpha\gamma})$ is the contact radial distribution function for a hard core diameter $\lambda d_{\alpha\gamma}$. F and F_o are the Helmholtz free energies of the fluid of interest and a corresponding ideal gas, respectively. In Eq. (3.9b) the hard core diameter is turned on as the "charging parameter" λ changes from 0 to 1. The pressure follows from differentiation of F with respect to volume.

Yethiraj and coworkers[67] calculated the hard core contribution to the equation-of-state of polyethylene by various thermodynamic routes using PRISM theory. It can be seen from the results plotted in Fig. 3.12 that very large differences are found between the compressibility and charging

3.12 The hard sphere equation-of-state (d=3.9 A) as a function of reduced fluid density computed[67] for polyethylene at T=430 K and N=6429 by various thermodynamic routes: free energy (upper solid), compressibility (lower solid), wall (dashed), and GFD (dot/dash). The inset includes attractions by perturbation theory using the GFD curve as the reference system.

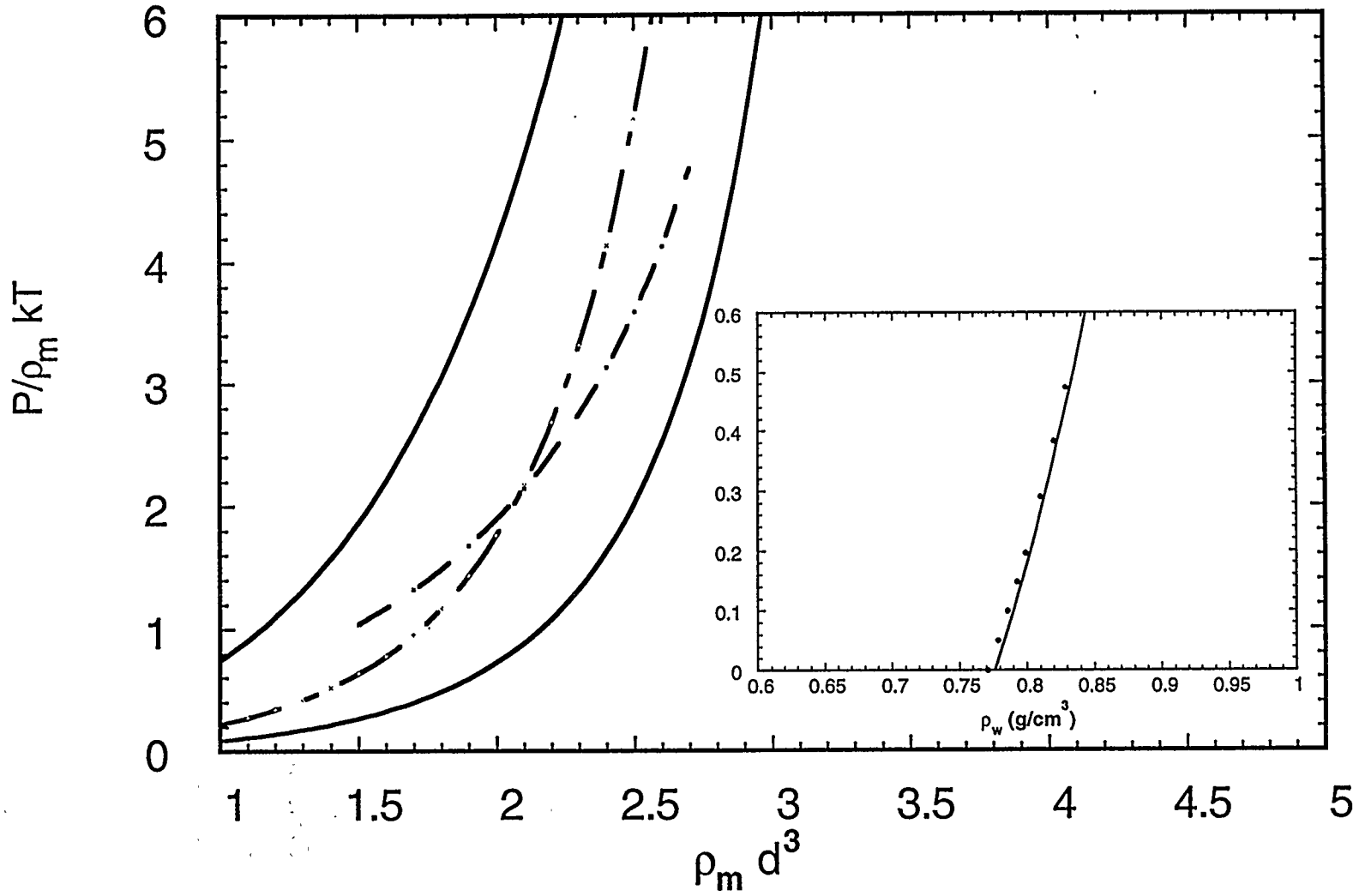

routes. Qualitatively similar results are seen for ethane and n-butane[67], however, the thermodynamic inconsistency appears to increase significantly with N. One contributing reason for this large, N-dependent thermodynamic inconsistency is traceable to the fact that RISM theory[7,8], unlike the PY theory[5] for atomic liquids, is not exact in the low density limit. Both Eqs. (3.9a) and (3.9b) effectively integrate the structure of the fluid over the complete range of density. A route which uses only structural information at liquid-like density, where RISM theory is accurate, might produce better results.

Based on an argument by Percus[76], another route to the pressure was proposed by Dickman and Hall[77] making use of the density of sites in a nonuniform molecular liquid at a hard wall $\rho_w(0)$:

$$P = \rho_w(0) k_B T \tag{3.9c}$$

Yethiraj and Hall[78] developed a "wall PRISM" theory to compute $\rho_w(0)$. The wall PRISM theory prediction for hard sphere polyethylene is also shown in Fig. 3.12. It can be seen that pressures intermediate between the charging and compressibility route predictions are found.

Also plotted in Fig. 3.12 is the predictions of a statistical thermodynamic approacg : the generalized Flory dimer equation-of-state (GFD) of Dickman, Hall and Honnell[79] suitably modified by Yethiraj and coworkers to rotational isomeric state chains of overlapping sites[67]. Monte Carlo studies[79] have documented the accuracy of the GFD equation-of-state for chain molecule liquids at high densities. It can be seen from Fig. 3.12 that the wall PRISM and GFD predictions for hard core polyethylene chains are in reasonable accord at densities $\rho_m d^3 \sim 2$ characteristic of polyethylene melts. It can be seen from the slopes of the curves, however, that the isothermal compressibility from wall PRISM calculations is somewhat higher than from the GFD model. Recently density functional theory has been combined with PRISM theory by McCoy and coworkers[80] as an alternative to wall PRISM in computing the density profile of sites near a wall. This approach avoids the wall-PRISM assumption of intramolecular chain ideality in the vicinity of the wall. Preliminary calculations[80] for the pressure by this approach are in close agreement with corresponding GFD calculations. Direct comparisons of PRISM predictions for the equation-of-

state of hard core n-alkane fluids with simulations have been recently carried out by Yethiraj[81a], and for the interchain structure by Dodd and Theodorou[81b].

Although the intermolecular packing of a dense polymeric melt is generally believed to be controlled by the repulsive part of the potential, attractions will have a strong influence on the equation-of-state. The conceptually and computationally simplest way to incorporate the effects of attractions on the pressure is through thermodynamic perturbation theory[5] about a hard core reference system. For convenience we employ the Barker - Henderson[5,82] version of perturbation theory in which the intersite Lennard-Jones potential v(r) is divided into a repulsive branch $v_0(r)$ and an attractive branch $v_a(r)$.

$$v(r) = 4\varepsilon\left[(\sigma/r)^{12} - (\sigma/r)^{6}\right] \tag{3.10}$$

$$v_0(r) = v(r); \quad r \le \sigma$$
$$= 0; \quad r > \sigma$$

$$v_a(r) = 0; \quad r \le \sigma$$
$$= v(r); \quad r > \sigma$$

The Helmholtz free energy can then be written to first order as

$$\frac{F}{k_B T} = \frac{F_{HS}}{k_B T} + \tfrac{1}{2}\rho_m^2 \int \frac{v_a(r)}{k_B T} g_o(r) d\vec{r} + \ldots \tag{3.11}$$

where F_{HS} and $g_o(r)$ are the free energy and intermolecular radial distribution function of the corresponding hard core reference system. Eq. (3.11) is written for a single site monomer but is easily generalized to monomers consisting of multiple sites. The pressure is then found by differentiation of Eq. (3.11) with respect to volume. The optimum diameter d of the hard core reference system is given by

$$d = \int_0^\infty \left\{1 - \exp\left[-v_0(r)/k_B T\right]\right\} 4\pi r^2 dr \tag{3.12}$$

Any of the four hard core equation-of state-curves in Fig. 3.12 could be used in conjunction with Eq. (3.11) to obtain the pressure of a polyethylene melt at any desired temperature. The method which appears to be most

accurate is to use the GFD equation-of-state for the reference system and PRISM theory for the structure $g_0(r)$ of the reference system. The results[67] of this procedure are shown in the inset of Fig. (3.12) along with experimental PVT data of Olabisi and Simha[83]. In calculating the polyethylene pressure curve the hard core diameter d was maintained at 3.9 A in order to be consistent with x-ray scattering measurements[64,66] on polyethylene at 430 K. The Lennard-Jones well depth parameter was then adjusted in order to *fit* the experimental data ; this procedure yields ε/k_B = 38.7 K, which fixes σ = 4.36 Angstrom according to Eq(3.12). It can be seen from the inset in Fig. 3.12 that excellent agreement is obtained with experiment. However, this approach is not completely satisfying since PRISM theory is not used for the equation-of-state of the reference system. On the other hand, the simulation studies of Yethiraj and Hall have shown that the use of the PRISM theory $g_0(r)$ leads to an accurate prediction of the attractive potential contribution to the pressure *within* a perturbative HTA framework.[84]

Reasonable *ab initio* results have also been obtained for the thermal expansion coefficient and isothermal compressibility($\hat{S}(k=0)$) of polyethylene melts[52,67]. The latter was computed using the experimental T-dependent density, and the assumed dominance of soft repulsive forces. The resulting $\hat{S}(0)$ was found to be roughly 20% larger than the experimental values, although excellent agreement was obtained for the relative temperature dependence[52] over the entire experimental range of T = 380 - 525 Kelvin.

Finally, analytic predictions for the osmotic pressure of polymers in good and theta solvents can be derived based on the Gaussian thread model, PRISM theory, and the compressibility route[30]. The qualitative form of the prediction for large N is[54] : $\beta P \propto (\rho\sigma^2)^3$, which scales as ρ^3 for theta solvents and $\rho^{9/4}$ for good solvents. Remarkably, these power laws are in complete agreement with the predictions of scaling and field theoretic approaches, and also agree with experimental measurements in semidilute polymer solutions[2-4].

2. Melt Solubility Parameters

The internal or cohesive energy density U is also a useful thermodynamic parameter for polymer melts. It is defined as[85]

$$U = \frac{1}{V^2}\sum_{\alpha\gamma}\rho_\alpha\rho_\gamma\int v^a_{\alpha\gamma}(r)g_{\alpha\gamma}(r)d\vec{r} \qquad (3.13a)$$

where the integration is carried out over the attractive branch of the potential in Eq. (3.10). In first order perturbation theory the radial distribution function is approximated by its reference hard core melt value $g^o_{\alpha\gamma}(r)$ thereby yielding

$$U \cong \frac{1}{V^2}\sum_{\alpha\gamma}\rho_\alpha\rho_\gamma\int v^a_{\alpha\gamma}(r)g^o_{\alpha\gamma}(r)d\vec{r} \qquad (3.13b)$$

In the absence of correlations, or the random mixing limit,the radial distribution functions are all unity. In this "mean field" limit the cohesive energy density reduces to : $U_{MF} = \frac{-32}{9}\pi\varepsilon\rho_m^2\sigma^3$ for the Lennard-Jones potential.

The melt solubility parameter δ can be computed from[85]

$$\delta = \sqrt{-U} \qquad (3.14)$$

For small molecule liquids δ can be measured directly from the heat of vaporization. For polymer melts the solubility parameter can only be indirectly estimated from solubility data in various solvents[86], group contribution tables[87], or model-dependent fitting of PVT measurements[88].

The cohesive energy density for polyethylene as a function of temperature has been computed from Eq. (3.13b)[52]. In agreement with experiment, $|U|$ was found to decrease nearly linearly with temperature[89]. This trend arises from the fact that the correlation hole of polyethylene deepens as the temperature is increased due to the combined effects of decreased density, and an increase in the number of gauche states of the polyethylene chain backbone(see Fig. 3.4). The magnitude of the predicted solubility parameter is in good agreement with experimentally inferred values for polyethylene in the range 15 - 19 $(J/cm^3)^{1/2}$ based on PVT measurements[45] and group contributions[87].

The cohesive energy of isotactic polypropylene has also been calculated from Eq. (3.13a) using the intermolecular structural information in Fig. 3.11 for the hard core system. The united atom Lennard-Jones potentials of

Jorgensen and coworkers[90] for CH_2, CH, and CH_3 groups with $\sigma \equiv \sigma_{\alpha\gamma}$ were employed, along with appropriate values for the CH_2 group well depth energy $\varepsilon \equiv \varepsilon_{AA}$ and relative values for the CH_3 and CH groups of

$$\lambda_1 = \sqrt{\varepsilon_{CC}/\varepsilon_{AA}}\ , \quad \lambda_2 = \sqrt{\varepsilon_{BB}/\varepsilon_{AA}} \tag{3.15}$$

Based on the Jorgenson parameters[90], the relative solubility parameter is predicted[52] to be $\delta_{PE}/\delta_{IPP} = 1.24$. If as a simplfying approximation one sets $\lambda_1 = \lambda_2 = 1$ then $\delta_{PE}/\delta_{IPP} = 1.26$ is predicted[52]. These predicted ratios are in good agreement with $\delta_{PE}/\delta_{IPP} = 1.20$ inferred by Rodgers et. al.[88] from equation-of-state data for isotactic polypropylene. For the case of syndiotactic polypropylene one finds[52] that $\delta_{PE}/\delta_{SPP} = 1.07$ under the assumption $\lambda_1 = \lambda_2 = 1$. Thus, polypropylene is predicted to have a smaller solubility parameter than polyethylene because of differences in packing on local length scales(see Figure 11b).

Schweizer and coworkers[52] have estimated the cohesive energy of a range of polymers of varying chain architecture using both the single-site semiflexible chain model, and the analytic Gaussian thread model. Model calculations of the reduced solubility parameter are shown in Figure 3.13. As discussed in section II.B.2, for experimental applications a system-specific effective aspect ratio was employed to map the semiflexible chain model to a particular polymer of interest. As described in detail elsewhere[52], the relative solubility parameters computed with the SFC approach are in good agreement with the atomistic values quoted above for both polyethylene and the various tacticities of polypropylene. Moreover, predictions for many other hydrocarbon polymer melts have also been made and compared with experimental solubility parameters[87,88,91]. Good agreement is found which provides a simple understanding of how local polymer structure influences melt solubility parameters[52].

The Gaussian thread model, in conjunction with a Yukawa form for the attractive interchain potential of spatial range a :

$$v(r) = -\varepsilon a \frac{e^{-r/a}}{r}, \quad \varepsilon > 0 \tag{3.16}$$

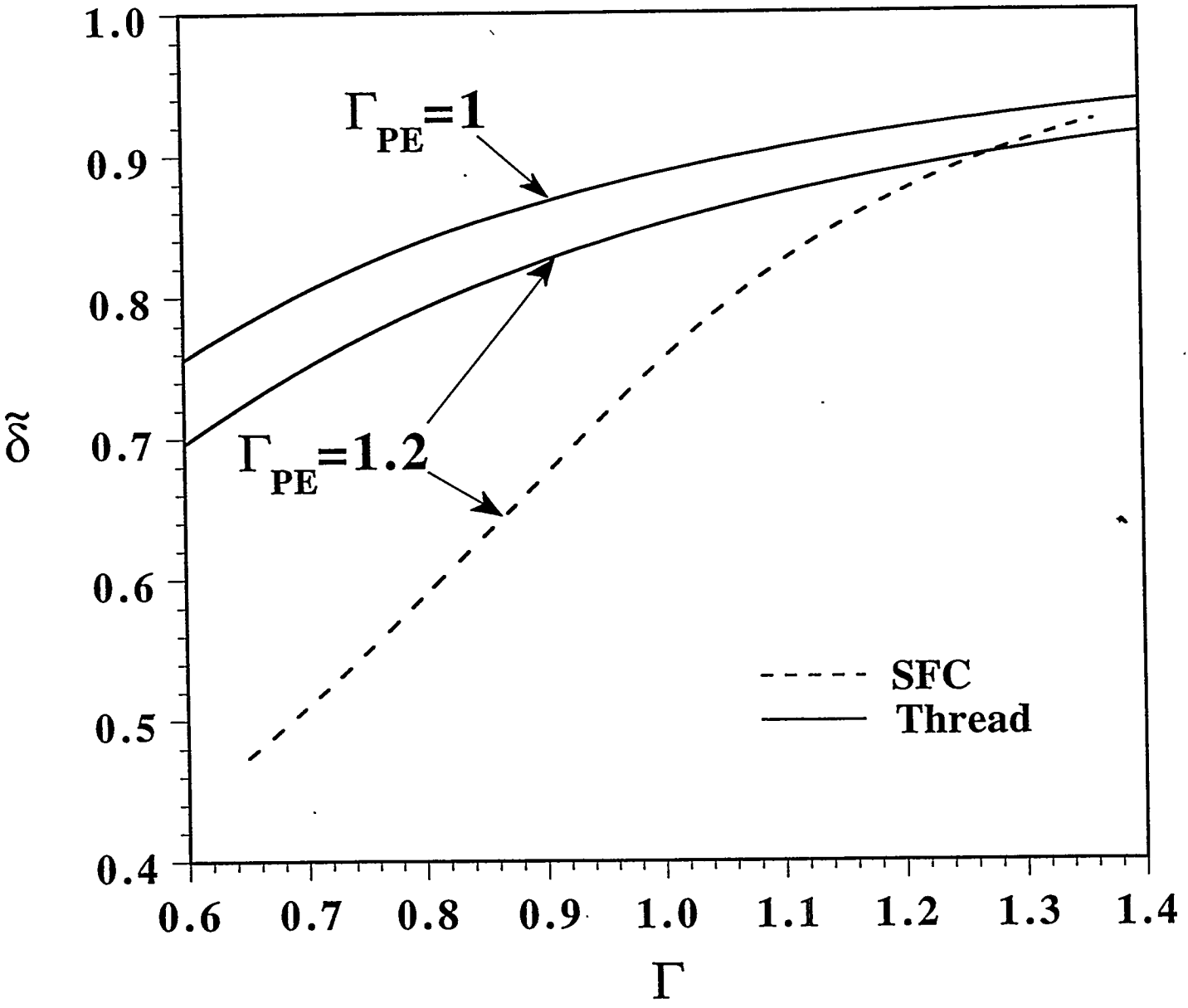

3.13 Reduced solubility parameter as a function of chain aspect ratio for the l/d=0.5 SFC model and the analytic Gaussian thread model[52]. Two choices of polyethylene aspect ratio at 430 Kelvin are shown. The liquid density is determined by the calibration procedure discussed in ref.52.

yields a simple analytic expression for the reduced solubility parameter. The result can be written in several alternative, but equivalent , forms[52]

$$\tilde{\delta} = \frac{1}{\sqrt{1+\frac{3}{\pi\rho_m\sigma^2 a}}} = \frac{1}{\sqrt{1+\frac{\sigma}{a}\sqrt{\frac{\hat{S}(0)}{12}}}} = \frac{1}{\sqrt{1+\frac{d}{2a\eta}\Gamma^{-2}}} \qquad (3.17)$$

This form is plotted in Figure 3.13 for two experimentally relevant choices[52] of the parameter d/2aη. The prediction of a direct connection between polymer density, aspect ratio(or packing length $(\rho_m\sigma^2)^{-1}$), and spatial range of the attractive potential is intuitively reasonable. Eq(3.17) has been shown by Lohse to provide an excellent representation of experimentally deduced solubility parameters of polyolefin melts[92].

As a cautionary remark, we note that significant quantitative differences between the SFC and Gaussian thread model predictions are evident in Figure 3.13. These differences are not surprising, and reflect the poorer local packing of Gaussian threads relative to semiflexible chains. These differences also highlight the potential subtleties of the proposed mapping schemes, i.e. the need to separately "calibrate" the different coarse-grained model parameters against experimental data or atomistic PRISM computations[52].

IV. ATHERMAL POLYMER BLENDS

Mixtures of polymers, or "blends", are of major scientific and materials engineering interest.[93-95] Moreover, the phase behavior of high polymer blends is very subtle due to the enormous reduction of the ideal(combinatorial) entropy of mixing due to chain connectivity.[1] "Athermal" blends are defined to be mixtures of two or more polymer components for which the heat of mixing is zero. An example of such a blend is one in which all intermolecular site-site interactions are entirely repulsive hard core in nature. Although athermal blends do *not* exist in reality, their behavior is important from a theoretical point of view. Based on studies of atomic[5,11] and small molecule liquids[8] the structure of one-component liquids at high density is believed to be primarily determined by

the repulsive part of the potential. This suggests that a useful strategy for describing general polymer blend thermodynamics might be to treat the attractive interactions by a perturbation expansion about an athermal reference system. Thus the problem of determining the intermolecular packing in athermal polymer blends is a fundamental one and forms the basis of the simplest conceivable general blend theory. In addition, the role of excess entropic effects on mixing, and possible athermal phase separation, are questions of basic statistical mechanical interest.

The well known mean field incompressible Flory-Huggins theory[1] of polymer mixtures assumes random mixing of polymer repeat units. However, it has been demonstrated that the radial distribution functions $g_{\alpha\gamma}(r)$ of polymer melts are sensitive to the details of the polymer architecture on short length scales. Hence, one expects that in polymer mixtures the radial distribution functions will likewise depend on the intramolecular structure of the components, and that the packing will not be random. Since by definition the heat of mixing is zero for an athermal blend, Flory-Huggins theory predicts athermal mixtures are ideal solutions which exhibit complete miscibility.

In this section we examine athermal binary mixtures using PRISM theory. Tests of both the structural and thermodynamic predictions of PRISM theory with the PY closure against large scale computer simulations are discussed in section A. Atomistic level PRISM calculations are presented in section B, and the possibility of nonlocal entropy-driven phase separation is discussed in section C at the SFC model level. Section D presents analytic predictions based on the idealized Gaussain thread model. The limitations of overly coarse-grained chain models for treating athermal polymer blends are briefly discussed.

A. Comparison with Computer Simulations

An important question is whether PRISM theory can predict the packing in athermal blends with the same good accuracy found for one-component melts. To address this question Stevenson and coworkers[96] performed molecular dynamics simulations on binary, repulsive force blends of 50 unit chains at a liquid-like packing fraction of η=0.465. The monomeric interactions were very similar to earlier one-component melt simulations by Grest and Kremer[51], which served as benchmark tests of

melt PRISM theory. Nonbonded pairs of sites (both on the same and different chains) were taken to interact via shifted, purely repulsive Lennard-Jones potentials. These repulsive potentials were adjusted so that the effective hard site diameters, obtained from Eq. (3.12), were $d_{AA} = 1.015$ and $d_{BB} = 1.215$ for the chains of type A or B respectively. Chain connectivity was maintained using an intramolecular FENE potential[51] between bonded sites on the same chain. The resulting chain model has nearly constant bond lengths which are nearly equal to the effective hard core site diameter.

The three intermolecular radial distribution functions $g_{AA}(r)$, $g_{AB}(r)$, $g_{BB}(r)$ in the blend were obtained from the simulation as a function of the concentration. Corrections were made for finite size effects in the simulation[96]. Likewise, the intramolecular structure factors $\hat{\Omega}_{AA}(k)$ and $\hat{\Omega}_{BB}(k)$ were obtained from the simulation and used as input for PRISM calculations on the athermal blend. In the PRISM calculation the PY closure of Eq(2.5a) was used for the same soft repulsive potentials as in the simulation. A comparison between the results from the molecular dynamics simulation and PRISM theory is shown in Fig. 4.1 for the case of volume fraction of A chains $\phi = 0.368$. Although deviations are seen at small distances, overall the agreement is quite good and comparable to similar studies[51,60] done earlier on one-component polymer melts(see Fig. 3.3). Similar agreement was found at other blend concentrations[96].

The simulations of Stevenson and coworkers allow a direct test of the random mixing approximation. Strictly speaking, at the structural level the random mixing approximation in its polymeric Flory-Huggins form[1] implies that all the radial distribution functions in the mixture are identically unity, $g_{\alpha\gamma}(r) = 1$. As can be seen from Fig. 4.1 this is obviously a poor approximation. A less restrictive definition of random mixing might be that the packing is the same for both species in the blend, in other words all the $g_{\alpha\gamma}(r)$ are the same. We can probe this approximation by defining an excess correlation function $\Delta g(r)$ based on the differences in radial distribution functions between species.

$$\Delta g(r) = g_{AA}(r) + g_{BB}(r) - 2g_{AB}(r) \tag{4.1}$$

4.1 A comparison between PRISM theory and the MD simulations[96] for the radial distribution functions in an athermal blend of 50 unit chains. The composition was maintained at f=0.368. The points are the simulations and the curves are the PRISM predictions.

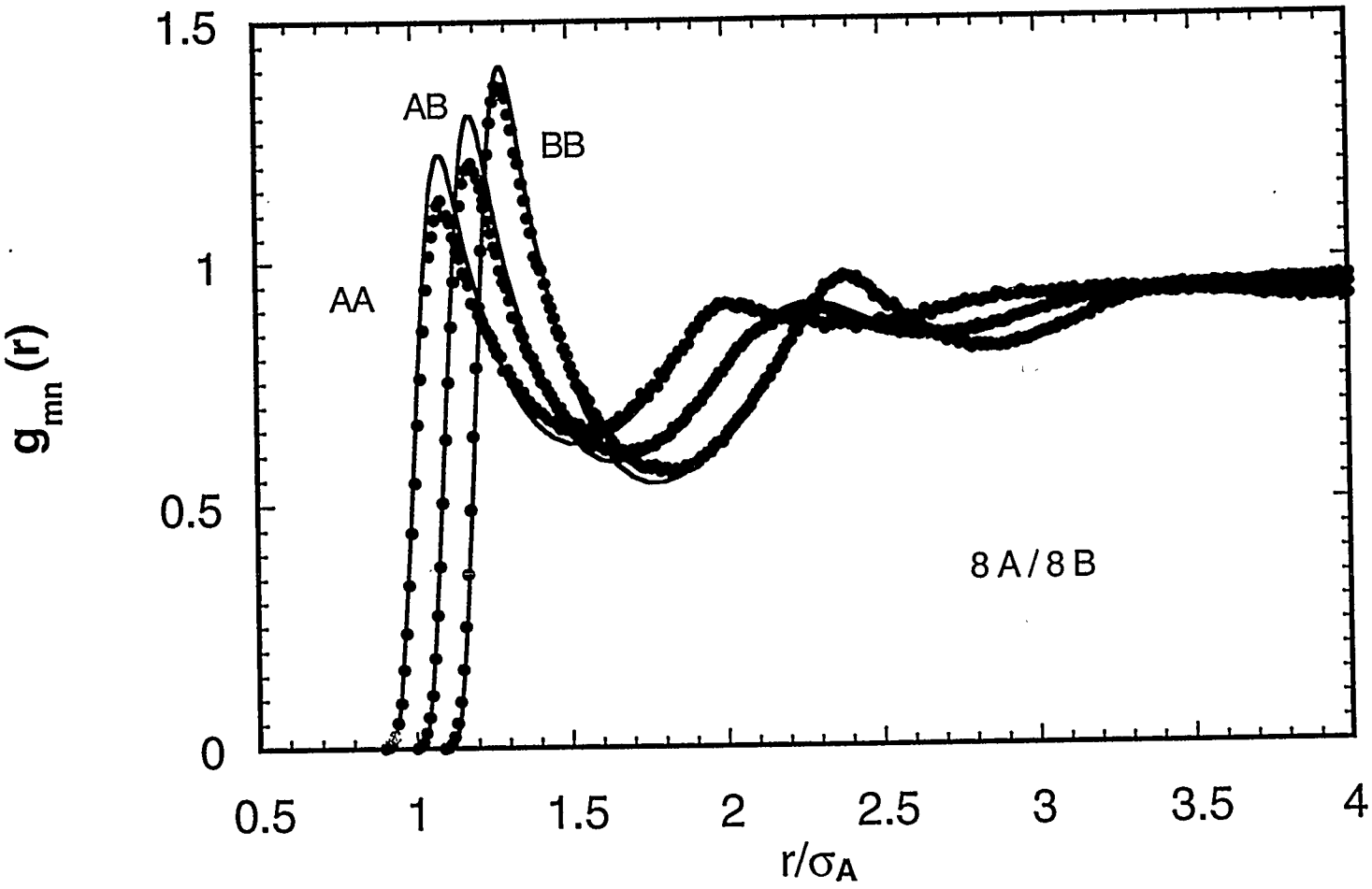

This function quantifies the tendency for "pairing" or physical clustering of like species. Figure 4.2 depicts $\Delta g(r)$ for the $\phi = 0.368$ case obtained from the simulation. Significant departures from random mixing, caused by local differences in monomer size, are evident at short length scales. Remarkably, PRISM theory is able to capture these subtle packing effects as seen by the solid line in Fig. 4.2.

Another important question regarding the structure of athermal blends is whether the single-chain conformation changes with composition. In the molecular dynamics simulations[96], small changes (at most 10-15 %) were observed in $\hat{\Omega}_{AA}(k)$ and in the mean square end-to-end distance $<R^2>$ of the chains in the blend. However, such changes are barely within the statistical error of the simulation. The collective partial structure factors were also monitored in the simulation and no evidence for incipient phase separation was detected in this athermal mixture[96].

Benchmark Monte Carlo simulations of a different class of athermal polymer mixtures have recently been carried out by Weinhold and Kumar[97] An equimolar(ϕ=0.5), constant volume binary blend was considered. The polymers were modeled as semiflexible, tangent bead chains of equal degrees of polymerization, N, interacting via a purely hard core potential of the same diameter for all sites. The reduced fluid density was $\rho_m d^3 = 0.65$ ($\eta \cong 0.34$) representative of a concentrated solution. The only difference between and A and B species was the local chain bending energy which controls the chain aspect ratio. A statistical segment length was defined as $a = (6R_g^2/N)^{1/2}$, and an aspect ratio as $\Gamma = a/d$. The A ("flexible") chain aspect ratio was fixed at $\Gamma_f = 1.5$, and the B ("stiff") chain aspect ratio was varied over the wide range of $\Gamma_S = 1.7 - 4.2$. Various model blends were studied for N=20 with the "stiffness asymmetry" of each characterized by the variable $\xi = 2(\Gamma_S-\Gamma_f)/(\Gamma_S+\Gamma_f)$. Besides providing exact results to test PRISM theory for athermal blends, these studies were motivated by scientific questions related to the relevance of a purely entropic "packing frustration" mechanism for phase separation in chemically similiar polymer blends such as the saturated polyolefins[98-100].

Here representative examples are given of the PRISM/simulation comparisons and the main conclusions are summarized[97]. The PRISM calculations were carried out assuming conformational ideality, and the required single chain structure factor was computed using the discrete,

4.2 The nonrandom mixing $\Delta g(r)$ in an athermal blend of composition f=0.368. The points are the simulations and the curves are the PRISM predictions[96].

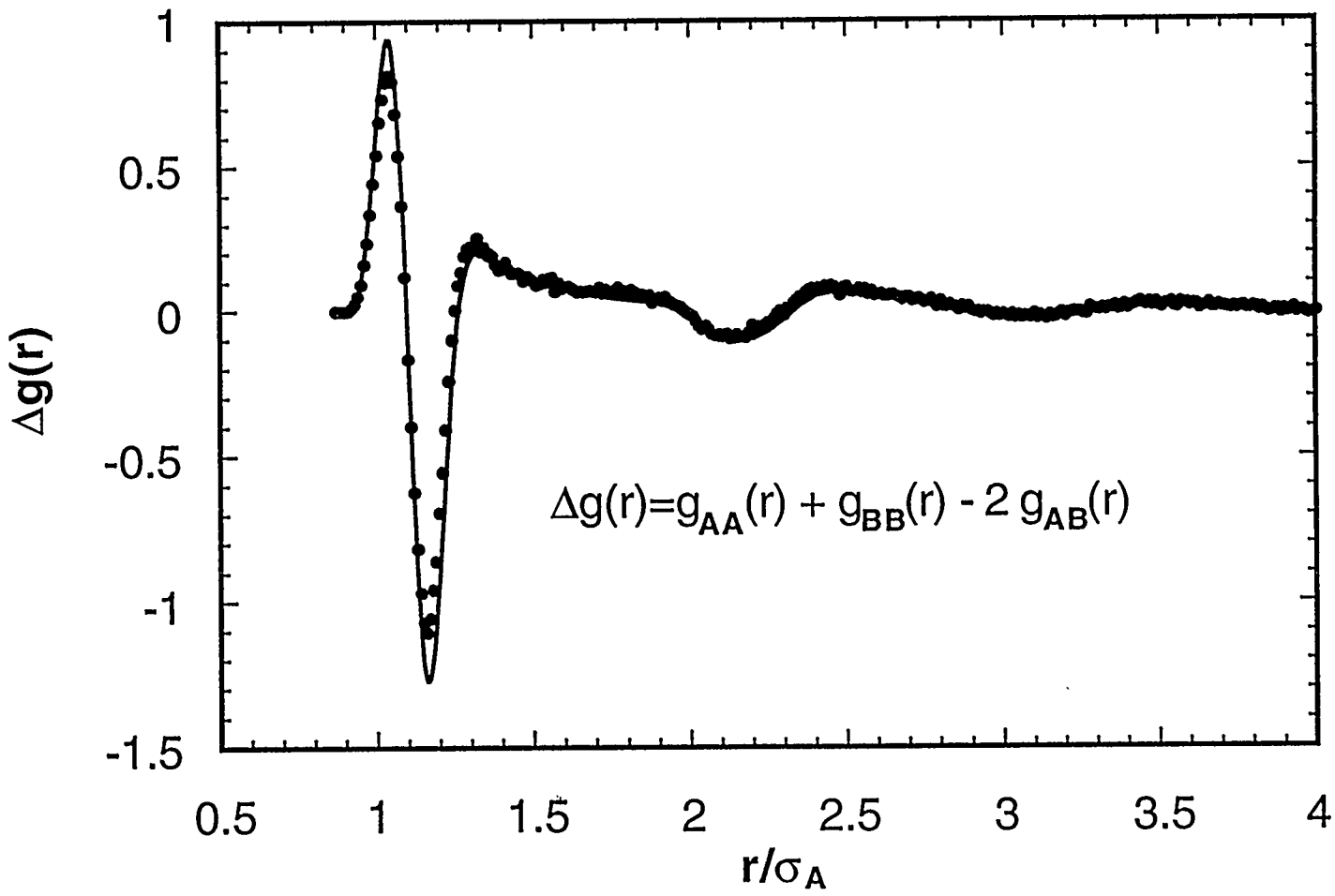

tangent site Koyama model[55] adjusted such that it reproduced the radius-of-gyration of the chains in the *one-component melt*. To within the statistical errors of the simulations, *no* changes in single chain conformation on going from the melt to the equimolar mixture were detected.

The agreement of PRISM theory with simulations for the three blend pair correlation functions, $g_{ss}(r)$, $g_{ff}(r)$, and $g_{fs}(r)$, was found to be typical of prior studies of dense melts, i.e. errors of roughly 10-20% close to contact, but much more accurate as r increases. More importantly, the *relative* form of the three g(r)'s, and their changes with increasing blend stiffness asymmetry, were accurately described by PRISM theory.[97] One simulation was carried out for N=200 and ξ =0.28. No loss of accuracy of PRISM for structural properties was found as N was increased from 20 to 200.

Blend thermodynamic properties were also computed. Comparisons of PRISM theory and simulation for the partial excess(interaction entropic) free energies of mixing per site, $\Delta F_{mix,i}$, are listed in Table 1 for N=20 and 200.

****

Table 1. Comparison of theory(computed based on free energy charging method) and simulation values of excess partial free energy of mixing changes defined in text[97]. The statistical uncertainties of the simulation values is roughly ± 0.005. Subscripts "s" and "f" denote stiff and flexible components. The flexible statistical segment length, a_f, is fixed at 1.50±0.01 and the stiffness asymmetry variable is $\xi = 2(a_s-a_f)/(a_s+a_f)$. $\beta\Delta F_{exc}$ is total excess free energy of mixing predicted by PRISM theory ; to within statistical uncertainty this quantity is found to be zero in the simulations for all cases shown. All results shown are for N=20, except for the one N=200 case.

	Simulation		**Theory**		
ξ	$\beta\Delta F_s$	$\beta\Delta F_f$	$\beta\Delta F_s$	$\beta\Delta F_f$	$\beta\Delta F_{exc}$
0.024	--	--	-0.0063	0.0063	0.00003
0.14	-0.022	0.020	-0.0175	0.0179	0.0004
0.28	-0.032	0.031	-0.0276	0.0296	0.0017
N=200:	-0.065	0.069	-0.0539	0.0549	0.0010
0.41	-0.036	0.035	-0.0306	0.0337	0.0031

0.53	-0.038	0.036	--	--	--

****

The PRISM results are based on the free energy charging route expressions, which for ϕ=1/2 are given by[97]

$$\beta\Delta F_{A,mix} = \frac{\pi\rho d^3}{2}\int_0^1 d\lambda\lambda^2\left[g^{\lambda}_{AA}(\lambda d^+) + g^{\lambda}_{BB}(\lambda d^+) - 2g^{\lambda}_{AB}(\lambda d^+)\right] \qquad (4.2)$$

for the A species. The B-species expression is obtained by interchanging A and B labels in Eq(4.2). Surprisingly good agreement between theory and simulation is obtained for all stiffness asymmetries and both values of N. Note that the "stiff" and "flexible" excess free energy of mixing are opposite signs, which implies that the flexible(stiff) chain is destablized(stabilized) upon transfer from the melt to the blend. Such behavior reflects local packing differences and equation-of-state effects[93,101], which cannot be described within an incompressible theory as often employed in polymer science[2]. Note, however, the *total* net excess free energy was extremely small in all cases(even much smaller than the ideal entropy of mixing per segment = N^{-1} ln(2)).

Thus, for the short and moderately long chains studied the athermal stiffness blend behaves as a *nearly ideal mixture in a thermodynamic sense* even though there are significant differences in segmental packing among the different species consistent with the MD simulations described above[96]. PRISM computations of an effective interaction (or "chi" in polymer science) parameter based on the free energy or compressibility route have also been shown to be in surprisingly good agreement with simulation[97], and are very small thus supporting the above conclusions.

We note that there are hints in Table 1, and structural fluctuation quantities such as $\Delta g(r)$ discussed elsewhere[97], that as N or stiffness mismatch increase the excess free energy of mixing also increases and the blend is less stable. Thus, the possibly of entropy-driven phase separation due to packing frustration of dissimiliar flexibility chains as N increases beyond 200 remains open based on the simulation studies of ref.97.

Summarizing, the major conclusion of this section is that PRISM theory provides an excellent description of the structure and (constant

volume) free energy of mixing of high density athermal polymer blends composed of the short and modest chain length molecules presently accessible to computer simulation. This has motivated the application of the theory to experimentally relevant situations such as long chains($N \approx 10^3$) and chemically-realistic atomistic models.

B. Multiple Site Homopolymer Blends

It was demonstrated in section IIIB for one-component melts that subtle screening effects resulted from the packing of nonspherical monomers. It is natural to expect that similar screening effects would also be operable in athermal blends of vinyl polymers. In order to probe this aspect at a *chemically realistic* level Rajasekaran, Curro, and Honeycutt[32] studied an athermal mixture of polyethylene and isotactic polypropylene. The chains in this mixture were modeled as illustrated in Fig. 3.7 with three sites (A, B, C) making up a polypropylene monomer, and a single D site representing the CH_2 group of polyethylene. Application of Eqs. (2.2) - (2.5) lead to a set of 10 coupled integral equations which were solved numerically using standard Picard iteration techniques.

Assuming that the intramolecular structure of the chains in the athermal blend is independent of composition, then the elements of the 4x4 $\hat{\Omega}_{\alpha\gamma}(k)$ intramolecular matrix for the blend are already available from the corresponding one-component melt intramolecular structure functions. The $\hat{\Omega}_{\alpha\gamma}(k)$for $\alpha,\gamma = A,B,C$ were obtained from Monte Carlo simulations of a single, rotational isomeric state chain using the parameterization of Suter and Flory[73] discussed in section IIIB. Likewise, $\hat{\Omega}_{DD}(k)$ was obtained from the RIS calculations of Honnell and coworkers for polyethylene[63,64].

Fig. 4.3 depicts the intermolecular packing in the athermal PE/i-PP blend for chains of 200 *monomers* at a volume fraction of polyethylene sites of $\phi = 0.50$. Although there are 10 independent correlations, only the diagonal components are shown. The radial distributions in the blend are qualitatively similar to those in the one-component melt (see Fig. 3.11). However, as demonstrated elsewhere[32], the detailed structure is found to be significantly composition dependent. For example, the local peaks in the polyethylene $g_{DD}(r)$ increase monotonically in magnitude as more polypropylene is added to the mixture(by roughly 30% at ϕ = 0.1 relative to

4.3 The radial distribution functions[32] for a blend of polyethylene and isotactic polypropylene($N_{PE}=N_{PP}=200$) at a volume fraction of polyethylene of f=0.5. The 4 diagonal correlations are shown.

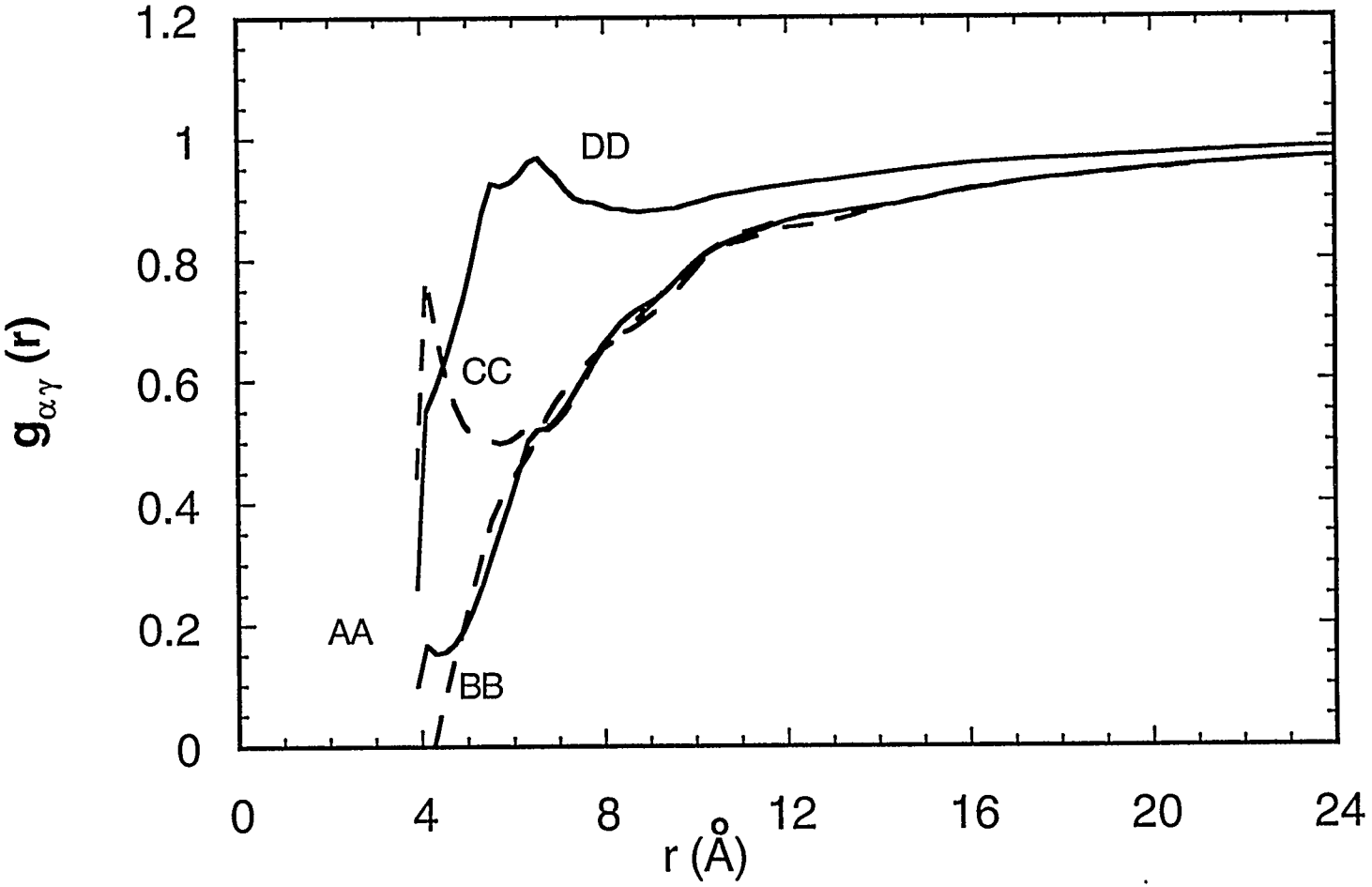

the pure PE melt). This suggests a tendency of the polyethylene to cluster in the mixture as a result of unfavorable cross correlations between the PE and i-PP chains. Despite this clustering tendency, no thermodynamic evidence was found for macroscopic phase separation in the athermal mixture at any composition.

From a knowledge of the radial distribution functions in the blend as a function of composition, one can obtain the various thermodynamic state functions by applying the analysis of Kirkwood and Buff[102]. For the present case the following relationship for the entropy of mixing ΔS_{mix} can be derived[32]

$$\left(\frac{\partial^2 \Delta S_{mix}}{\partial \phi^2}\right)_{TP} = \frac{-k_B(\eta/\nu)^2 V}{\left[9\phi^2 \hat{S}_{AA}(0) - 6\phi(1-\phi)\hat{S}_{AD}(0) + (1-\phi)^2 \hat{S}_{DD}(0)\right]} \tag{4.3}$$

where η is the overall blend packing fraction and ν is the volume of one of the sites (assumed to be all equal). If incompressibility ($\kappa \to 0$) and random mixing ($g_{\alpha\gamma}(r) = 1$) are enforced, then the continuous space analog of the Flory-Huggins or ideal solution relationship is obtained[32]

$$\left(\frac{\partial^2 \Delta S_{mix}}{\partial \phi^2}\right)_{TV} = -k_B\left(\frac{\eta}{\nu}\right)V\left[\frac{1}{2N_{PE}\phi} + \frac{1}{3N_{PP}(1-\phi)}\right] \tag{4.4}$$

Calculations by Rajasekaran and coworkers[32] of the entropy of mixing derivative for the polyethylene/polypropylene blend using Eq. (4.3) predict a *smaller* entropy stabilization of the mixture, by approximately a factor of two, relative to ideal solution behavior[32]. Thus, excess entropic effects do destabilize this PE/iPP blend relative to the ideal solution behavior, but no athermal phase separation is found even for this very structurally asymmetric case. Experimentally, an equimolar PE/PP mixture is *immiscible* for all accessible temperatures and values of N_{mon} *far less* than 200. Thus, explanation of the experimental behavior requires consideration of thermal effects(attractive forces) as discussed in Section V.

It should be mentioned that Eq. (4.3) is only one of several possible thermodynamic routes to the entropy of mixing in the athermal blend.

Another possible route is through the "charging formula" of Chandler[8] used earlier in Eq. (3.9b) for the one-component polymer melt.

C. Semiflexible Blends and Entropy-Driven Phase Segregation

Motivated by both scientific questions related to the origin of phase separation in saturated polyolefin alloys[97-100], and the basic statistical mechanical question of entropy-driven phase segregation, Singh and Schweizer[100] have carried out a detailed numerical PRISM study of the structure and phase behavior of the binary athermal "stiffness" blend discussed in section A. A wide range of chain aspect ratios of the tangent SFC chain, fluid density, blend composition, and ratio of A and B site diameters were investigated. Liquid-liquid spinodal phase separation is defined as when all the partial collective structures at zero wavevector, $\hat{S}_{MM'}(k=0)$, simultaneously diverge. This condition is precisely given as

$$0 = 1 - \rho_A N_A C_{AA} - \rho_B N_B C_{BB} + \rho_A \rho_B N_A N_B (C_{AA} C_{BB} - C_{AB}^2) \qquad (4.5)$$

where $C_{MM'} = C_{MM'}(0)$. For the cases of interest here $N_A=N_B=N$, $\rho_A = \phi\,\rho$, $\rho_B = (1-\phi)\,\rho$, and ρ is the total site number density of the binary blend.

The possibility of "entropy-driven" phase separation in purely hard core fluids has been of considerable recent interest experimentally, theoretically, and via computer simulations. Systems studied include binary mixtures of spheres(or colloids) of different diameters[103], mixtures of large colloidal spheres and flexible polymers[104], mixtures of colloidal spheres and rods[105], and a polymer/small molecule solvent mixture under *infinite dilution* conditions(here an athermal conformational "coil-to-globule" transition can occur)[106]. For the latter three problems, PRISM theory could be applied, but to the best of our knowledge has not. The first problem is an old one solved analytically using PY integral equation theory by Lebowitz and Rowlinson[107]. *No liquid-liquid phase separation was found, i.e. the hard sphere mixture is completely miscible.* Recent simulations and experiments suggest this is not true for *highly* size-asymmetric cases[103], and modifications of the atomic closures have been proposed to account for the observed phase separation[108]. For the polymer problem, we are also using the site-site PY closure. However, entropy-driven phase separation, if it occurs, is associated with the difficulty of

packing chains of different stiffnesses or bending rigidity. In analogy with liquid crystal systems[109], one might expect phase separation if the "packing frustration" is sufficiently great(although for mixtures of rods and coils segregation into an isotropic and nematic phase generally occurs). Relevant variables for such an entropy-driven phenomenon would include the individual chain aspect ratios, overall packing fraction, and degree of polymerization.

Here only a few of the highlights of the extensive study[100] will be mentioned for the simplest case of equal A and B chain site hard core diameters, and an equimolar mixture of chains of N sites each(ϕ=1/2). The A chain aspect ratio is fixed at approximately 1.3, which is representative of a polymer such as polyethylene[52]. Thus, the structural asymmetry variable $\xi = 2(\Gamma_B - \Gamma_A)/(\Gamma_B + \Gamma_A) < 0$ for most experimental polyolefin mixtures since unbranched polyethylene generally has the largest aspect ratio of the saturated hydrocarbon polymers[52,97,100]. Figure 4.4 shows spinodal phase boundaries based on Eq(4.5) for two reduced densities representative of a dense melt and concentrated solution(as studied by simulation)[97]. There are several important features[100].

(1) *No* phase separation is found for a stiffness asymmetry variable less than roughly 0.4, or for low values of N and any value of stiffness mismatch(consistent with simulation)[97]. Since experimentally one expects $\xi < 0$, this result suggests purely entropy-driven mechanism cannot account for the facile tendency of polyolefins to demix. Moreover, for chain parameter values typical of most semiflexible polymers of interest, the excess entropic effects appear small and much weaker than enthalpy related consideration associated with *local* packing differences between species(see Section V).

(2) Phase separation can occur at *large enough N* under the appropriate conditions. It seems clear that since large N is required, the predicted phase separation is driven by spatially long range, or nonlocal, aspects of polymer connectivity and excluded volume interactions. *Thus, nonlocal entropy-driven phase segregation requires a large enough N and sufficient absolute stiffness and aspect ratio mismatch of the polymer backbones.* This deduction seems natural in that packing frustration is created locally and then propagated to macromolecular length scales via a backbone stiffness dependent chain connectivity mechanism. This scenario

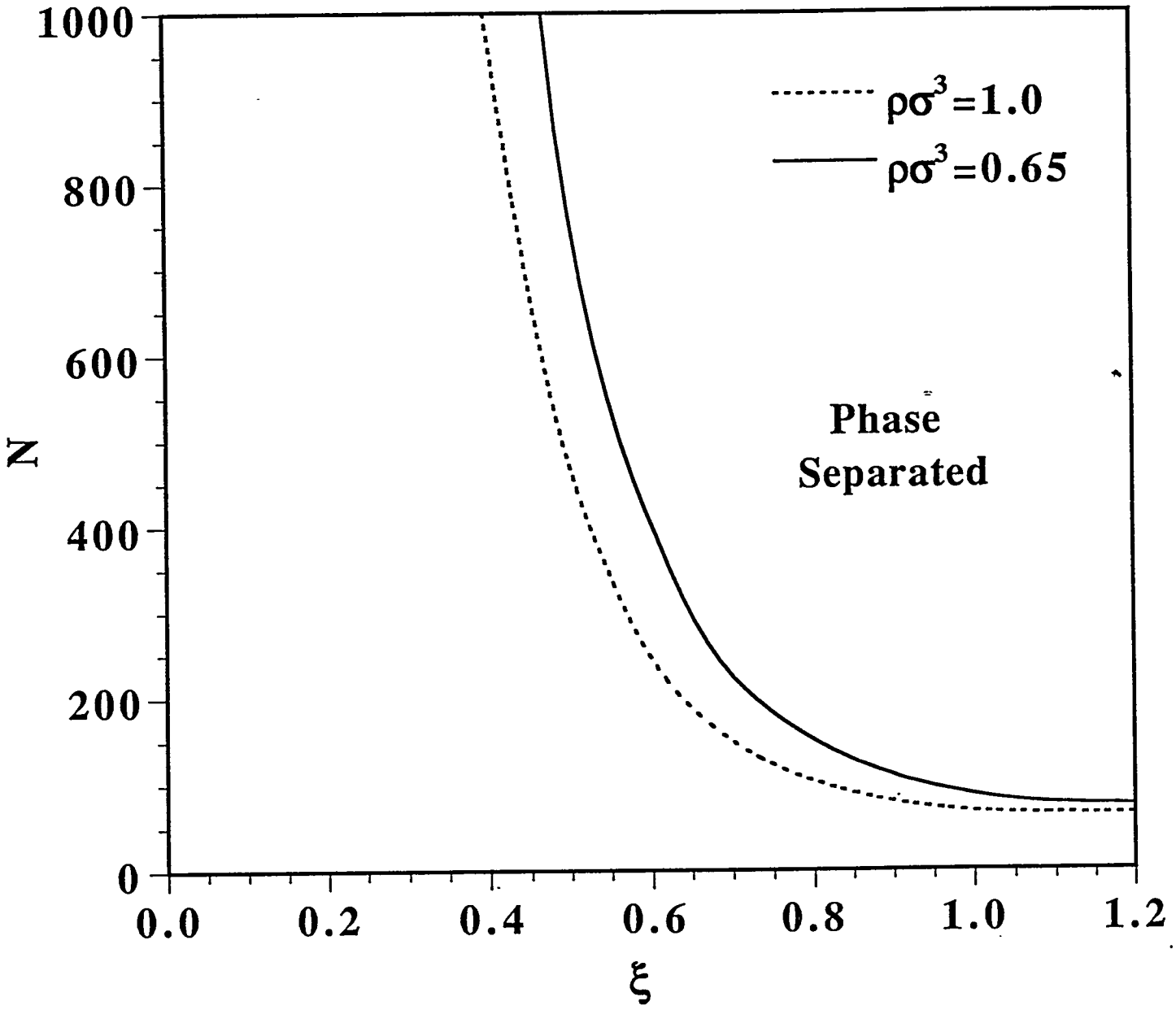

4.4 Athermal spinodal phase diagram obtained using PRISM theory[100] and the compressibility route for two reduced fluid densities($d=\sigma$) and a flexible chain aspect ratio of 1.3.

is further reinforced by the fact that PRISM theory studies to date have found *no* athermal phase separation for highly flexible chain models such as Gaussian or freely-jointed models[27-29](see also section D below) which lack completely the local rod-like stiffness on length scales comparable and shorter than the chain persistence length.

(3) The effect of fluid density is relatively weak but phase separation is enhanced at higher density consistent with intuition.

A structural interpretation of the predicted nonlocal entropy-driven phase separation can be deduced by examining the spatially-resolved pair correlation function measure of incompatibility or clustering, $\Delta g(r)$ defined in Eq(4.1). Figure 4.5a shows this function for the case of fixed chain aspect ratios and several values of N and fluid packing fraction. As the chains become longer, local clustering of like segments is enhanced but tends to "saturate" at large N. However, the growth of a much larger amplitude and longer spatial range component is dramatic. It coincides with increasingly large long wavelength concentration fluctuations and ultimately spinodal phase separation. This N-dependent correlation feature is associated with the chain connectivity and inpenetrability on intermediate "correlation hole" length scales.

The dependence of $\Delta g(r)$ on chain stiffness mismatch at fixed N=100 is shown in Figure 4.5b. Again, local segregation increases with stiffness mismatch but tends to saturate. However, *non*local segregation continues to grow in both amplitude and range ultimately resulting in phase separation. The latter behavior is particularly striking since at fixed N the size of the polymers, and hence the spatial range the correlation hole associated with melt-like density fluctuations, is nearly fixed. This plot also illustrates an intriguing empirical observation that the contact value $\Delta g(r=d)$ tends to acquire a common critical value at the spinodal phase boundary(roughly 0.1 in the cases of Figures 4.5) which is nearly independent of how the phase transition is driven(increasing N at fixed $\gamma = \Gamma_B/\Gamma_A$ or increasing γ at fixed N)[100].

The detailed nature of single phase blend correlations, effective interaction parameters, and the entropy-driven phase separation phenomenon have been found to be sensitive to system-specific factors such as composition, differences in A and B site diameter, density, and local

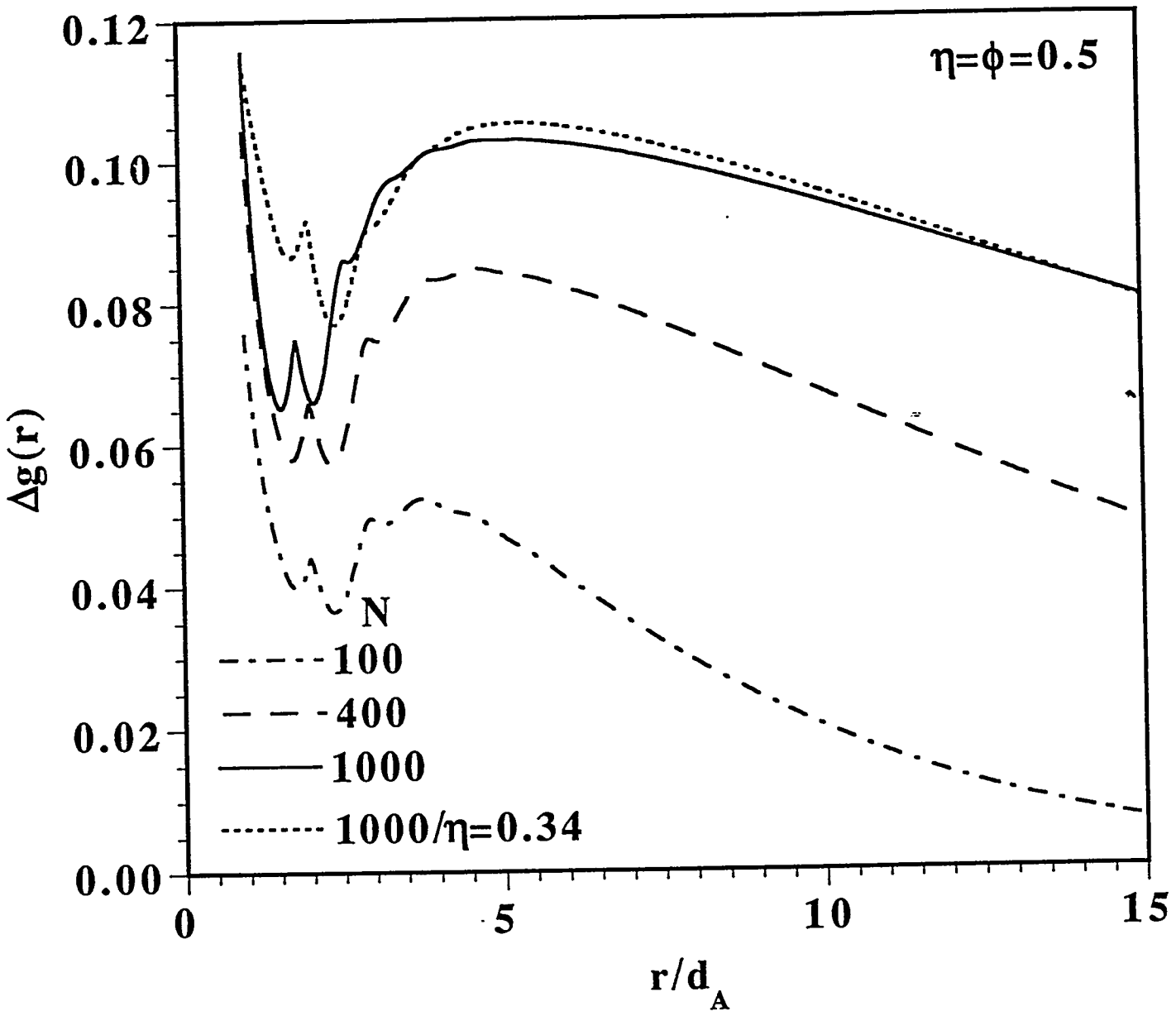

4.5a Intermolecular pairing function in the equimolar athermal stiffness blend[100]. Except as explicitly noted all curves are for the melt like packing fraction of 0.5. Results for fixed aspect ratio asymmetry of $\gamma = \Gamma_B/\Gamma_A = 1.49$ and various values of N. (b) Dependence on aspect ratio asymmetry for Fixed N=100. From top to bottom the curves correspond to γ = 2.319(spinodal boundary), 2.199,1.979,1.734,1.343 and 1.219.

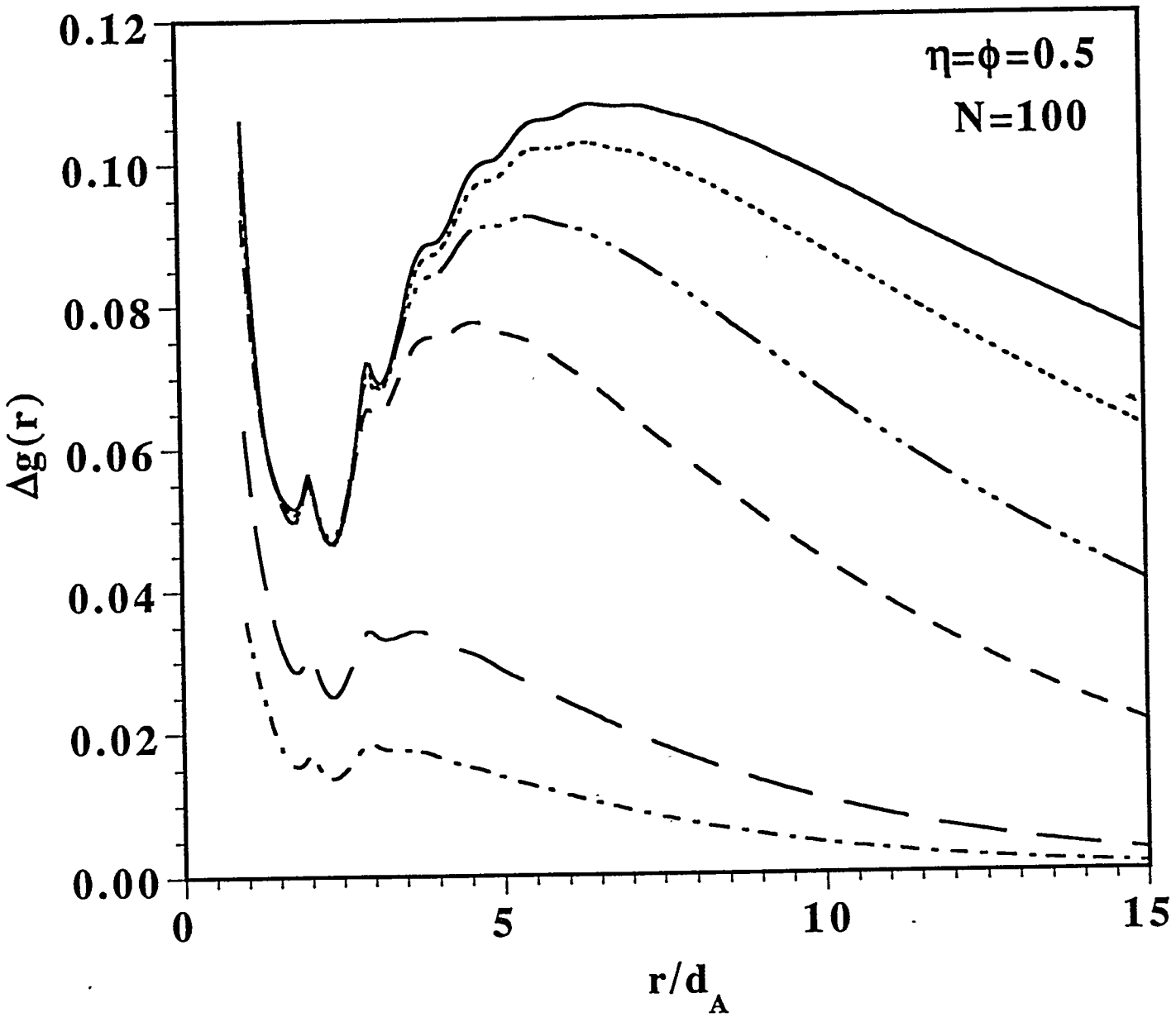

4.5b Intermolecular pairing function in the equimolar athermal stiffness blend[100]. Except as explicitly noted all curves are for the melt like packing fraction of 0.5. Dependence on aspect ratio asymmetry for Fixed N=100. From top to bottom the curves correspond to γ = 2.319(spinodal boundary), 2.199,1.979,1.734,1.343 and 1.219.

architectural details[100]. However, the basic conclusions summarized above seem qualitatively general.

A limited number of numerical studies have been carried out using the free energy charging approach to blend thermodynamics instead of the compressibility route described above[100]. In the miscible region, quantitative differences in the excess free energy of mixing, or interaction parameter, have been found but these differences are generally no more than a factor of 2 or 3. More work is required to establish the severity of the thermodynamic inconsistency problem for this athermal stiffness blend system. Another caveat is that it is well known that PRISM does not properly incorporate "nematic-like" orientational corrleations in the one phase fluid[8,39,40]. This should represent a technical limitation to describing liquid-liquid phase separation which becomes more severe as the chain aspect ratios increase. Description of isotropic-nematic phase separation is not possible. However, for the experimental applications to conformationally flexible polyolefins and polydienes of current interest, strong nematic correlations seem improbable.

D. Analytic Gaussian Thread Model

PRISM theory for the athermal "stiffness asymmetric blend" model described in section C can be analytically solved[29,30] in the idealized Gaussian thread limit for $N \rightarrow \infty$. For many physical problems(e.g., polymer solutions and melts, liquid-vapor equilibria, and thermal polymer blends and block copolymers), the Gaussian thread model has been shown to be reliable *in the sense* that it is qualitatively consistent with many aspects of the behavior predicted by numerical PRISM for more realistic semi-flexible, nonzero thickness chain models. However, there are classes of physical problems where this is not the case. The athermal stiffness blend in certain regions of parameter space is one case, both in the bulk[100] and near surfaces[110]. Nevertheless, even for this problem the thread model does correctly capture certain aspects, and when it does fail this provides considerable insight into the key factors which control the behavior of real polymer systems[100].

Employing the simplified Gaussian forms of Eq(3.1), and enforcing the three point-like core conditions within the PY closure approximation($g_{MM'}(r=0)=0$) , results in three nonlinear transcendental

equations for the three direct correlation parameters $C_{MM'}$. In the long chain limit, the Gaussian chain structure factors take on a perfectly self-similiar form : $\hat{\omega}_M(k) = 12(k\sigma_M)^{-2}$, and no large k crossover to locally rigid behavior , $\hat{\omega}(k) \propto (k\xi_p)^{-1}$, occurs. This mathematical feature allows an exact analytic solution which has a scaling form[29,30,100]

$$C_{BB} = \gamma^4 C_{AA} \ , \quad C_{AB} = \gamma^2 C_{AA} \tag{4.6}$$

$$\sigma_A^{-3} C_{AA}(\phi) = \frac{-\pi\eta\Gamma^3}{18}[\phi + \gamma^2(1-\phi)] \tag{4.7}$$

where $\Gamma = \sigma_A/d$ and $\gamma = \sigma_B/\sigma_A$ is the "structural or conformational" asymmetry variable. The perfect scaling relations among the blend composition-dependent $C_{MM'}$ are a consequence of the self-similiar intrachain correlations and the PY closure treatment of the (point-like) excluded volume constraints.

Eq(4.6) predicts the repulsive effective potential between segments of like species, $-k_BT\ C_{MM}$, is larger in the blend for the conformationally stiffer chain than the more flexible one. This result is in accord with physical intuition and is mathematically required to satisfy the local hard core (point) exclusion constraint. Moreover, the repulsive pseudopotential between the more flexible(stiffer) species is predicted to increase(decrease) upon transfer from a one-component melt to the blend environment. This trend is intuitively sensible, consistent with the signs of the species-dependent effective chi-parameters derived elsewhere[100], and agrees with numerical SFC PRISM calculations and Monte Carlo simulations of the partial excess free energies of mixing and effective chi-parameters[97].

The thread model is predicted to be miscible under all conditions due to the perfect scaling relations of Eq(4.6). Although this complete miscibility conclusion is in agreement with numerical SFC PRISM for low aspect ratio chains(those best described by a Gaussian model), it misses the entropy-driven phase separation phenomenon found numerically for sufficiently stiff polymers[100]. This point emphasizes the limitations of the thread model: it ignores the consequences of local chain rigidity on packing which appears to be central to the athermal phase segregation phenomenon. Another example of the limitations of the Gaussian thread model is its prediction[29,30] of interchain random mixing, or conformal solution

behavior, corresponding to $g_{MM'}(r) = g_{eff}(r;\phi)$. Again, this is a consequence of the (assumed) perfectly self-similiar Gaussian single polymer structure and the $d \to 0$ idealization. In reality, there are always differences in the $g_{MM'}(r)$ functions due to local, nonuniversal breaking of the self-similiar chain correlations.

Finally, field theoretic approaches[99] have recently predicted athermal phase separation driven by nonlocal-entropic considerations for *incompressible blends of Gaussian thread polymers.* This prediction is at odds with PRISM theory in the thread limit. However, for the effective chi-parameter PRISM theory has been shown[100] to be equivalent to the field theory *if* the free energy route is employed in conjunction with the extremely simple RPA closure(not PY). The RPA closure, $C_{MM'}(r) = -\beta u_{MM'}(r)$ *for all r*, is known to be very poor for repulsive force systems and violates the hard core impenetrability condition. Thus, the field theoretic prediction has been suggested to be a consequence of the combined use of a long wavelength incompressibility approximation in conjunction with anRPA closure[100].

V. THERMAL EFFECTS IN POLYMER BLENDS: PERTURBATION APPROACH

In reality, polymer mixtures are not athermal and attractive interactions can play a crucial role in determining their miscibility and thermodynamic properties[1,93-95]. This fact is evident in the mean field Flory-Huggins theory where phase separation and the interaction parameter are entirely of an enthalpic origin. For a binary blend of A and B single site chains composed of N repeat units the free energy of mixing per segment is given in the *incompressible* Flory theory as[1]

$$\beta\Delta F_{mix} = \frac{\phi_A \ln \phi_A}{N_A} + \frac{\phi_B \ln \phi_B}{N_B} + \chi_o \phi_A \phi_B \qquad (5.1a)$$

where $\phi_A + \phi_B = 1$, and the interaction or "chi" parameter in its off-lattice version is of an extremely simple, purely energetic mean field form

$$\chi_o = \frac{-\rho}{2k_BT}\int d\vec{r}[v_{AA}(r)+v_{BB}(r)-2v_{AB}(r)] \qquad (5.1b)$$

Here, $v_{MM'}(r)$ are the (generally attractive) tail potentials between species M and M'. The spinodal instability corresponds to a vanishing of the second compositional derivative of the free energy of mixing yielding the condition

$$2\chi_{o,s}N\phi(1-\phi) = 1 \qquad (5.2a)$$

where $\phi \equiv \phi_A$ and $N_A = N_B = N$. This implies a liquid-liquid spinodal phase separation temperature of

$$k_BT_s = N\frac{\rho\,\phi(1-\phi)}{2}\int d\vec{r}[2v_{AB}(r)-v_{AA}(r)-v_{BB}(r)] \qquad (5.2b)$$

The critical composition is $\phi_A = \phi_B = 1/2$ by symmetry.

The two prime predictions of Flory theory are as follows. (i) $T_S \propto N$ due to the extreme loss of ideal entropy of mixing associated with global chain connectivity. Hence, it is correctly predicted to be generally very difficult to create a miscible polymer blend[93-95]. (ii) Immiscibility is promoted as the A and B monomers become more *chemically* distinct as quantified by their intermolecular tail potentials (e.g. London dispersion interactions).

Eq(5.1) includes only the ideal, combinatorial entropy of mixing and the simplest conceivable "regular solution" type estimate of the enthalpy of mixing based on completely random mixing of monomers : $g_{MM'}(r) = 1$ in the liquid state language. χ_o is refered to as the "bare" chi-parameter since it ignores all aspects of polymer architecture and interchain nonrandom correlations. For these reasons, the model blend for which Eq(5.1) is thought to be most appropriate for is an *interaction and structurally symmetric* polymer mixture. The latter is defined such that the *only difference* between the A and B chains is a $v_{AB}(r)$ tail potential which favors phase separation at low temperatures. The closest real system to this idealized mixture is an "isotopic blend" where the A and B chains are hydrogenated and deuterated versions of the same polymer[111]. The symmetric model has played a central role in theoretical and simulation studies due to its great simplicity from a chemical viewpoint[112].

In real systems, nonrandom mixing effects, potentially caused by local polymer architecture and interchain forces, can have profound consequences on how intermolecular attractive potentials influence miscibility. Such nonideal effects can lead to large corrections, of both excess entropic and enthalpic origin, to the mean-field Flory-Huggins theory. As discussed in section IV, for flexible chain blends of prime experimental interest the excess entropic contribution seems very small. Thus, attractive interactions, or enthalpy of mixing effects, are expected to often play a dominant role in determining blend miscibility. In this section we examine these enthalpic effects within the context of thermodynamic pertubation theory for atomistic, semiflexible, and Gaussian thread models. In addition, the validity of a Hildebrand-like molecular solubility parameter approach based on pure component properties is examined.

A. Thermodynamic Perturbation Theory

For *dense* nonpolar polymers the intersite interactions are of the van der Waals type and one anticipates that the attractive branch of the potential may exert little influence on interchain packing. Although obviously true if the tail potentials are weak relative to k_BT, such "repulsive force screening"[5,11] may also be operative in polymer mixtures for several reasons discussed below. Although there will undoubtably be errors made by such a simplification, it represents a conceptually and computationally convenient starting point. In such a thermodynamic perturbation , or high temperature approximation(HTA), approach the polymer liquid structure is *assumed* to be determined solely by an appropriately constructed repulsive reference system.

The starting point is the the reduced Helmholtz free energy of the *blend* in the standard "charging parameter" form[8]

$$\frac{\beta F}{V} = \frac{\beta F_o}{V} + \frac{1}{2}\sum_{\alpha\gamma}\rho_\alpha\rho_\gamma\int_0^1 d\lambda\int \beta v_{\alpha\gamma}(r)g^{\lambda}_{\alpha\gamma}(r)d\bar{r} \qquad (5.3)$$

where the attractive branch of the potential $\lambda w_{\alpha\gamma}(r)$ is gradually turned on as the charging parameter λ varies from 0 to 1. F_0 is the free energy of the corresponding athermal, or reference repulsive force, system and may depend on temperature *implicitly* through the density, single chain

conformation, and/or effective hard core diameter. Eq(5.3) ignores *single chain intramolecular* contributions associated with the attractive branch of the potentials. This generally represents an additional approximation, *but* within the the context of the conformational ideality simplification such contributions would only contribute terms *linear* in polymer concentration and blend density. Such terms then *cancel out* in the free energy of mixing relevant to blend mixing thermodynamics. Since all PRISM work on blend thermodynamics to date has employed this conformational ideality assumption, Eq(5.3) is appropriate. Future work based on the "self-consistent" formulation of PRISM discussed in Section VIII needs to be done in order to investigate the corrections to blend thermodynamics due to *nonideal* conformational effects(e.g., changes in polymer structure on going from the melt to blend, or mixture composition-dependent conformational changes).

Within the HTA scheme, the liquid structure of the mixture is approximated by the structure of the athermal system, ie. $g^{\lambda}_{\alpha\gamma}(r) \approx g^{o}_{\alpha\gamma}(r)$. Thus to first order Eq. (5.3) can be approximated as

$$\frac{\beta F}{V} \approx \frac{\beta F_o}{V} + \frac{1}{2}\sum_{\alpha\gamma}\rho_\alpha\rho_\gamma \int \beta v_{\alpha\gamma}(r) g^{o}_{\alpha\gamma}(r) d\vec{r} \qquad (5.4)$$

Such a HTA might be expected to be particularly accurate for polymers since the critical temperature grows without bound as N increases. Thus, the literal perturbative condition that $\beta v_{\alpha\gamma}(r) << 1$ might be expected to hold in the one phase region for long chains. Although this argument is sound *in principle*, in practice the experimentally accessible temperatures are restricted to T = 200 -500 Kelvin so such a weak coupling condition will not necessarily be valid for laboratory blends *for which* the demixing transition is measurable.

At constant pressure P, the Gibbs free energy of mixing ΔG_{mix} of the blend relative to the pure components can be expressed as

$$\Delta G_{mix} = \Delta F_{mix} + P\Delta V_{mix} \qquad (5.5)$$

where ΔV_{mix} is the volume change of mixing. In first order perturbation theory, the Helmholtz free energy of mixing of the reference athermal

system is entirely due to the entropy of mixing, ie. $\Delta F^{\circ}_{mix} = -T\Delta S_{mix}$. Thus, from a knowledge of the structure of the athermal reference blend one can calculate the free energy of mixing and phase behavior of the general blend. Any theory based on Eqs(5.4) and (5.5) is expected to yield classical critical exponents.

Incompressible Flory mean field theory[1] is recovered from Eq(5.4) and (5.5) if one assumes : (i) No excess volume of mixing, (ii) a blend composition-independent total packing fraction, (iii) the athermal reference system is an ideal solution, i.e. zero excess entropy of mixing, and (iv) literal random mixing, i.e. $g_{MM'}(r) = 1$.

In the PRISM studies carried out to date, simplification (i) has been invoked. An effective interaction or chi-parameter can be defined in the usual manner as the second derivative of the *excess* free energy of mixing

$$\begin{aligned}\chi &\equiv -\frac{1}{2}\frac{\partial^2}{\partial\phi^2}\Delta F^{exc}_{mix} \\ &= -\frac{1}{2}\frac{\partial^2}{\partial\phi^2}\left[-T\Delta S^{exc}_{mix} + \Delta H_{mix}\right] \\ &\equiv \chi_a + \chi_B\end{aligned} \tag{5.6}$$

where the third line defines excess entropic and enthalpic interaction parameters. Spinodal phase boundaries are determinable from this quantity.

B. Phase Behavior of Atomistic Models

Rajasekaran and coworkers[32] applied Eq. (5.4) to the PE/i-PP blend using the 10 radial distribution functions determined from the athermal mixture as discussed in section IVB. For this case Eq. (5.5) can be written in the form

$$\frac{\beta\Delta G_{mix}}{V} = -\frac{\Delta S_{mix}}{k_B V} + \left(\frac{\eta}{\nu}\right)\chi_H\phi(1-\phi) + \frac{\beta P\Delta V_{mix}}{V} \tag{5.7}$$

with an enthalpic interaction parameter χ_H defined implicitly in terms of the heat of mixing. Alternative definitions of an effective chi-parameter,

such as Eq(5.6), are equally valid since *as a matter of principle* a single interaction parameter cannot completely characterize the nonideal aspects of a compressible binary mixture. For purposes of computing the spinodal phase boundary the precise definition of a homogeneous phase interaction parameter is *irrelevant*. For the PE/i-PP blend, χ_H can be written in the form

$$\chi_H(\phi) = -\frac{1}{2}\left(\frac{\eta}{v}\right)\left[\Delta H_{PE} + \Delta H_{PP} - 2\Delta H_{PE/PP}\right] \tag{5.8a}$$

with the various contributions to the heat of mixing taking the form

$$\Delta H_{PE} = (1-\phi)^{-1}\int \beta v_{DD}\left[g_{DD}^{melt} - \phi g_{DD}^{o}\right]d\bar{r} \tag{5.8b}$$

$$\Delta H_{PP} = \frac{1}{9\phi}\sum_{a,b=A}^{C}\int \beta v_{ab}\left[g_{ab}^{melt} - (1-\phi)g_{ab}^{o}\right]d\bar{r} \tag{5.8c}$$

$$\Delta H_{PE/PP} = \frac{1}{3}\sum_{a=A}^{C}\int \beta v_{aD} g_{aD}^{o} d\bar{r} \tag{5.8d}$$

where the arguments of the relevant functions have been suppressed. In the literal random mixing limit, in which all the radial distribution functions are unity, Eqs. (5.8) reduces to the continuum analog of the Flory-Huggins "bare" chi parameter

$$\chi_o = \frac{16\pi\beta\varepsilon\sigma^3}{9}\left(\frac{\eta}{v}\right)\left(\frac{1+\lambda_1+\lambda_2}{3} - 1\right)^2 \tag{5.9}$$

where the λ's are ratios of attractive well depth parameters as defined in Eq. (3.15), and σ and ε are the Lennard-Jones parameters for interactions between a pair of methylene sites.

Using Eq. (4.3) for the second derivative of the entropy of mixing together with Eqs. (5.8) for the heat of mixing permits the evaluation of the Gibbs free energy of mixing as a function of volume fraction ϕ of polyethylene. In their application to the PE/i-PP blend, Rajasekaran and coworkers[32] approximated the volume change of mixing as zero. This is equivalent to approximating the partial molar volumes in the mixture by the pure component molar volumes. It should be emphasized that making the assumption that $\Delta V_{mix} = 0$ does *not* neglect the effect of density

fluctuations (or equation-of-state effects), which are still present in the free energy of mixing through the composition dependence of the packing fraction $\eta(\phi)$. If the polarizability ratios are estimated from group additivity tables[86], or from Jorgensen's potential functions[90] for alkanes, the heat of mixing for PE/i-PP is found to be positive. Furthermore the critical temperatures found from PRISM theory[32] are much higher than the corresponding Flory-Huggins estimates. This can be seen from the spinodal curves plotted in Fig. 5.1 obtained using Small's estimate[86] for λ_1 and λ_2. The critical temperature for this mixture is predicted by PRISM theory to be approximately 11 times larger than from the corresponding mean field Flory value. This is in qualitative accordance with experimental observations indicating a high degree of incompatibility between polyethylene and polypropylene. Thus, one concludes that local nonrandom packing effects, induced by local structural asymmetries in the monomeric structure of PE and i-PP, lead to gross (primarily enthalpic) destabilization of the blend.

In the case of polyolefin chains one expects the site polarizability increases with the number of hydrogens present. For example the polarizability of CH_3 is larger than for a CH group. Thus, in terms of Eq(3.15) $\lambda_1 > 1$ and $\lambda_2 < 1$ for polyolefins. It is interesting to observe that if λ_1 and λ_2 are switched (keeping the bare Flory-Huggins chi parameter in Eq. (5.9) *unchanged*), then PRISM theory predicts a *negative* heat of mixing and a miscibility for this hypothetical PE/iPP blend. Such an intriguing possibility of "compensation" of the demixing consequences of structural and interaction potential differences between species was first discovered by Singh and Schweizer[113] as described in the next section.

Finally, Honeycutt[114] has applied blend PRISM theory at an atomistic RIS model level to study the effect of tacticity(stereochemical differences) on the phase behavior of a commercially important binary polymer mixture. Tacticity is found to result in significant changes of the computed spinodal boundaries, which serves to again emphasize the importance of monomer structure and local packing on the free energy of mixing.

VI. SOLVATION POTENTIALS AND SELF-CONSISTENT PRISM

5.1 The spinodal curve calculated[32] using PRISM theory for a blend of polyethylene and isotactic polypropylene (NPE=NPP=200). The ratios l_1 and l_2 were estimated from the group contribution tables of Small[86]. The ordinate is a reduced temperature defined as $T^* = k_B T / \varepsilon$ where ε is the united atom, Lennard-Jones parameter for a pair of methylene sites.

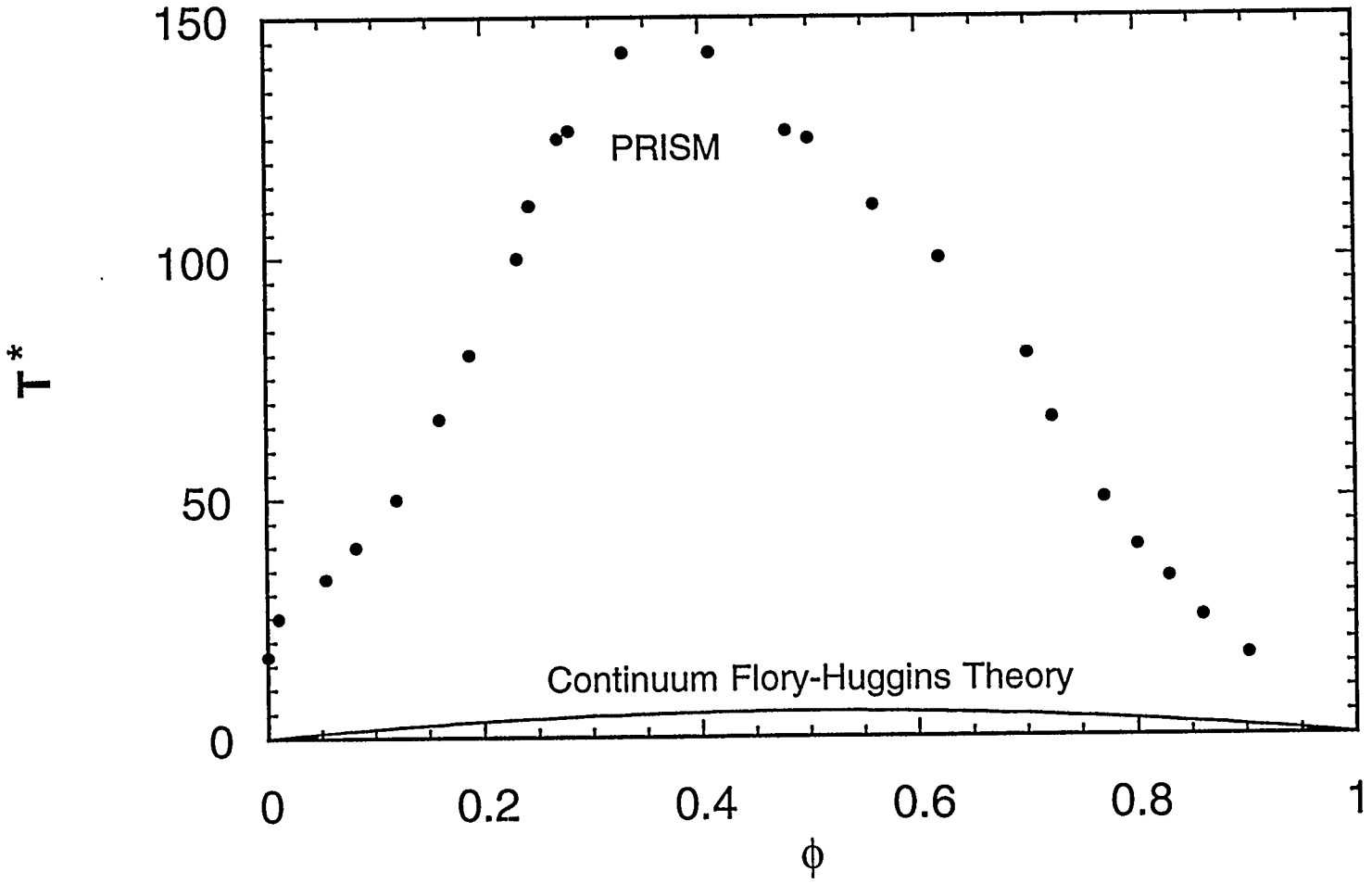

All the theoretical work described so far has assumed "conformational ideality". That is, the intramolecular pair correlations are presumed to be independent of fluid density(and composition in an alloy) and can be computed based on a chain model which only accounts for "short range" interactions between monomers close in chemical sequence. This assumption can fail spectacularly in dilute "good" solution where the effective intrachain monomer-monomer interaction is repulsive in a second virial coefficient sense[1-4]. For such good solvent conditions, the polymer mass/size relationship no longer obeys the ideal random walk scaling law $R \propto N^{1/2}$, but follows the "self-avoiding walk"(SAW) law $R \propto N^{\nu}$ with $\nu \cong 3/5$ corresponding to the "swollen" coil behavior. As the dilute solution is concentrated by increasing a dimensionless measure of monomer concentration (e.g., ρ), the polymers begin to interpenetrate and the excluded volume swelling effect is progressively screened. The precise manner this occurs is predicted by scaling theories[2] to be of a power law form *under large N, semidilute* solution conditions, $R \propto \rho^{-1/8}$, for $\rho^* << \rho << 1$. Here, $\rho = 1$ corresponds to the neat melt, and in good solvents $\rho^* \propto N^{-4/5}$,which represents the "semidilute overlap" density when different chains just begin to touch. The semidilute regime is characterized by strong interchain overlap conditions, but still small *overall* concentration of polymer. At high, melt-concentrations the polymer behaves as an ideal random walk, and it is widely believed(but not proven) that chain dimensions "saturate", i.e. become ρ independent[1-3].

Phenomenological scaling theories, based on analogies with critical phenemena, have been developed to qualitatively describe semidilute solutions in the asymptotic long chain limit($N \rightarrow \infty$)[2] Self-consistent field theoretic approaches have also been constructed by Edwards and co-workers to describe the physical behavior summarized above[3]. However, such theories are based on the most idealized Gaussian thread chain model, and *integrable delta-function* two and three body psuedopotentials between monomers. The latter can loosely be identified as describing effective monomer-monomer interactions in solution at the second and third virial coefficient level; in practice they are treated as empirical parameters. Neither scaling nor field theoretic approaches are appropriate for dense solutions and melts.

As Edwards has recently emphasized[115], a truly microscopic theory of phenomena such as discussed above would be very valuable since it would provide not only quantitative system-specific information, but also could establish the range of validity of phenomenological scaling ansatzes. In this section we summarize recent progress towards this goal in the framework of PRISM and liquid state theory. We note that Chandler and Pratt carried out pioneering work in this area by developing a statistical mechanical framework for the self-consistent calculation of single molecule conformation within the RISM formalism[8,12].

The effective single macromolecule potential surface, U(R), consists of three physically distinct contributions[43]

$$U(\underset{\sim}{R}) = U_0 + U_E + W(\underset{\sim}{R}) \tag{6.1}$$

where $\underset{\sim}{R}$ denotes a complete set of coordinates required to specify the configuration of a polymer molecule composed of N sites. The first term, U_0, describes the "bare" local intramolecular interactions which specify chemical bonding constraints(e.g., fixed bond length and bond angle) and local chain flexibility(e.g., dihedral angle rotations in an atomistic model or bending energy in a SFC model). All the "ideal" models discussed in Section III contain *only* this type of energy term. The second contribution, U_E, describes non-bonded "long range" (in chemical sequence) excluded volume type intramolecular interactions which are taken to be *pair-decomposable*. Under good solvent conditions, U_E favors chain swelling to reduce *intra*molecular repulsive contacts. The third term, W(R), describes the "solvation free energy", i.e. the reversible work required to achieve a configuration R in the condensed phase due to *inter*molecular solute-solvent potentials only. In principle, this solvation potential is an N-body function. However, mathematical tractability would seem to require reduction to an (effective) pair-decomposable form, i.e.

$$W(\underset{\sim}{R}) = \sum_{\alpha<\gamma=1}^{N} W_{\alpha\gamma}(|\bar{r}_\alpha - \bar{r}_\gamma|) \tag{6.2}$$

All work to date has employed this simplification.

Pratt, Chandler, and others have developed and applied approximate "solvation potentials" for flexible n-alkane fluids such as butane and decane and other relatively small molecules[2,116,117]. The original approaches invoked a "superposition" approximation[12], which in its most naive form corresponds to assuming pair decomposability of W(R) *and* calculation of the effective pair potential based solely on consideration of the two sites. A more accurate solvation potential approach was then developed by Chandler and coworkers[23,24] in the context of a quantum electron in dilute (classical) solution which led to new and more accurate self-consistent approximations for the effective pair potential in W(R)[117]. This work represents the starting point for our self-consistent PRISM-based studies of polymer fluids,and the development of novel solvation potential approximations required for an adequate qualitative treatment of some macromolecular systems.

A. Solvation Potential Theories

Chandler et.al have proposed a self-consistent pair interaction, called the "Gaussian fluctuation"(GF) potential, of the form[23,24]

$$\beta W_{\alpha\gamma}(r) = -\sum_{\lambda\delta}\int d\vec{r}'\int d\vec{r}''C_{\alpha\lambda}(|\vec{r}-\vec{r}'|)S_{\lambda\beta}(|\vec{r}'-\vec{r}''|)C_{\delta\gamma}(r'') \qquad (6.3)$$

where $S_{\alpha\gamma}(r)$ is the total density-density correlation function between sites α and γ separated by a distance r. For molecules composed of symmetry equivalent sites Eq(6.3) simplifies in Fourier space to

$$-\beta\hat{W}(k) = -\hat{C}^2(k)\hat{S}(k) \qquad (6.4)$$

This approximate form can be derived many ways : from renormalized second order perturbation theory[23], Gaussian(linear response) density field theory[23], or via density functional expansions[44,118]. Pictorially, the medium-induced potential between a pair of tagged sites is determined by coupling to the surroundings via an effective potential (direct correlation function) which is mediated by density fluctuations of the condensed phase. The integrated strength of the medium-induced potential is

$$\hat{W}(k) = -k_B T \hat{C}^2(0)\hat{S}(0) = -\frac{1}{\rho^2 \kappa_T} \qquad (6.5)$$

where the second equality follows from use of the PRISM Eq(2.2). Eq(6.5) shows W(r) is (on average) attractive favoring compressed polymer conformations, and hence will tend to cancel or "screen" the expansive consequences of the bare intramolecular repulsions. Thus, the effective attraction is expected to become stronger as fluid density increases, chain length decreases, and/or polymer backbone stiffness increases, since all these changes enhance intermolecular packing and reduce bulk compressibility. Moreover, W(r) becomes increasingly structured(e.g. oscillatory) as the above changes are made[24,43].

The basic feature of a self-consistent mean pair approximation such as Eqs(6.2) and (6.3) is that the effective interaction between two sites on the polymer depends on their instantaneous position, and only on the entire macomolecule conformation in an *average* (implicit) sense via the direct and collective pair correlations. This simplification does *not* preclude describing situations of broken conformational symmetry, such as polymer collapse, solvated electron localization, or inhomogeneous conformational characteristics such as occur in star polymers(see section IX below)[23,24,46].

Grayce and Schweizer[46], based on graph theoretical and hueristic arguments, suggested a modified form for the solvation potential("PY-style") which is in the spirit of the Percus-Yevick closure

$$\beta W^{PY}_{\alpha\gamma}(r) = -\ln\left[1 + \int d\vec{r}' \int d\vec{r}'' C(|\vec{r} - \vec{r}'|) S(|\vec{r}' - \vec{r}''|) C(r'')\right] \qquad (6.6)$$

Eq(6.3), by contrast, was argued to be in the HNC closure spirit ("HNC-style" solvation potential). On general grounds, one expects the PY-style solvation potential to be *weaker (e.g., less compressive)* than its HNC-style analog. However, the two solvation potentials do become equal in the limit of weak interactions, $\beta W(r) << 1$. This limit may occur for many reasons such as high temperature, low fluid density, and/or large intersite separations. Moreover, the theoretical *model* adopted (e.g. thread, SFC,RIS) and/or the

statistical mechanical approximations invoked may result in such a weak coupling regime for differing regimes of thermodynamic state.

For simple fluids[5], the PY and HNC closure approximations are useful in different contexts, and this is probably also true of the corresponding solvation potentials. Based on analogies with atomic and small molecule liquids, and homopolymer fluids, one might expect the PY potential is better for bare interactions which are spatially short-ranged and repulsive[46]. This is the situation for the polymer/good solvent system of present interest. However, one might expect that the HNC-style potential is useful for longer-range, more slowly varying potentials such as Coulombic or possibly Lennard-Jones attractive tails. The role of macromolecular architecture(or precise single polymer model) in such qualitative ideas may be subtle and is not well understood at present.

B. Self-Consistent Solution of Single Macromolecule Problem

Implementation of self-consistent PRISM theory requires addressing the difficult technical question of how to iteratively solve the effective N-body single polymer problem with "long range" intramolecular interactions, *in conjunction* with PRISM theory for interchain pair correlations and hence the solvation potential itself. For the homopolymer/good solvent problem, successful field theoretic approximate approaches have been developed[2-4]. However, these methods *explicitly* rely on the use of an *integrable*, delta-function psuedopotential description of segment-segment interactions within an *effective* Gaussian thread framework. The use of more realistic models with local chemical constraints and a finite chain thickness (hard core constraint) requires the development of different approaches.

Over the past several years, we and our collaborators have constructed and applied several approaches[43-47] which vary greatly in both computational convenience and level of statistical mechanical approximation. These various approaches often have distinct(and often limited) regimes of applicability and level of accuracy. Here we sketch the essential physical features and statistical mechanical approximations of the different numerical approaches.

1. Single Chain Monte Carlo

The most rigorous *and* computationally demanding approach to solving the statistical mechanics of an effective Hamiltonian given by Eqs(6.1) and (6.2) is to perform a *single chain* Monte Carlo simulation in the framework of a self-consistent PRISM calculation. This approach was first explored by Melenkevitz et.al. using a standard "kink-jump" algorithm[44], and subsequently by Grayce, Yethiraj and Schweizer[47] using the more accurate "pivot algorithm"[119].

Although straightforward in principle, and much simpler than a many chain simulation, there are several practical difficulties associated with proper sampling and equilibration. For example, at high fluid densities the solvation pair potential is strong and oscillatory (see Figure 6.1) which makes sampling and equilibration difficult. Early work using the kink-jump method was found to fail at such high densities[44], and the pivot algorithm with its "long range moves" was required for proper statistical sampling[47].

2. Free Energy Variational Approaches

A simpler, analytic approach is to employ the standard idea of replacing the real system with a computationally tractable "reference system" (polymer chain model in our case), the parameters of which are variationally optimized using an approximate single chain free energy expression. Two such schemes have been explored[45,47], which differ in *both* the choice of reference chain model and the form of the approximate free energy.

Earlier work by Melenkevitz et. al.[45] was based on the standard Gibbs-Bogoliubov inequality for the single chain free energy

$$\beta F \le \beta F^{o} + \sum_{\alpha<\gamma=1}^{N} \int d\bar{r} \beta \Delta\phi_{\alpha\gamma}(r) \omega^{o}_{\alpha\gamma}(r) \qquad (6.7)$$

where $\omega^{o}{}_{\alpha\gamma}(r)$ is the *reference system* intrachain pair correlation function matrix, and $\Delta\phi_{\alpha\gamma}(r)$ is the *difference* in single chain effective interaction pair potential between the real and reference systems.

In numerical applications, the "solvent" is treated as a vacuum, i.e. it enters solely in determining the polymer concentration or packing fraction η. Thus, the real two-component polymer/solvent mixture is abstracted to a

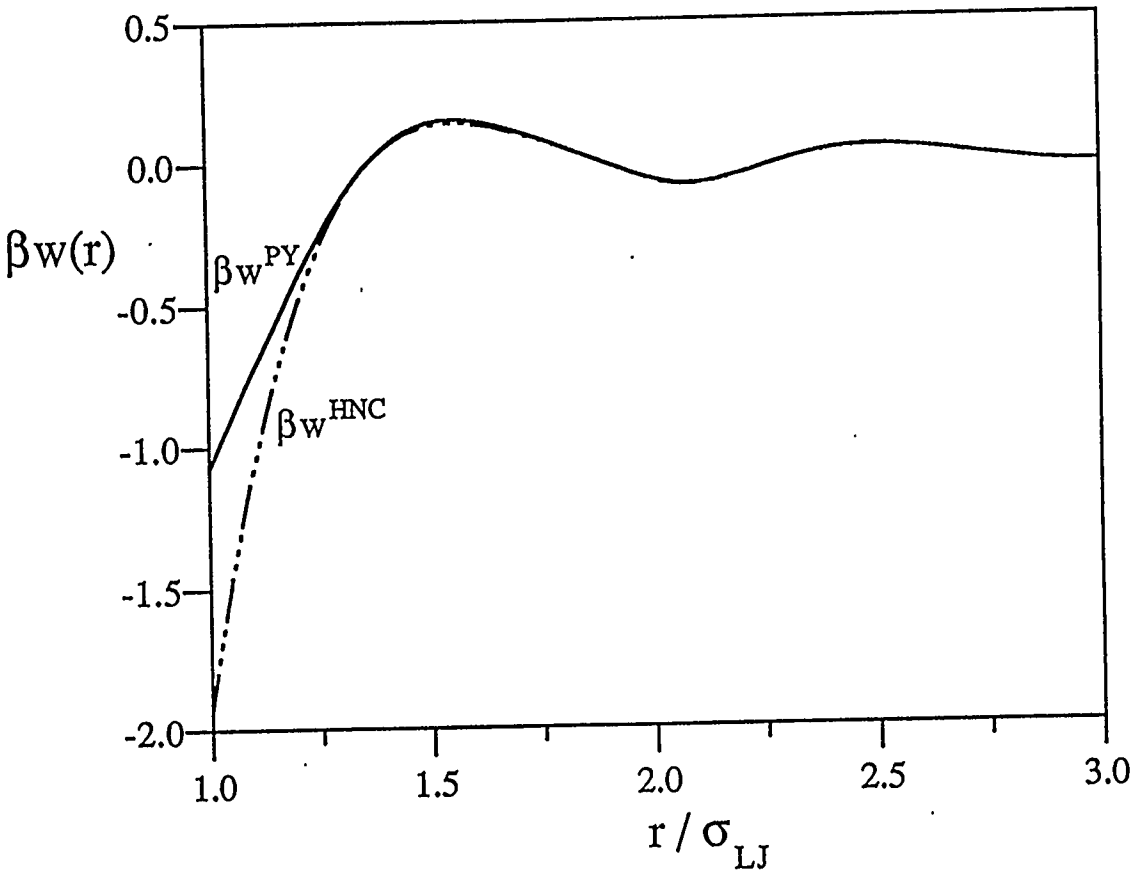

6.1 Typical high density($\rho\sigma_{LJ}^3 = \beta\varepsilon_{LJ} = 1$) medium-induced potential between monomers of a repulsive Lennard-Jones N=100 chain as predicted by self-consistent PRISM theory based on the HNC-style and PY-style solvation potentials and the variational generating functional method[47].

one-component polymer fluid of variable density. For the homopolymer/good solvent system, the reference system is chosen to be an *ideal* SFC(as computed with the discrete Koyama approximation)[55] with an effective, or "renormalized", bending energy ε_r. The repulsive interactions between sites separated by two bonds ($\omega^0_{\alpha,\alpha+2}(r)$) is also included in the reference system and treated *exactly*. Thus, the effective bending energy describes both the *bare* bending efficiency of the real chain, plus the combined consequences of the bare intramolecular repulsions and medium-induced potential. Since the explicit effect of intrachain excluded volume is absent in the ideal SFC model, it is introduced *approximately* by defining an effective bond length , l_{eff} , determined such that in the dilute solution limit SAW scaling for $<R^2>$ is recovered. This approach is in the spirit of field theoretic studies[3], and is capable of treating the entire polymer concentration regime in good solvents. Values of the density-independent quantity l_{eff} as a function of N are determined from Monte Carlo simulation of a *single self-avoiding* chain[45]. Explicit forms of Eq(6.7) for this model and variational theory are given elsewhere[45] ; it is important to mention that the bare (singular) intrachain repulsions are *omitted* in the evaluation of $\Delta\phi_{\alpha\gamma}(r)$ in Eq(6.7).

More recently, a second free energy variational approach has been developed by Grayce,Yethiraj and Schweizer[47] An approximate single chain free energy is constructed in the spirit of a functional expansion about an ideal reference state with an explicit accounting of intrachain excluded volume. The latter cannot be naively treated via perturbation theory since it is singular and nonintegrable for the finite hard core diameter models of interest. Rather, a virial-like treatment of the nonbonded intrachain repulsions and medium-induced potentials is employed by carrying out an expansion about an ideal reference system through second order in the appropriate Mayer f-bonds.

In applications, the reference system is again chosen as an ideal SFC with renormalized bending energy ε_r ,and next-nearest neighbor pair correlations, $\omega^0_{\alpha,\alpha+2}(r)$, exactly computed. The resulting approximate single chain free energy is[47]

$$\beta F(\varepsilon_r,\varepsilon_{eq}) \approx \beta F^0(\varepsilon_r) + \beta \int d\bar{r} \sum_{\alpha=1} \omega^0_{\alpha,\alpha+2}(r;\varepsilon_r) \quad \Delta\phi_{\alpha,\alpha+2}(r)$$
$$- \sum_{\alpha+2<\gamma} \omega^0_{\alpha,\gamma}(r;\varepsilon_r)\left[-1+\exp(-\beta\Delta\phi_{\alpha\gamma}(r)\right] \qquad (6.8)$$

where $\Delta\phi_{\alpha\gamma}(r) = u(r) + W(r;\varepsilon_{eq})$ for $|\alpha-\gamma| \geq 3$ (where u is the bare intrapolymer "excluded volume" potential), and $\Delta\phi_{\alpha\gamma}(r)$ also includes the difference between the bare and renormalized bending potential for $|\alpha-\gamma| = 2$. Here, ε_{eq} and ε_r must be determined self-consistently by free energy minimization and a recursive generating functional procedure[47]. Under certain conditions it is possible to bypass this process by treating W not as an external field but as a functional of the intrachain correlations, and therefore directly minimizing F. That is, $\varepsilon_{eq} = \varepsilon_r$ is enforced at the start of the self-consistent iteration procedure and $F(\varepsilon_r)$ is mimimized. Such a "direct" method[47] is generally much faster to numerically implement than the full recursive procedure. As a matter of priniciple it does not yield the same predictions as the recursive approach, but in applications studied to date *based* on the PY-style solvation potential the results are quite similiar(see section C).

Both the accuracy of variational approaches and their range of applicability are expected to depend strongly the physical problem, thermodynamic state conditions, and the choice of reference system and form of the approximate free energy. The approach of Melenkevitz et. al.[45] is relatively crude, but is expected to be qualitatively useful over the entire range of polymer concentration and degree of polymerization. The approach of Grayce et. al.[47] is more general with regards to describing the chemical structure of macromolecules, but by construction is not capable of recovering the SAW dilute solution behavior due to the perturbative(in an f-bond sense) treatment of intrachain excluded volume interactions. Thus, this approach is expected to be most appropriate for dense solutions and melts, and hence is complementary to the heavily coarse-grained scaling and field theoretic approaches[2-4].

3. Optimized Perturbation Theory

The first self-consistent PRISM studies by Schweizer, Honnell and Curro[43] considered only the HNC-style solvation potential and were based

on an "optimized pertubative", not variational, determination of the ideal reference system effective bending energy. The starting point is a simple functional expansion of the true single chain free energy about an ideal reference system[43]

$$\beta F = \beta F^{o} + \sum_{\alpha>\gamma}^{N} \int d\bar{r} \frac{\delta \beta F}{\delta f_{\alpha\gamma}(r)}\Bigg]_{o} \left[f_{\alpha\gamma}(r) - f^{o}_{\alpha\gamma}(r) \right] + \ \ldots \qquad (6.9a)$$

where the full and reference Mayer f-bonds are

$$\begin{aligned} f_{\alpha\gamma}(r) &\equiv \Theta_{+}(r-d)\exp\left[-\beta(v_b(\varepsilon_o)+W)\right]-1\,, \quad |\alpha-\gamma|=2 \\ &\equiv \Theta_{+}(r-d)\exp(-\beta W)-1\,, \quad |\alpha-\gamma|\geq 3 \end{aligned} \qquad (6.9b)$$

$$\begin{aligned} f^{o}_{\alpha\gamma}(r) &\equiv \Theta_{+}(r-d)\exp\left[-\beta v_b(\varepsilon_r)\right]-1\,, \quad |\alpha-\gamma|=2 \\ &\equiv 0\,, \quad |\alpha-\gamma|\geq 3 \end{aligned}$$

, where ε_o is the bare SFC bending energy which quantifies the potential v_b, and ε_r is the corresponding renormalized value of the reference system. The required functional derivative (evaluated in the reference system) is easily determined. The reference system effective bending energy is chosen by requiring the first correction to F-F^o vanishes. This scheme is analagous to well-known "blip-function" theories of Chandler, Weeks and Andersen[5,11] for determining a hard core diameter of soft repulsive force simple fluids. Such a simple approach is *not* adequate for *low* polymer densities and does not recover SAW scaling in the dilute limit. It is believed to be most adequate for describing "small" nonideal conformational corrections, e.g. nearly melt-like conditions. Moreover, this non-variational approach can only be implemented for ideal reference systems characterized by only *one* parameter, and it has been shown to *not* properly describe the *rigid rod* limit where all condensed phase modifications of chain conformation must vanish[43].

C. Theory/Simulation Comparisons for Homopolymer Good Solutions

The best test of self-consistent PRISM theory and the different solvation potential approximations is via comparison of its predictions against exact computer simulation studies of the *same model*. The drawback is that

present computer power limits such comparisons to short and intermediate length chains(N less than roughly 200). Many detailed comparisons have been carried at all levels of approximation discussed in section B. Here we give a few examples and along with summarizing remarks. The reader is refered to the original papers for details and a complete discussion.

Two similiar freely-jointed(zero bare bending energy) models of a homopolymer/solvent system have been studied by many-chain simulation. Yethiraj and Hall[60] investigated a purely hard core, tangent bead model for N = 20 -100 and monomer packing fractions of η = 0.1 - 0.35(concentrated solution). A shifted repulsive Lennard-Jones model of nearly tangent chains has been studied by Kremer and Grest(N=20-200 at fixed $\eta \cong 0.45$) and by Gao and Weiner[158](N=16, η = 0.1 - 0.47). The intramolecular structure factor $\hat{\omega}(k)$ and chain-averaged g(r) were monitored, along with average chain dimensions R and R_g. Here we focus on R_g, which for dense solutions is also a direct measure of the chain persistence length or stiffness.

We begin with the most "rigorous" version of self-consistent PRISM based on a Monte Carlo evaluation of the effective single chain problem. Theoretical predictions of Grayce, Yethiraj and Schweizer[47] are compared with many chain simulation results for the mean square end-to-end distance of the hard core chain model as a function of polymer packing fraction in Figures 6.2 for N=20 and 100. (The corresponding *estimates* of the dilute-semidilute crossover points are $\eta^* \cong 0.06$ and 0.015, respectively.) *Over* the many chain simulation range of density studied, the PRISM/Monte Carlo results based on the pivot algorthim and full self-consistent evaluation of $\omega(k)$ are in good (but not perfect) agreement with the simplified self-consistent PRISM/Monte Carlo approach of Melenkevitz et. al.[45] based on the kink-jump algorithm. Moreover, the theoretical predictions based on both the HNC-style and PY-style solvation potential are in *qualitative* agreement with the exact results. Motivated by blob scaling arguments for *semidilute* solutions[2], the density dependence of $\langle R^2 \rangle$ was fit to a power law form : $\langle R^2 \rangle \propto \eta^{-\alpha}$ for $0.1 < \eta < 0.35$. Over this very limited range, the power law form is adequate and an exponent in agreement(to within statistical error) with the many chain simulation value[60] of 0.25 $\pm$ 0.1 was found. The latter value is consistent with the long chain blob

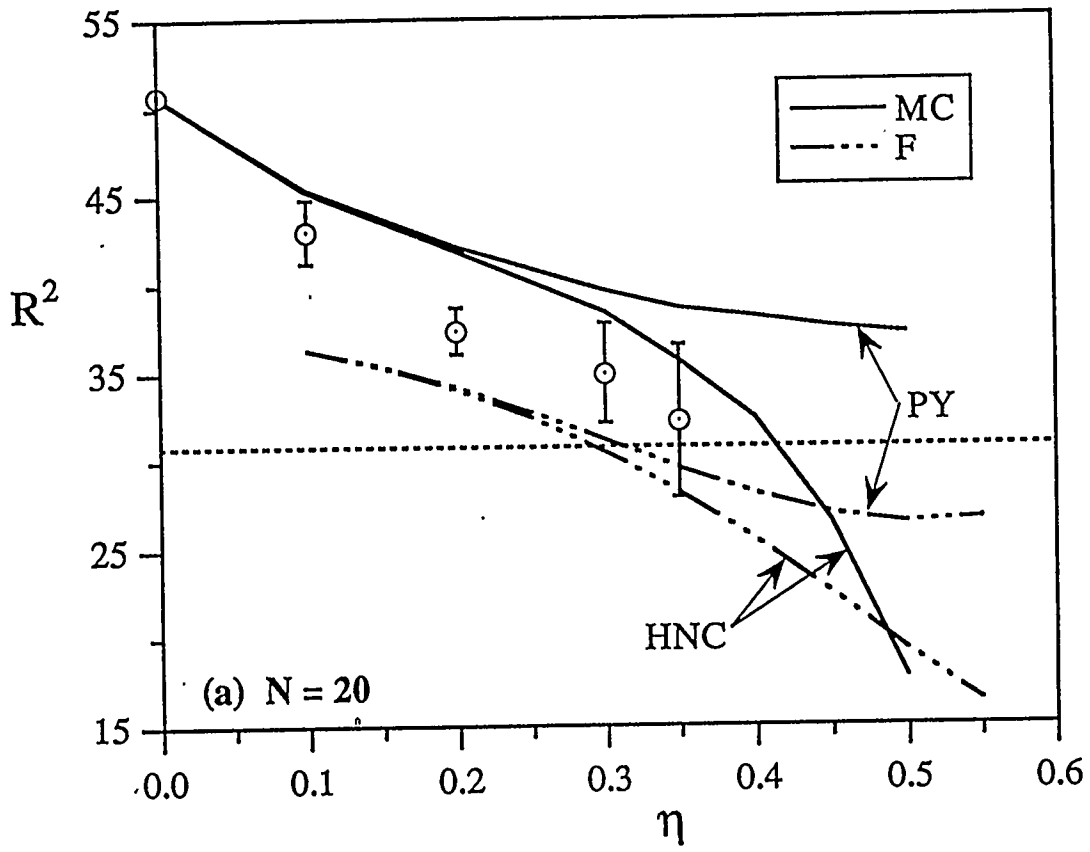

6.2a The change with polymer density of the mean square end-to-end distance of hard core chains of length N=20. The data points are exact many chain simulation results[60] and the solid (dash-dot) lines are the self-consistent PRISM/Monte Carlo (free energy generating functional) predictions using the two solvation potentials[47]. The dashed horizontal line is the value of R^2 for an ideal freely joined chain *with* a minimum next nearest neighbor bending angle of 60° which mimic the local hard core repulsion.

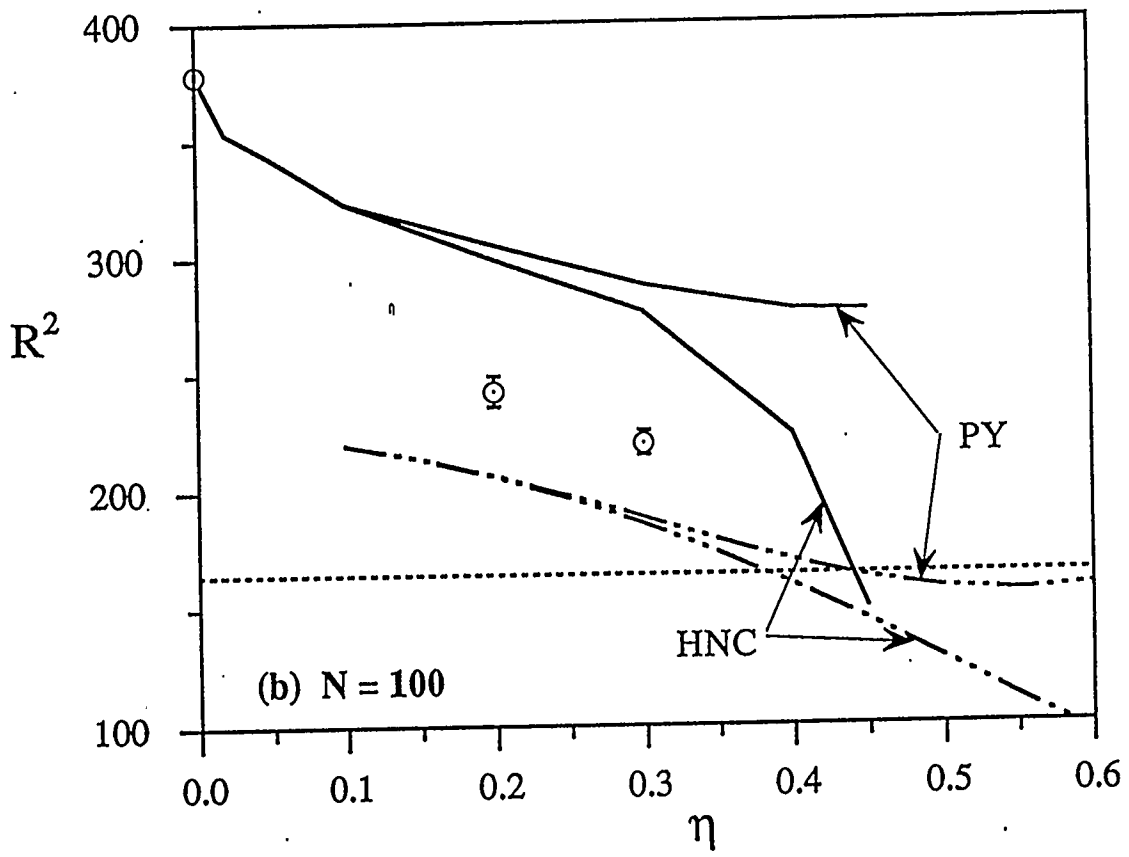

6.2b The change with polymer density of the mean square end-to-end distance of hard core chains of length N=100. The data points are exact many chain simulation results[60] and the solid (dash-dot) lines are the self-consistent PRISM/Monte Carlo (free energy generating functional) predictions using the two solvation potentials[47]. The dashed horizontal line is the value of R^2 for an ideal freely joined chain *with* a minimum next nearest neighbor bending angle of 60° which mimic the local hard core repulsion.

scaling prediction, but the agreement may be accidental since the chains studied are rather short and the density regime very limited.

Quantitatively, the calculations based on the HNC-style solvation potential appear to be superior *for the density range studied by the full many chain simulations*. This is misleading, however, since(as seen in Figure 6.2) the more compressive HNC-style solvation potential leads to a very strong, rapidly varying reduction of chain dimensions at high concentrations. This behavior conflicts with basic Flory arguments[1-3] and the limited experimental data available suggesting that chain dimensions tend to saturate, or at least become very slowly varying in dense melts[121,122]. Examination of typical chain configurations in the PRISM Monte Carlo calculation based on the HNC style solvation potential reveals a form of local collapse, or condensation, of closely bound sites along the chain[44,47].

Further comparisons are given in Table 3 for relatively dense solutions and two values of N. Note that the polymer size is very different than the ideal freely-jointed, ideal Koyama with local swelling, or the self-avoiding walk behavior. The accuracy and predicted trends of the HNC-style and PY-style approaches are relatively(but not completely) insensitive to N over the range of 20-100 for the choice of purely hard core interactions. Summarizing, it appears the HNC-style solvation potential predicts too strong a compressive solvation force at high densities and is inadequate in this regime. Based on all the studies to date[44,47], the PY-style solvation potential coupled with PRISM/Monte Carlo seems qualitatively sensible under all conditions, and typically makes errors of 10-20% in the prediction of the *absolute* magnitude of R^2 and R_g^2. *Relative* trends seem to be predicted significantly more accurately.

****

Table 3. Mean squared end-to-end distances, R^2, in units of the hard core diameter of N=20 and 100 linear hard core chains at several packing fractions η. The many chain simulation results of Yethiraj and Hall[60] are listed along with theoretical predictions based on various approximate implementations of the self-consistent PRISM scheme described in detail in the text[47]. MC refers to the single chain Monte Carlo method and F refers to the variational generating functional method. The HNC or PY in parentheses refers to the style of solvation potential approximation

employed. Percent error of the theoretical predictions relative to the simulation values are also listed. For the simulation data the percentage error gives the statistical margin of error.

	$\eta = 0.2$, N=100		$\eta = 0.3$, N=100		$\eta = 0.35$, N = 20	
Method	R^2	**% error**	R^2	**% error**	R^2	**% error**
Simulation	242.5	±2.7	220.1	±2.1	32.2	±13.3
MC (HNC)	299.6	23.5	276.7	25.7	35.7	10.7
MC(PY)	305.4	26.0	288.3	31.0	38.6	19.9
F(HNC)	206.1	-15.0	185.7	-15.6	28.2	-12.5
F(PY)	206.5	-14.9	188.4	-14.4	29.6	-8.2
F(HNC) [a]	221.2	-8.8	201.3	-8.5	30.4	-5.6
F(PY) [a]	220.8	-8.9	200.6	-8.8	30.7	-4.8
S.A.W.[b]	348.5	43.7	348.5	58.3	50.8	57.6
F.J.C.[c]	99.0	-59.2	99.0	-55.0	19.0	-41.1
S.F.C. [d]	164.1	-32.3	164.1	-25.4	30.8	-4.5

[a]Using a direct minimization of F as described in text and Appendix of ref. 47

[b]Value for a self-avoiding random walk

[c]Value for an ideal freely-jointed chain.

[d] Value for the SFC model with local intrachain repulsion between next nearest neighbors included.

****

The predictions of the variational free energy method(see Eq(6.8)) of Grayce et. al.[47] are also listed in Table 3. Results are shown for both the rigorous generating functional approach and the more approximate, but computationally simpler, "direct" minimization scheme. Reasonable agreement between the two technical implementions are found. Generally, the generating functional method predicts consistently smaller polymer sizes than found based on the Monte Carlo method. This is true for both the HNC and PY-style potentials, and presumably reflects nonideality effects lost by the truncation of the virial expansion in Eq(6.8) and by the assumption of ideal trial conformations invoked by the generating functional approach. For the shifted repulsive Lennard-Jones models(not

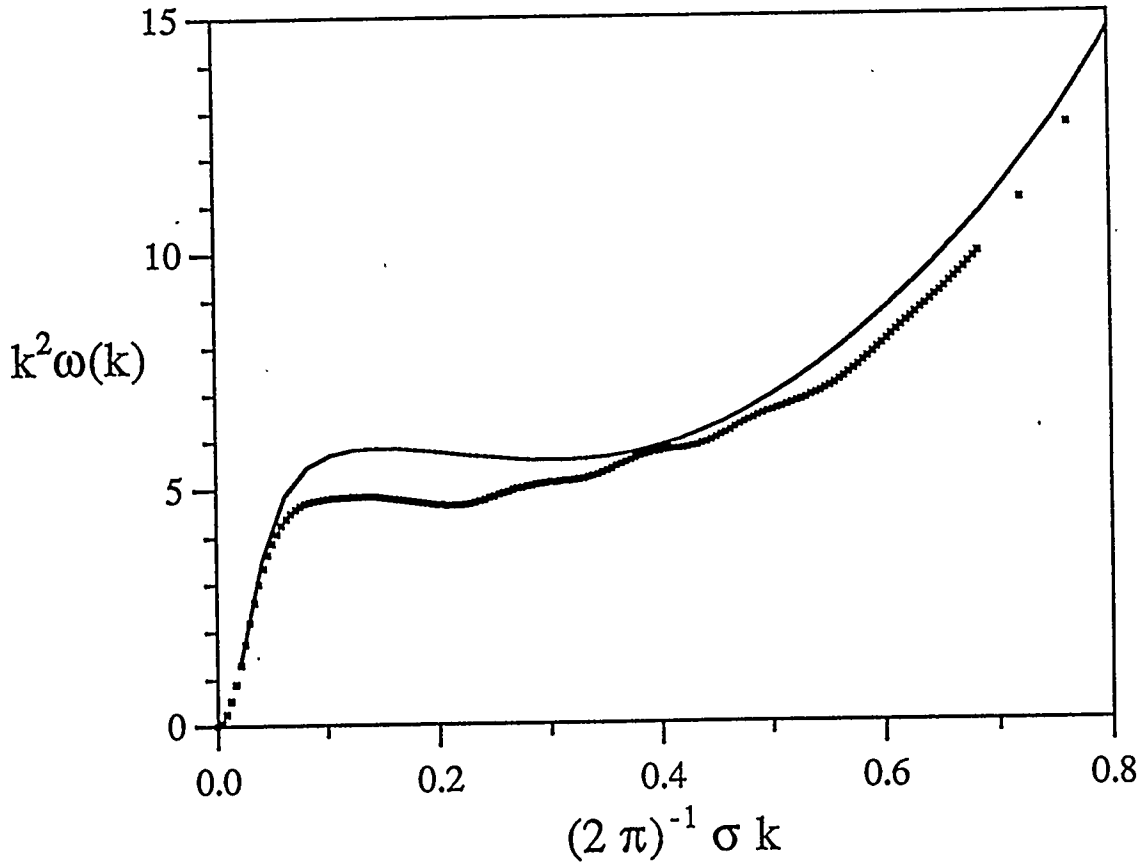

6.3a Self-consistent PRISM structural predictions for the average intramolecular structure factor plotted in Kratky form for N=100 hard core chains at a concentrated solution packing fraction of 0.3. The points are the many chain simulation results[60] and the lines are the PRISM results based on the PY-style solvation potential and the simplified version of the variational generating functional method of Grayce et.al. discussed in the appendix of ref. 47.

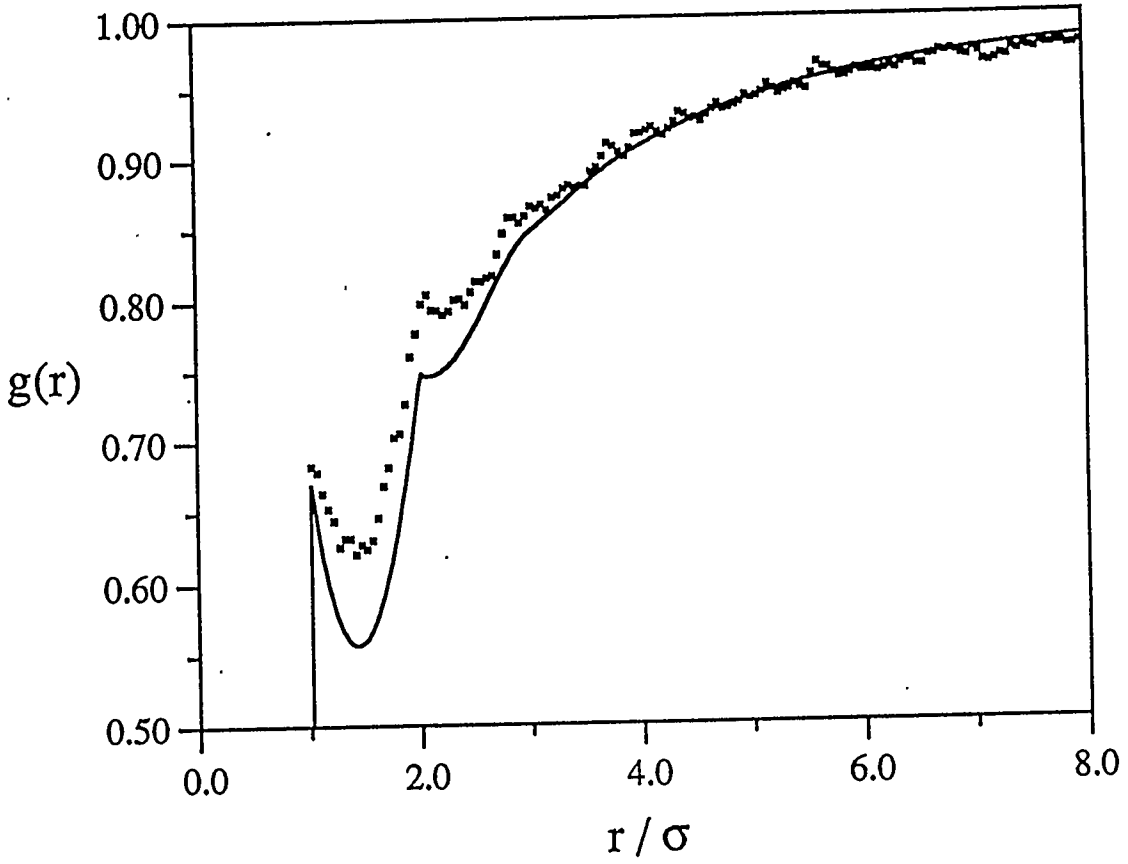

6.3b Self-consistent PRISM structural predictions for the site-site intermolecular radial distribution function for N=100 hard core chains at a concentrated solution packing fraction of 0.3. The points are the many chain simulation results[60] and the lines are the PRISM results based on the PY-style solvation potential and the simplified version of the variational generating functional method of Grayce et.al. discussed in the appendix of ref. 47.

employed. Percent error of the theoretical predictions relative to the simulation values are also listed. For the simulation data the percentage error gives the statistical margin of error.

	$\eta = 0.2$, N=100		$\eta = 0.3$, N=100		$\eta = 0.35$, N = 20	
Method	R^2	**% error**	R^2	**% error**	R^2	**% error**
Simulation	242.5	±2.7	220.1	±2.1	32.2	±13.3
MC (HNC)	299.6	23.5	276.7	25.7	35.7	10.7
MC(PY)	305.4	26.0	288.3	31.0	38.6	19.9
F(HNC)	206.1	-15.0	185.7	-15.6	28.2	-12.5
F(PY)	206.5	-14.9	188.4	-14.4	29.6	-8.2
F(HNC) [a]	221.2	-8.8	201.3	-8.5	30.4	-5.6
F(PY) [a]	220.8	-8.9	200.6	-8.8	30.7	-4.8
S.A.W.[b]	348.5	43.7	348.5	58.3	50.8	57.6
F.J.C.[c]	99.0	-59.2	99.0	-55.0	19.0	-41.1
S.F.C. [d]	164.1	-32.3	164.1	-25.4	30.8	-4.5

[a]Using a direct minimization of F as described in text and Appendix of ref. 47

[b]Value for a self-avoiding random walk

[c]Value for an ideal freely-jointed chain.

[d] Value for the SFC model with local intrachain repulsion between next nearest neighbors included.

The predictions of the variational free energy method(see Eq(6.8)) of Grayce et. al.[47] are also listed in Table 3. Results are shown for both the rigorous generating functional approach and the more approximate, but computationally simpler, "direct" minimization scheme. Reasonable agreement between the two technical implementions are found. Generally, the generating functional method predicts consistently smaller polymer sizes than found based on the Monte Carlo method. This is true for both the HNC and PY-style potentials, and presumably reflects nonideality effects lost by the truncation of the virial expansion in Eq(6.8) and by the assumption of ideal trial conformations invoked by the generating functional approach. For the shifted repulsive Lennard-Jones models(not

shown), the PY-style approach is much more accurate than the HNC-style, and significantly more accurate(typical errors of 5-8%) in an absolute sense than for the hard core models(typical errors of 14-19%).

The gross qualitative trend of the HNC-style potential predicting much too small, "collapsed" conformations at high density is again found based on the approximate variational/generating functional approach of Grayce et.al.[47] A more traditional polymer science demonstration of the origin of this fact is the trend with polymer density of the *monomeric* second virial coefficient, defined in normalized dimensionless form as

$$v_o \equiv -\frac{3}{4\pi\sigma^3}\int d\vec{r}[\exp[-\beta\{u(r)+W(r)\}]-1] \qquad (6.10)$$

where u(r) is the bare intrachain, and W(r) is the solvation, pair potential between nonbonded sites. Traditionally, v_o is taken as a measure of "solvent quality" , with positive values indicating a good solvent and coil swelling, negative values indicating a poor solvent and a collapsed conformation, and a zero value defining an ideal, "theta" state[1-4]. It has been shown based on the generating functional approach that $v_o > 0$ for the PY-style potential, and approaches zero gradually at high melt densities consistent with the Flory concept of the melt as a theta solvent[47]. However, for the HNC-style potential v_o changes from positive to negative around $\eta \cong 0.4\text{-}0.45$, consistent with the observation of overly compressed polymer dimensions.

Comparisons between theory and exact many-chain simulations have also been carried for the structural properties g(r) and $\hat{\omega}(k)$ by Grayce, Yethiraj and Schweizer based on the PY-style potential and the variational generating functional method[47]. An example is given in Figures 6.3 for N=100 and the medium-density case of $\eta = 0.3$. The general shape of $\hat{\omega}(k)$ is well-predicted by the effective SFC ideal model, although the "plateau" at intermediate wavevectors is too high since the theory underpredicts chain dimensions(see Table 3) and hence local stiffness. Other comparisons suggests improved agreement of both g(r) and $\hat{\omega}(k)$ (see, for example, Fig. 3.3) at higher, melt-like densities where the chains are conformationally more ideal, and where the differences between self-consistent and non-self-consistent PRISM predictions become incresingly small.

Based on the all the above results, and many others not shown, it has been demonstrated that the generating functional method(with PY-style solvation potential) is more accurate at high densities than the single chain Monte Carlo/PRISM method when compared against the exact many chain simulation results. This suggests the additional approximations employed by the generating functional method compensate for other errors in the PRISM-based theory. Thus, the generating functional method at high density seems complementary to the PRISM/Monte Carlo method since the computational demands of the latter become very heavy at high densities and /or high N.

Application and generalization of the self-consistent PRISM theory to flexible trimer fluids, and detailed comparison with many molecule simulations, has also been performed by both Grayce and dePablo[42], and Yethiraj[123].

Finally, we briefly summarize the first application of self-consistent PRISM theory by Schweizer, Honnell and Curro based on the HNC-style potential and a simple optimized pertubation("blip function") approach[43]. Detailed comparisons of the predicted chain dimensions and g(r) for the N=50,100 and 150 repulsive Lennard-Jones fluid model of concentrated solutions studied by Kremer and Grest[51] have been carried out. R^2 was predicted to be 3-7% *too small,* and in all cases deviations from ideal behavior(SFC with next nearest neighbor 1-3 repulsions explicitly accounted for) was extremely weak. The self-consistently determined g(r) was in excellent agreement with simulations except near the first peak where the theory underestimated the maximum by roughly 10% as a consequence of the underpredicted chain dimensions and hence local stiffness. A key finding here is that at very high melt-like densities, all but the most local aspects of intrachain repulsion (and concommitant swelling) are screened out consistent with the basic tenets of the Flory ideality ansatz. Thus, as expected, the need for a fully self-consistent theory becomes far less important under high density conditions. However, the fact that such "reasonable" behavior is found based on the HNC-style potential is again an indication of the subtle role played by the approximate single chain theory, choice of reference system, and solvation potential in determining the theoretical predictions for the screening problem.

D. Numerical and Analytic Model Calculations

Besides benchmark comparisons with exact simulation results, model calculations have been performed to numerically explore additional issues.

(1) The large N behavior, inaccessible to many chain simulation(and very difficult for PRISM/Monte Carlo), but relevant to experiments and field theoretic and scaling predictions, has been studied numerically based mainly on the HNC-style/variational approach of Melenkevitz, Curro and Schweizer.[45] For fixed large N of the order of 10^3, a power law scaling behavior of $<R^2>$ with density has been found for intermediate(semidilute) solution densities in rough accord with phenomenological scaling predictions[2]. The question of global screening of intrachain excluded volume interactions, as quantified in the effective exponent ν in the relationship $<R^2> \propto N^{\nu}$, has also been studied. Over a range of N values less than or equal to 2000, Melenkevitz et. al.[45] find $\nu \cong 0.56$ for η=0.4 (intermediate between the ideal 0.5 and SAW 0.6 values), $\nu \cong 0.51$ for η=0.54 (melt-like), and $\nu \cong 0.50$ for higher liquid packing fractions in agreement with the Flory ideality hypothesis. The latter result has also been derived based on the Edwards psuedopotential field theoretic method[3], but is a highly nontrivial achievement for a microscopic theory based on *non*integrable, singular hard core interactions between monomers. Thus, a truly microscopic basis for the ideality and semidilute scaling ideas has been established, and the nature of the corrections and limitations of these simple concepts can be elucidated.

(2) The subtle question of "incomplete" screening of the excluded volume swelling at very high densities has been studied by several PRISM based approaches[43,45,47]. At issue is whether chain dimensions approach a density-independent value, and whether it is truly "ideal", in the high packing fraction limit. Experiments are unclear on this point[122], and PRISM studies yield differing conclusions depending on solvation potential choice and approximate free energy based scheme to evaluate the effective single chain problem. Benchmark simulations which address this question would be of great value.

(3) The subtle question of whether the *relative* changes in polymer dimensions as a function of solution density become N-independent in the semidilute and concentrated regime has been considered by Grayce et.al.[47] within the PY-style/generating function framework.

(4) The question of how variable bare chain stiffness(aspect ratio) influences the predicted nonideal conformational corrections. Predictions of the renormalized persistence length, relative to its bare value, have been obtained by Grayce and Schweizer[124] based on the PY-style solvation potential and the variational generating functional method, and also by Schweizer, Honnell and Curro[43] based on the optimized perturbation approach and the HNC-style potential. At high densities the predicted renormalizations are rather modest(typically ± 10 % or less). The most interesting feature is the nonmonotonic dependence of the renormalization ratio or bare persistence length, indicating a crossover from the condensed phase effects favoring chain compression(relative to the ideal limit) to a type of "induced rigidity". The latter is a subtle consequence of the emergence of strong solvation shells in the liquid for stiff polymers at high density. However, we do not overly emphasize this feature for two reasons: (i) for high aspect ratio chains nematic/orientational correlations are expected to become increasingly important, a physical feature not properly described by RISM-based approaches[8,38-40] ; (ii) the theories[43,47] do not properly recover the "trivial" rod limit where the renormalization ratio should approach unity. Many chain simulations would be particularly helpful in guiding the further development of the self-consistent approach for such semiflexible polymer systems.

Finally, we point out that *analytic* results have been derived and discussed based on the HNC-style solvation potential in the idealized Gaussian thread limit[43]. The variational free energy theory of Melenkevitz et. al. has also been worked out within the analytic thread model framework[45]. Interesting connections and differences between the thread PRISM theory, the field theoretic approaches of Edwards, Muthukumar and others[3], and blob scaling arguments[2] have been established. The work of Melenkevitz et. al.[45] is novel in the sense that it combines the liquid state PRISM approach to effective interactions(direct correlations, solvation potentials) with field theoretic schemes for solving the effective single chain problem in a manner which is qualitatively correct for all density. The construction of "hybrid" liquid state/field theoretic approaches, applicable for large N macromolecular systems, is an attractive direction for future development.

E. Other Applications

There are many other physical problems and macromolecular systems for which the self-consistent PRISM approach should be useful. The following represents an incomplete list of problems for which preliminary work has been done or which appear to be attackable based on the present state-of-the-art.

(1) Theta and poor solvents. A key question here is how to generalize the intermolecular closure approximation and the intramolecular solvation potential to simultaneously treat the competing repulsive and attractive bare forces. The problem of low temperature polymer collapse in dilute solution is a classic problem in this area.

(2) Polymer Alloys. Perturbation of melt-like conformation upon transfer to a multicomponent environment is not understood. The influence of proximity to phase boundaries, coupled density and concentration fluctuations, and mixture composition on both single chain dimensions and miscibility are problems which have begun to be addressed within the PRISM formalism for the simple "symmetric" blend model by Singh and Schweizer[163] and symmetric diblock copolymer model by David and Schweizer[140], and other more coarse-grained field theoretic approaches[126]. Comparisons with the few available simulations[126,130,146-148] have also been performed. However, the experimentally relevant conformationally and interaction asymmetric alloy cases[140] remains to be carefully considered.

(3) Atomistic Models. Self-consistent conformational calculations at the atomistic level have not been studied although a tractable scheme for RIS models has been proposed[43]. One might expect much less perturbation of single chain structure at an atomistic level where there are constant bond lengths, bond angles etcetera. However, rotational isomers generally differ in energy only by of order k_BT, so *a priori* it is not clear what happens for specific polymer systems.

(4) Constrained Polymers. The conformation of polymers constrained in various ways, e.g. grafted to a flat surface("brush"), adsorbed on a spherical colloidal particle, or tethered to a central branch point as in "star" polymers[127]. All such problems involve potentially large "nonideal" conformational effects, and also introduce additional complications

associated with site inequivalence within the PRISM formalism. Progress for star polymers is briefly described in the next section.

VII. STAR-BRANCHED POLYMER FLUIDS

Star polymers represent an interesting and important class of macromolecules of nonlinear global architecture. They consist of "f" linear chains or arms (with N_a monomers per arm) connected at a central branch structure, as schematically shown in Figure 7.1. This architecture is characterized by a spatially inhomogeneous single molecule density which decreases as one moves away from the star center. Thus, relative to linear chains, a new and stronger form of *site nonequivalency* is present which results in spatially nonuniform screening of the intramolecular excluded volume interactions. In particular, the reduced exposure of the central "core" regions of the star to other polymers suggest less screening and hence more "swollen" conformations near the star center. However, very far from the branch point the star is still a low density fractal object, and hence is expected to display conformational behavior similiar to the linear chain case.

The above physical features imply a fully self-consistent treatment of intramolecular and intermolecular pair correlations is more important for star polymers than linear chains, and the concept of "ideality" is expected to be of much less utility even at high melt densities. The treatment of star polymers within a self-consistent PRISM formalism has been very recently pursued by Grayce and Schweizer[128,129]. Here we give a brief description of some of the essential theoretical modifications required to treat stars, and a few conformational and structural results which emphasize the distinctive new phenomena characteristic of the star architecture. We note that the star polymer fluid is a model for other physical systems such as spherical micellar fluids and sterically-stabilized colloids[127].

A. Basic Model and Theory

The basic theory of star polymer fluids developed by Grayce and Schweizer is general in its ability to treat polymer models of variable chemical detail[128]. For simplicity, we discuss the theory in the context of

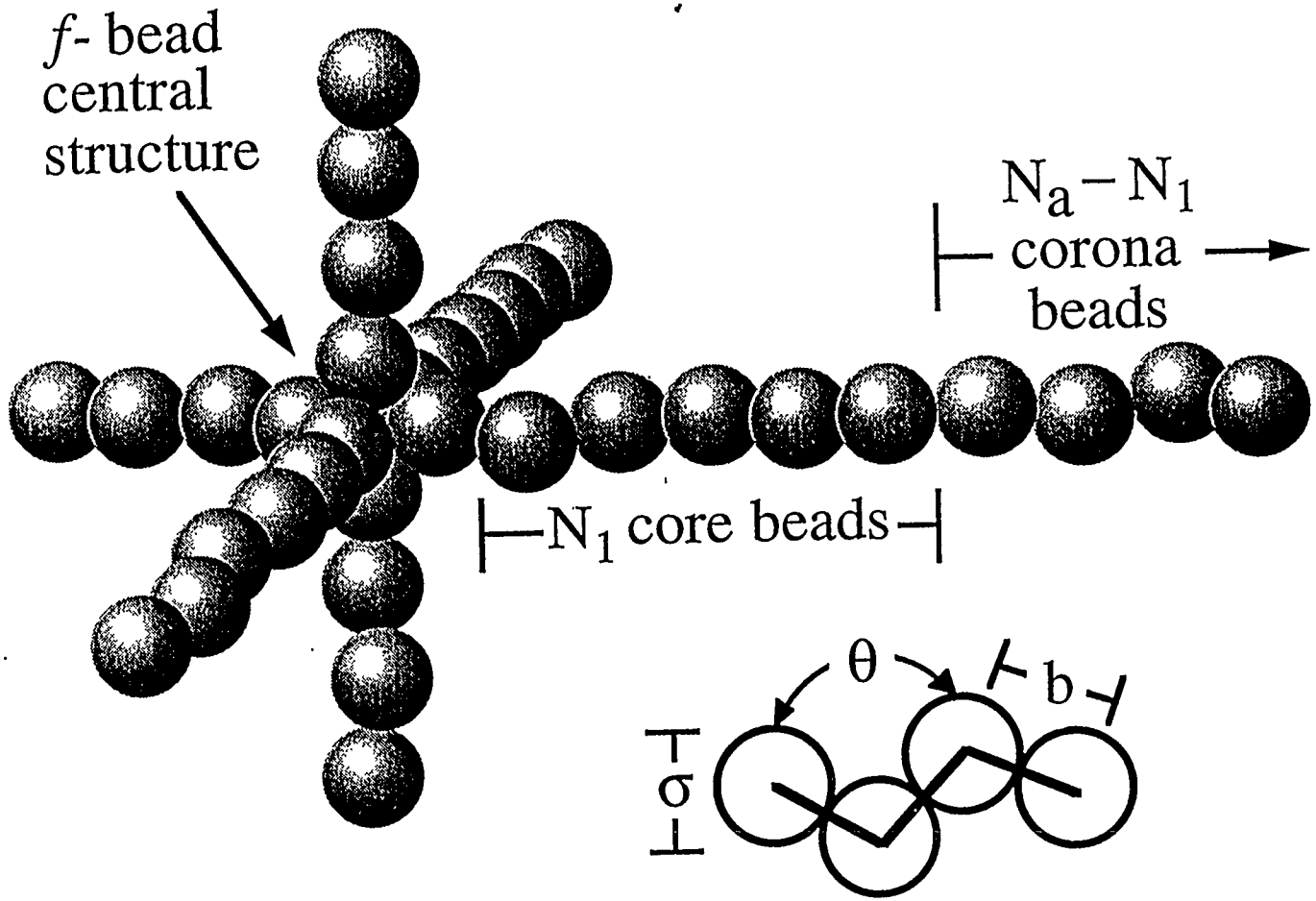

7.1 The star-branched tangent SFC model of an "f x N_a" star, where N_a is the number of sites per arm and the arm number f=6 in the example shown. The total number of sites comprising the star is f(N_a+1). The number of "core" sites is denoted N_1 and is determined variationally as described in the text.

the tangent, semiflexible chain model. As true for most of the results discussed in Section VIII, the bare bending energy is set equal to zero and pure hard core interactions(athermal or good solvent conditions) are employed in numerical studies carried out so far.

A sketch of the model star polymer is shown in Figure 7.1. Site equivalence is clearly broken by the presence of the central branch point, and in principle one expects the local stiffness of the arms varies continuously as one proceeds from the star core to its outer "corona" region. The development of a technically tractable theory requires some simplification, or "preaveraging", of this complete site *in*equivalence. As indicated in Figure 7.1, a "3-region" scheme has been adopted motivated by both conceptual simplicity, and by analogy with coarse-grained polymer physics type approaches[130,131]. The model star has a rigid branch point structure consisting of f sites(site type 0), a "core" region of fN_1 sites(site type 1), and an outer arm or "corona" region(site type 2, N_a-N_1 sites per arm).

For the "3-site" model there are 6 independent intramolecular partial structure factors, radial distibution functions, and solvation pair potentials which must be determined self-consistently. PRISM theory has been implemented at the level of the variational generating functional theory of Grayce et.al.[47] as described in section VIII.B.2 using the PY-style solvation potential. However, two new features arise for star polymers. (i) Two distinct effective bending energies , ε_1 and ε_2 , associated with the core and corona regions, respectively, are required. (ii) The number of sites which comprise the core region is not *a priori* known, but is treated as a variational parameter in the free energy minimization process. Thus, there are 3 variational parameters to be determined self-consistently[128].

B. Conformation and Liquid Structure

Detailed numerical predictions have been obtained for average conformational properties such as the mean square end-to-end distance of the core region, the overall star radius-of-gyration, the number of sites in the core, the effective persistence lengths of the core and corona regions, and the single star structure factor $\hat{\omega}(k)$. The influence of variables such as number of arms(f=4-12), arm degree of polymerization, and fluid packing fraction on these properties has been established[128]. In a rough qualitative

sense, the chain segments which comprise the corona region behave similiarly to the analogous linear chain case. However, the core region is always found to be strongly swollen relative to the "ideal" state even at melt densities, and results in a transfer of monomer density outwards from the central region of the star to the coronal region. As a consequence, there is an increase of overall star dimensions, and distinctive changes in the star collective structure factor and intramolecular radial distribution function occur, relative to *either* the analogous linear chain case *or* the ideal Gaussian star model behavior[128].

The predicted overall star dimensions as a function of (concentrated) fluid packing fraction and arm number is shown in Figure 7.2 for a macromolecule of modest size(N_a=100). A simple power law form, $R_g^2 \propto f^{0.38}\,\eta^{-0.3}$, fits the numerical results very well. Curiously, the predicted density scaling exponent is rather close to the scaling theory[2] exponent of 0.25 *for long chains in semidilute solution*, although the significance of this near agreement is unclear. Note that no density-independent chain dimensions are attained, in conflict with common assumptions of ideal behavior at high melt-like densities.

Both the core swelling, and the fraction of arm sites in the core, grow as the fluid density decreases, the number of arms increases, and/or the arm molecular weight increases[128]. The latter trend is rather surprising since the core size appears to (weakly)increase without bound as arm degree of polymerization increases according to the power law $\langle R_1^2 \rangle \propto N_a^{1/3}$. Convincing physical interpretation of this intriguing behavior is lacking.

The fundamental origin of all the conformational trends discussed above is the strong reduction of the solvation potential, and hence screening effect, in the core region relative to the corona region. An example of the predicted self-consistent solvation pair potentials $W_{ij}(r)$ is given in Figure 7.3.

The predicted nonideal conformational effects can be probed by SANS experiments, and theoretical/experimental comparisons are given elsewhere[128]. A detailed physical picture of the origin of the nonideal conformational behavior in terms of the thermodynamic forces a star experiences has been constructed. Comparison of the self-consistent PRISM theory results with phenomenological scaling and other coarse-

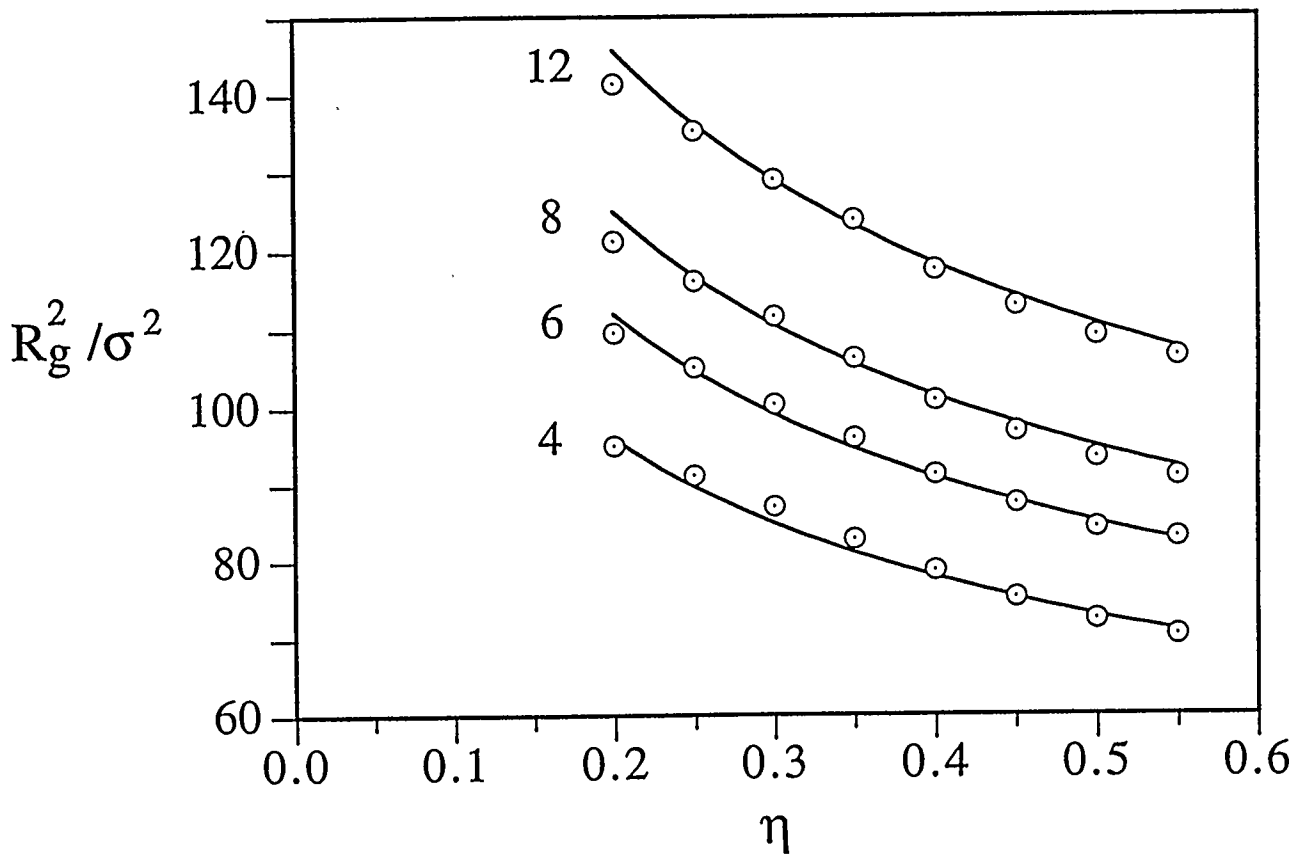

7.2 Mean squared radius-of-gyration of f x 100 stars as a function of monomer packing fraction and the indicated number of arms. The curves are an empirical power law fit given by $35\ f^{0.38}\ \eta^{-0.30}$.

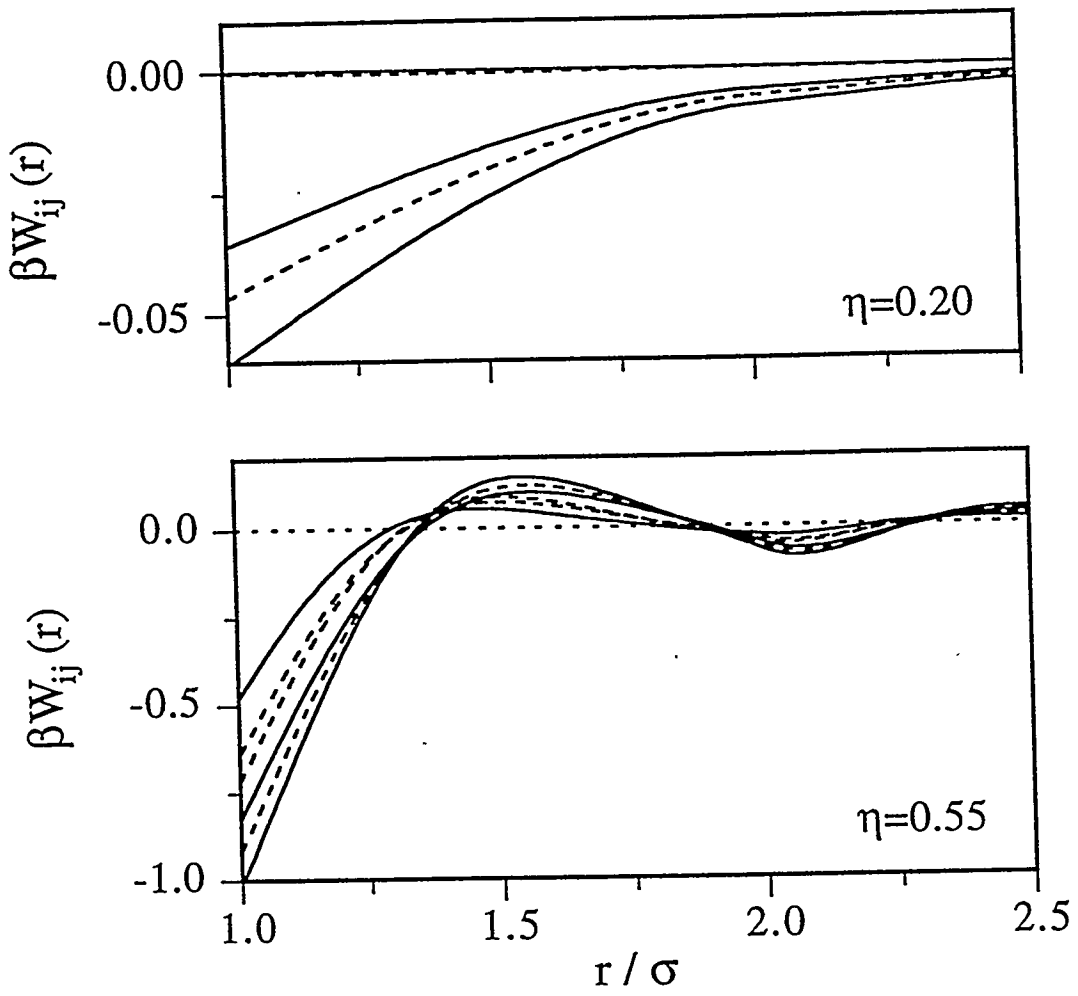

7.3 The six pair components W_{ij} ({i,j} = 0,1,2) of the self-consistently determined solvation potential W acting on a 8 x 100 star for two values of fluid packing fraction. The three "diagonal" ("off-diagonal")components W_{ii} ($W_{ij}, j \neq i$) are drawn with solid(dashed) lines. The strengths of the components at contact ($r=\sigma$) are, from weakest(least negative) to strongest(most negative), {0,0}, {0,1}, {0,2}, {1,1}, {1,2} and {2,2}, respectively. Only the three strongest (W_{11},W_{12},W_{22}) can be discerned on the lower density plot.

grained polymer physics approaches has also been presented, and distinctive qualitative and quantiative differences have been identified[128].

The self-consistently determined intermolecular pair correlations, $g_{ij}(r)$, and collective partial structure factors, $\hat{S}_{ij}(k)$, also display several unique physical features due to the star-branched architecture[129]. An example for the pair correlations is shown in Figure 7.4 for a melt-like density. The corona region is quite similiar to the analogous linear tangent SFC[55] case : a local solvation shell regime followed by a power law correlation hole region out to intersite separations of order R_g. However, the central branch structure and core region pair correlations show reduced local ordering(as expected), plus two new structural features : (i) a broad intermediate region where h(r) grows in a nearly linear fashion with increasing site-site separation, and (ii) a weak oscillation in the vicinity of the global chain dimension separation. The latter feature is hard to see on the scale of Figure 7.4, but is clearly visible on an expanded scale. Close examination reveals the characteristic oscillation wavelength scales as $N_a^{1/3}$, a distance corresponding to the mean separation of cores on different stars within the correlation volume containing of order $N_a^{1/2}$ interpenetrating star molecules.

The macromolecular scale solvation shell feature is clearly seen in the partial and total structure factors in Fourier space. An example is given in Figure 7.5. The very small and high k regions are weakly dependent on arm number, and are nearly identical to the analogous linear chain case. However, the low angle broad maximum at $k^* \propto N_a^{-1/3}$ is a unique star feature which becomes more intense, and shifts to slightly smaller wavevector, with increasing arm number. This feature implies there is a type of macroscale colloidal ordering in star polymer melts, which is also predicted to occur under semidilute and concentrated solution conditions[129].

The signature of macroscale colloidal ordering in semidilute star polymer solutions has been found experimentally using SANS[132], and these measurements are in good agreement with the PRISM predictions. Moreover, phenomenological scaling type arguments have been advanced by Witten and Pincus[131] which also predict such a low angle scattering maximum at $k^* \propto R_g^{-1} \propto N_a^{-3/5}$ *but only under semidilute($\rho \cong \rho^*$), long arm, good solvent* conditions. In the latter situation, the stars do not

7.4 Diagonal components of the self-consistently determined intermolecular site-site pair correlation functions, $h_{ij}(r) = g_{ij}(r)-1$ for a dense melt (η=0.55) of 8 x 400 star polymers. The overall star radius-of-gyration is indicated.

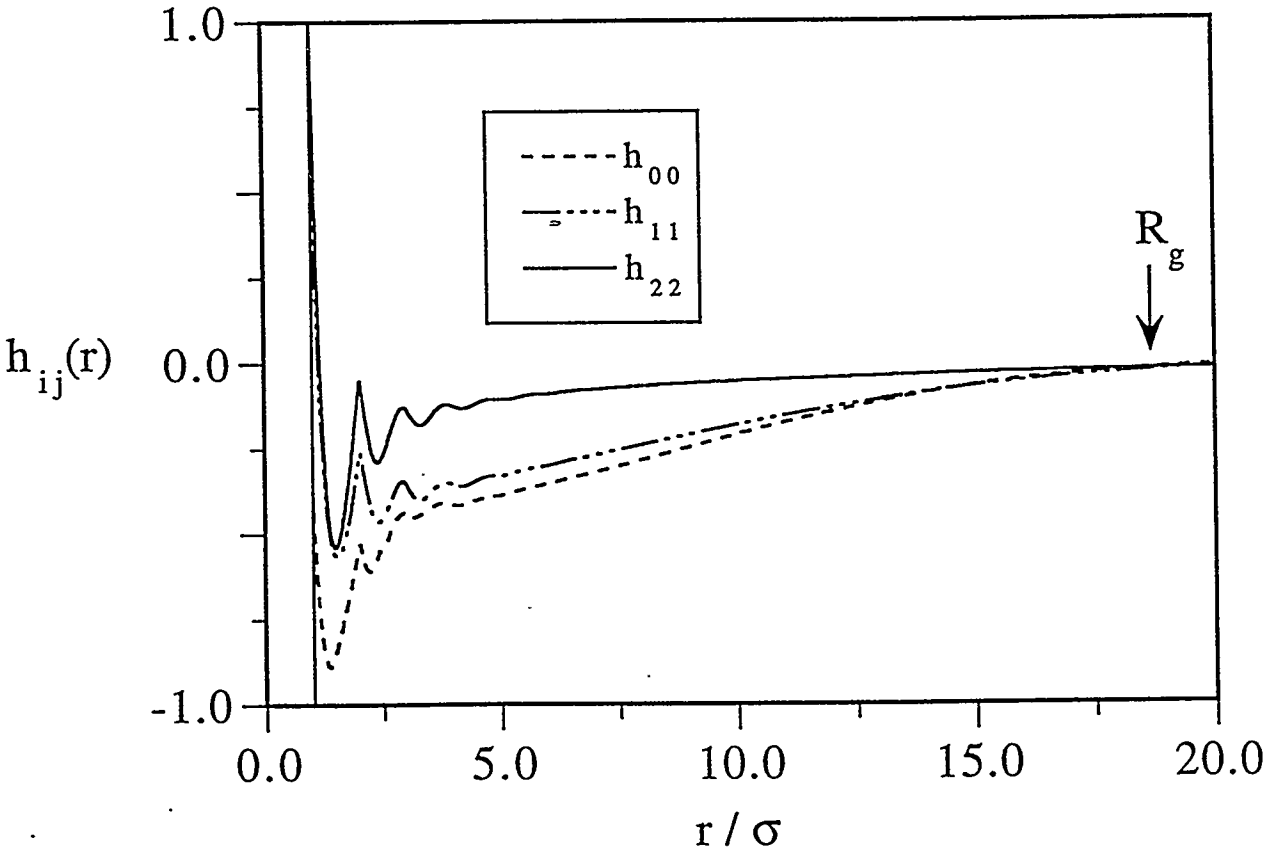

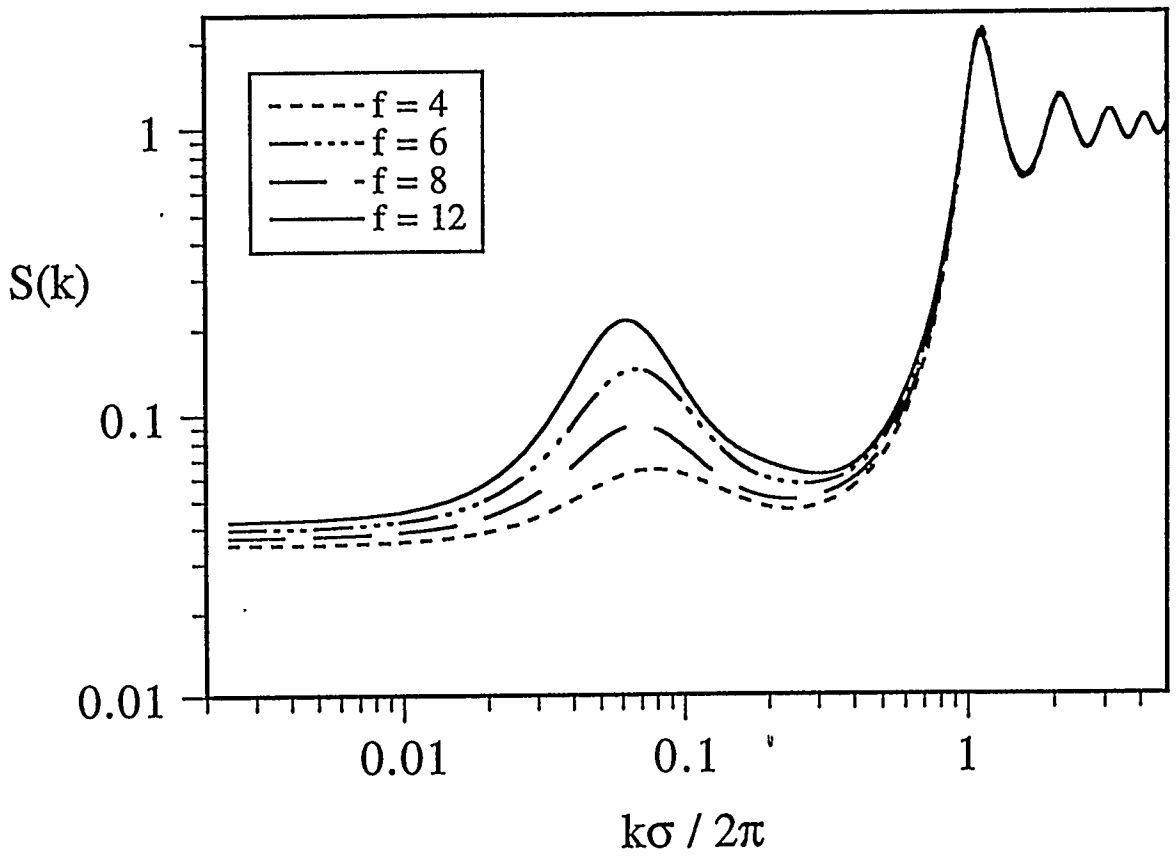

7.5 Total collective structure factor of a dense melt of f x 100 stars. Note the logarithmic scales.

interpenetrate appreciably and hence behave roughly as fuzzy spheres. However, PRISM theory predicts the colloidal ordering feature is a generic consequence of the star architecture and persists in dense solutions up to the melt state. Appropriate experiments to test the melt PRISM predictions have apparently not yet been carried out.

VIII. DISCUSSION AND FUTURE DIRECTIONS

This report has focused on describing progress made over the past 3 years on developing microscopic liquid state theories of the conformation, structure, thermodynamics, and phase transitions of macromolecular fluids within the context of interaction site models and the RISM integral equation method. Although much progress has been made, there remain many physical problems and systems which have either not been addressed at all, or are just beginning to be seriously attacked, from a liquid state integral equation perspective. An incomplete list is as follows. (1) Charged polymers, polyelectrolytes, and ionomers(strong dipolar interactions). The appropriate closure approximations and treatment of self-consistency in the presence of both hard core forces and long range Coulombic interactions are major unsolved problems. (2) Short range orientational correlations in isotropic fluids, and nematic and other liquid crystalline phases, of rigid and semiflexible polymers. (3) Incorporation of quenched disorder(beyond naive pre-averaging) associated with intramolecular features such as tacticity variations, molecular weight polydispersity, and sequence disorder in copolymers. (4) Polymer gels, rubbers, and associating fluids where strong intermolecular "attractive" interactions can result in network-like and/or fractal structures which can be either quenched in or thermoreversible. (5) Self-assembly of intermediate-sized molecules(e.g. surfactants) into supramolecular structures(e.g., micelles, microemulsions). (6) Ternary and more complex mixtures of homopolymers and copolymers where there is a competition between macrophase and microphase separation. A related phenomenon is the role of low concentration additives on phase stability.

All the above problems represent challenges to the further development of a general microscopic liquid state theory of macromolecular

systems, but we are hopeful that significant progress can be made in the near future.

REFERENCES

1. P.J.Flory, *Principles of Polymer Chemistry*,Cornell University Press, 1953.
2. P.-G. deGennes, *Scaling Concepts in Polymer Physics*, Cornell University Press, Ithaca, 1979.
3. M. Doi and S.F. Edwards, *Theory of Polymer Dynamics*, Oxford Press, Oxford,1986.
4. K.F.Freed, *Renormalization Group Theory of Macromolecules*, J.Wiley & Sons, New York, 1987.
5. J. P. Hansen and I. R. McDonald, *Theory of Simple Liquids*, 2nd Ed., Academic Press: London, 1986.
6. K. S. Schweizer and J. G. Curro *Phys. Rev. Lett.* **58**, 246 (1987).
   J. G. Curro, and K. S. Schweizer, *Macromolecules* , 20, 1928 (1987).
   J. G. Curro, and K. S. Schweizer, *J. Chem. Phys.* , **87**, 1842 (1987).
7. D. Chandler and H. C. Andersen, *J. Chem. Phys.*, **57**, 1930 (1972).
8. D. Chandler, in *Studies in Statistical Mechanics VIII*, edited by E. W. Montroll and J. L Lebowitz ,North-Holland, Amsterdam, 1982, p274 ; L. J. Lowden, and D. Chandler, *J. Chem. Phys.*, **61**, 5228 (1974) ; **59**, 6587 (1973); **62**, 4246 (1975).
9. K.S.Schweizer and J.G.Curro, *Adv. Chem. Phys.* (1995) submitted.
10. K. S. Schweizer and J. G. Curro *Adv. Polym. Sci.*, **116**, 321 (1994).
11. H.C. Andersen, D.Chandler and J.D.Weeks, Adv. Chem. Phys. **34**, 105 (1976) ; D.Chandler,J.D.Weeks and H.C.Andersen, *Science***220**,787(1983) ; J. A. Barker and D. Henderson, *Rev. Mod. Phys.*, **48**, 587 (1976).
12. D.Chandler and L.R.Pratt, *J.Chem.Phys.* **65**, 2925(1976) ; L.R.Pratt and D.Chandler, *ibid,* **66**,147(1977) ; L.R.Pratt, C.S.Hsu and D.Chandler,*ibid*, **68**, 4202 and 4213(1978).
13. P. J. Flory, *Statistical Mechanics of Chain Molecules*, Wiley: NY, 1969.
14. J. G. Kirkwood, *J. Chem. Phys.*, **3**, 300 (1935) ; J. Yvon, *Actualities Scientifiques et Industrielles*, Hermann and Cie, Paris (1935). M.Born and M. Green, *Proc. Roy. Soc.*, **A188**, 10 (1946).

15. J.K. Percus, in *Classical Fluids*, edited by H. L. Frisch and J. L. Lebowitz, Wiley, New York, 1964.
16. J. Percus and G. Yevick, *Phys. Rev.*, **110**, 1 (1958); J. von Leeuwen, J. Groeneveld, and J. deBoer, *Physica*, **25**, 792 (1959); G. Stell, *Physica*, **29**, 517 (1963).
17. See, for example, F.J.Rogers and D.A.Young, *Phys. Rev. A* **30**,999(1984); P.Ballone, G.Pastore, G.Galli and D.Gazillo, *Mol.Phys.* **59**,275(1986);B.Bernu,J.P.Hansen,Y.Hiwatari and G.Pastore, *Phys.Rev.A* **36**,4891(1987)
18. Q.Zhang and J.P.Badiali, *Phys.Rev.A* **45**,8666(1992) ; A.Parola and L.Reatto, *ibid*, **44**, 6600(1991).
19. See, for example, B.D'Aguanno, U.Genz and R.Klein, *J.Phys. Condens. Matter* **2**, SA379 (1990) and references cited therein.
20. P.A.Monson and G.P.Morris, *Adv.Chem.Phys.* **77**, 451(1990) ; P.Rossky, *Ann.Rev.Phys.Chem.* **36**, 321(1985).
21. D. Chandler, C. S. Hsu and W. B. Streett, *J. Chem. Phys.*, **66**, 5231 (1977); S. I. Sandler and A. H. Narten, *Mol. Phys.*, **32**, 1543 (1976). A. H. Narten, *J. Chem. Phys.*, **67**, 2102 (1977) ; C. S. Hsu and D. Chandler, *Mol. Phys.*, **36**, 215 (1978); *Mol. Phys.* **37**, 299 (1979).
22. L.R.Pratt and D.Chandler, *J.Chem.Phys.* **67**, 3683(1977) ; *in Methods in Enzymology* **127**, 48(1986).
23. D.Chandler,Y.Singh and D.M.Richardson, *J.Chem.Phys.* **81**,1975 (1984); A.L.Nichols, D. Chandler, Y.Singh and D.M.Richardson, *ibid* **81**, 5109(1984) ; D.Laria, D.Wu and D.Chandler, *ibid*, **95**, 4444(1991).
24. D.Chandler, p.193 in *Les Houches Lectures on "Liquids, Freezing and Glass Transition"*, eds. J.P.Hansen, D.Levesque and J.Zinn-Justin, North Holland, Amsterdam, 1991.
25. K. S. Schweizer and J. G. Curro, *Macromolecules* , **21**, 3070,3082 (1988).
26. J. G. Curro, ,*Macromolecules*, **27**, 4665 (1994) ; J. J. Rajasekaran and J. G. Curro, *J.Chem.Soc. Faraday Trans.*, **91**,2427 (1995).
27. K. S. Schweizer and J. G. Curro, *Phys. Rev. Lett.*, **60**, 809 (1988).
28. J. G. Curro and K. S. Schweizer, *J. Chem. Phys.*, **88**, 7242 (1988) . K. S. Schweizer and J. G. Curro, *J. Chem Phys.* **91**, 5059 (1989).
29. J. G. Curro, and K. S. Schweizer, *Macromolecules.*, **23**, 1402 (1990).
30. K. S. Schweizer and J. G. Curro, *Chemical Physics*, **149**, 105 (1990).

31. J. G. Curro and K. S. Schweizer, *Macromolecules.*, **24**, 6736 (1991).
32. J.J.Rajasekaran, J. G. Curro and J. D. Honeycutt, *Macromolecules*, **28**,6843(1995).
33. E. F. David and K. S. Schweizer, *J. Chem. Phys.* **100**, 7767 , 7784 (1994).
34. D. Chandler, *Chem.Phys.Lett.* **139**, 108(1987).
35. L.Lue and D.Blanckschtein, *J.Phys.Chem.* **96**, 8582(1991) ; J.R.Elliot and U.S.Kanetar, *Mol.Phys.* **71**,871 and 883(1990).
36. K.Kojima and K.Arakawa, *Bull.Chem.Soc.Japn.* **51**,1977(1978) ; **53**,1795(1980).
37. G.A.Martynov and G.N.Sarkisov, *Mol.Phys.* **49**, 1495(1983).
38. A.Yethiraj, *Mol.Phys.* **80**, 695(1993).
39. D. Chandler, R.Silbey and B.M.Ladanyi, *Mol.Phys.***46**, 1335(1982)
40. D.M.Richardson and D.Chandler, *J.Chem.Phys.* **80**, 4484(1984).
41. J.P.Donley, J.G.Curro and J.D.McCoy, *J.Chem.Phys.* **101**,3205(1994)
42. C.J.Grayce and J.J.dePablo, *J.Chem.Phys.* **101**, 6013(1994).
43. K.S.Schweizer, K.G.Honnell and J.G.Curro,*J.Chem.Phys.* **96**, 3211 (1992).
44. J.Melenkevitz, K.S. Schweizer and J.G. Curro, *Macromolecules* **26** 6190 (1993).
45. J.Melenkevitz, J.G. Curro and K.S. Schweizer, *J.Chem.Phys.***99**, 5571 (1993).
46. C.J.Grayce and K.S.Schweizer, *J.Chem.Phys.* **100** ,6846 (1994).
47. C.J.Grayce, A. Yethiraj and K.S. Schweizer, *J.Chem.Phys.***100**,6857(1994).
48. P. J. Flory, *J. Chem. Phys.*, **17**, 203 (1949).
49. D. G. Ballard, J. Schelton and G.D.Wignall, *Eur. Polymer Journal*, **9**, 965 (1973). J. P. Cotton, D. Decker, H. Benoit, B. Farnoux, J. Higgins, G. Jannick, R. Ober, J. des Cloizeaux, *Macromolecules,* **7**, 863 (1974).
50. J. G. Curro, *J. Chem. Phys.*, **64**, 2496 (1976); *Macromolecules,* **12**, 463 (1979) ; M. Vacatello, G. Avitabile, P. Corradini, A. Tuzi, *J. Chem. Phys.* **73**, 543 (1980).
51. J. G. Curro, K. S. Schweizer, G. S. Grest, K. Kremer,*J. Chem. Phys.*, **91**, 1357 (1989) ; K.Kremer and G.S.Grest, *ibid* **92**, 5057(1990).
52. K. S. Schweizer, E. F. David, C. Singh, J. G. Curro and J. J. Rajasekaran, *Macromolecules* **28,**1528 (1995).
53. L.J.Fetters,D.J.Lohse,D.Richter, T.A.Witten and A.Zirkel, *Macromolecules* **27**, 4639(1994).
54. K.S.Schweizer and G.Szamel, *J.Chem.Phys.* **103**, 1934(1995).

55. K.G.Honnell, J.G.Curro and K.S.Schweizer,*Macromolecules*, **23**, 3496 (1990).
56. R.Koyama, *J. Phys. Soc. Japan*, **22**, 1029 (1973).
57. See, for example, *Atomistic Modeling of Physical Properties*, Adv. Polym. Sci. , L.Monnerie and U.W.Suter eds. Springer-Verlag, 1994.
58. D. Theodorou and U.W.Suter, *Macromolecules* **18**,1467 (1985).
59. R.Khare, M.E.Paulaitis and S.R. Lustig, *Macromolecules* **26**,7203(1993).
60. A.Yethiraj, C.K.Hall and K.G.Honnell, *J.Chem.Phys.* **93**, 4453(1990); A.Yethiraj and C.K.Hall, *ibid*, **96**, 797(1992).
61. A.Yethriaj and K.S. Schweizer, *J. Chem. Phys.*, **97**, 1455 (1992).
62. A.Yethiraj, *J.Chem.Phys.* **101**, 9104(1994).
63. J. D. McCoy, K. G. Honnell, J. G. Curro, K. S. Schweizer, and J.D.Honeycutt, *Macromolecules,* **25**, 4905 (1992).
64. K. G. Honnell, J. D. McCoy, J. G. Curro, K. S. Schweizer, A. H. Narten, and A. Habenschuss, *J. Chem. Phys.*, **94**, 4905 (1991).
65. K.G.Honnell, J.D.McCoy,J.G.Curro,K.S.Schweizer,A.H.Narten and A. Habenshuss, *Bull.Am.Phys.Soc.* **36(3)**,481(1991).
66. A. H. Narten, A. Habenschuss, K. G. Honnell, J. D. McCoy, J. G. Curro, and K. S. Schweizer, *J. Chem. Soc. Faraday Trans.* **88**, 1791 (1992).
67. A. Yethiraj, J. G. Curro, K. S. Schweizer, and J. D. McCoy, *J. Chem. Phys.*, **98** 1635 (1993) ; J. G. Curro, A. Yethiraj, K. S. Schweizer, J. D. McCoy, and K. G. Honnell, *Macromolecules*, **26** 2655 (1993).
68. J.D.McCoy, K.G.Honnell, K.S.Schweizer and J.G.Curro, *Chem.Phys.Lett.* **179**, 374(1991); *J.Chem.Phys.* **95**, 9348(1991).
69. K.S.Schweizer and C.Singh, *Macromolecules* 28, 2063(1995).
70. A. Yethiraj, J. G. Curro, and J. J. Rajasekaran, *J. Chem. Phys*, **103**,2229(1995).
71. See for example, G. R. Mitchell, and A. H. Windle, *Polymer*, **25**, 906 (1984).
72. A. H. Habenschuss and D. Londono, private communication.
73. U. W. Suter and P. J. Flory, *Macromolecules* **8**, 765 (1975).
74. D. G. H. Ballard, P. Cheshire, G. W. Longman and J. Schelton, *Polymer,* **19,** 379 (1978).
75. J. G. Curro, J. J. Rajasekaran, A. H. Habenschuss, D. Londono, J. D. Honeycutt, *Macromolecules*, in preparation.

76. J. K. Percus, *J. Stat. Phys.*, **15**, 423 (1976).
77. R. Dickman and C. K. Hall, *J. Chem. Phys.*, **89**, 3168 (1988).
78. A. Yethiraj and C. K. Hall, *J. Chem. Phys.*, **95**, 3749 (1991).
79. R. Dickman and C. K. Hall, *J. Chem. Phys.*, **85**, 4108 (1986).
K. G. Honnell and C. K. Hall, *J. Chem. Phys.*, **90**, 1841 (1989).
80. S. Sen, J. M. Cohen, J. D. McCoy and J. G. Curro, *J. Chem. Phys.*, **101**, 9010 (1994); S. Sen, J. D. McCoy, S. K. Nath, J. P. Donley and J. G. Curro, *J. Chem. Phys.*, **102**, 3431 (1995).
81. (a) A.Yethiraj, *J.Chem.Phys.*, in press, 1995.
(b) L.R.Dodd and D.Theodorou, *Adv.Polym.Sci.* **116**, 249(1994).
82. J. A. Barker and D. Henderson,*Ann. Rev. Phys. Chem.* **23**, 439 (1972).
83. O. Olabisi and R. Simha, *Macromolecules*, **8**, 206 (1975).
84. A.Yethiraj and C.K.Hall, *J.Chem.Phys.* **95**,1999(1991).
85. J.S.Rowlinson and F.L.Swinton, *Liquids and Liquid Mixtures* , Butterworth Scientific, London, 1982; J. Hildebrand and R.Scott, *The Solubility of Nonelectrolytes*, 3rd Edition, Reinhold, New York, 1949.
86. E. A. Grulke, in *Polymer Handbook*, 3rd Edition, J. Brandrup, E. H. Immergut, Eds. ; John Wiley & Sons, NY (1989) ; P. A. Small, *J. App. Chem*, **3**, 71 (1953) ; D. W. Van Krevelen, *Fuel*, **44**, 229 (1965) ; K. L. Hoy, *J. Paint Tech.*, 42, 76 (1970).
87. P. A. Rodgers, *J. App. Polym. Sci.*, **48**, 1061 (1993).
88. M. M. Coleman, C. J. Serman, D. E. Bhagwager and P. Painter, *Polymer*, **31**, 1187 (1990).
89. D. J. Walsh, W. W. Graessley, S. Datta, D. J. Lohse and L. J. Fetters, *Macromolecules*, **25**, 5236 (1992).
90. W. L. Jorgensen, J. D. Madura and C. J. Swenson, *J. Am. Chem. Soc.*, **106**, 6638 (1984).
91. W.W.Graessley, R. Krishnamoorti, N.P.Balsara, L.J. Fetters, D.J. Lohse, D.Schulz and J. Sissano, *Macromolecules* **27**, 2574, 3073, 3896 (1994) and references cited therein ; R. Krishnamoorti, W.W. Graessley,L.J.Fetters,R.J.Garner and D.J. Lohse, *Macromolecules* **28**, 1252, 1260(1995)
92. D.J.Lohse, private communication, 1995.

93. *Polymer Compatibility and Incompatibility,* ed. K.Solc, MMI, Midland, Michigan, 1981 ; O.Olabisi, L.M.Robeson and M. Shaw ,*Polymer-Polymer Miscibilit"*: Academic Press : New York, 1979 ; R.Koningsveld, *Adv. Colloid and Interface Science* **1968**, 2, 151 ; P.J.Flory, *Proc. Roy. Soc. A*, **234**, 60 (1956).
94. I.C.Sanchez, *Ann.Rev.Mater.Sci.* **13**, 387(1983).
95. F.S.Bates,*Science* **251**, 898 (1991);
96. C. S. Stevenson, J. G. Curro, J. D. McCoy and S. J. Plimpton, *J. Chem. Phys.*, **103**, 1208 (1995); C. S. Stevenson, J. D. McCoy, S. J. Plimpton and J. G. Curro, *J. Chem. Phys*, **103**, 1200 (1995).
97. J.D. Weinhold,S.K.Kumar, C.Singh and K.S.Schweizer, *J.Chem.Phys.* , in press, December, 1995.
98. F.S.Bates, M.F. Schulz and J.Rosedale, *Macromolecules* **25**, 5547(1992); M.D.Gehlsen and F.S.Bates,*ibid*, **27**,3611(1994).
99. F.S. Bates and G.H. Fredrickson, *Macromolecules* **27**, 1065 (1994). G.H.Fredrickson,A.J.Liu, and F.S.Bates, *ibid,* **27**, 2503(1994). G.H.Fredrickson and A.J. Liu, *J.Poly.Sci.Poly.Phys*.**33**,1203(1995).
100. C.Singh and K.S. Schweizer, *J.Chem.Phys.* **103**, 5814(1995).
101. I.C.Sanchez and R.H. Lacombe, *J.Phys.Chem.* **80**,2352 & 2368(1976). D.J. Walsh and S.Rostami, *Adv.Polym.Sci.* **70**, 119(1985).
102. J. G. Kirkwood and F. P. Buff, *J. Chem. Phys.*, **19**, 774 (1951).
103. M. Dijkstra, D.Frenkel and J.P.Hansen, *J.Chem.Phys.* **101**, 3179(1994), and references cited therein.
104. E.J.Meijer and D.Frenkel, *J.Chem.Phys.* **100**, 6833(1994).
105. P.Bolhius and D.Frenkel, *J.Chem.Phys.* **101**,9869(1994).
106. D.Frenkel and A.A.Louis, *Phys.Rev.Lett.* **68**, 3363(1992).
107. J.Lebowitz and J.Rowlinson, *J.Chem.Phys.* **41**,133(1964).
108. T.Biben and J.P.Hansen, *Phys.Rev,Lett.* **66**, 2215(1991).
109. L.Onsager, *Proc. New York Acad.Sci.* **51**,627(1949).
110. A.Yethiraj, S. Kumar, A. Hariharan and K.S.Schweizer,*J.Chem.Phys.* **100,** 4691(1994) ; *ibid*, in press, 1995.
111. F.S.Bates, L.J. Fetters and G.D. Wignall, *Macromolecules* **21**,1086(1988),

and *Phys.Rev. Lett.* **55**,2425(1985) ; J.D.Londano, A.H. Narten, G.D.Wignall, K.G.Honnell, E.T. Hseih, T.W. Johnson, and F.S. Bates, *Macromolecules* **27**, 2864(1994).

112. For a recent review of polymer alloy theories see : K.Binder, *Adv.Polym,Sci.* **112**,181(1994).
113. C.Singh and K.S.Schweizer, *Macromolecules*, in press, 1995.
114. J.D.Honeycutt, *Makromol. Chem. Macromol. Symp.* **65**, 49(1993) ; *Macromolecules* **27**, 5377(1994) ; *ACS Polymer Preprints* **33**,529(1992).
115. S.F.Edwards, *Faraday Discussions* **98**,1 (1994).
116. B.M.Pettitt, M.Karplus and P.J.Rossky, *J.Phys.Chem.* **90**,6335(1986); T.Ichiye and D.Chandler, *ibid* **92**, 5257(1988) ; H.Yu, B.M.Pettitt and M.Karplus, *J.Am.Chem.Soc.* **113**, 2425(1991).
117. For a review see : G.E.Marlow, J.S.Perkyns and B.M.Pettitt, *Chem.Rev.*
93, 2503(1993).
118. Singh,Y., *J.Phys.A-Math Gen.*,**20**, 3949(1987).
119. M.Lal, *Mol.Phys.* **17**,57(1965).
120. J.Gao and J.Weiner,*J.Chem.Phys.* **91**, 3168(1989).
121. G.D.Wignall, in *Encyclopedia of Polymer Science and Engineering* , second edition, Wiley, New York, Vol.12, p.112 (1987).
122. M.Daoud, J.P.Cotton, B.Farnoux, G.Jannick, G.Sarma, H.Benoit, R.Duplessix, C.Picot and P.G.deGennes, *Macromolecules* **8**, 8041(1975)
J.S.King, W.Boyer, G.D.Wignall and R.Ullman, *ibid* **18**, 709(1985).
123. A.Yethiraj, *Mol.Phys.* , **82**, 957(1994).
124. C.J.Grayce and K.S.Schweizer, in preparation.
125. C.Singh and K.S.Schweizer, *J.Chem.Phys.*to be submitted.
126. J.Barrat and G.Fredrickson, *J.Chem.Phys.* **95**, 1281(1991).
T.A.Vilgis and R.Borsali, *Macromolecules* **23**,3171(1990).
H.Tang and K.F.Freed, *J.Chem.Phys.* **96**, 8621(1992).
Z.G.Wang, *Macromolecules* **28**, 570(1995).
127. S.T.Milner, *Science* **251**, 905(1991) ; D.H.Napper, *Polymeric Stabilization of Colloidal Dispersions*, Academic Press, NY, 1983; G.S.Grest and M.Murat in *Monte Carlo and Molecular Dynamics Simulations in Polymer Science*, ed. K.Binder, Clarendon Press Oxford, England, 1994.

128. C.J.Grayce and K.S.Schweizer, *Macromolecules*, October, 1995.
129. C.J.Grayce and K.S.Schweizer, *Macromolecules*, submitted,1995.
130. M.Daoud and J.P.Cotton, *J. de Physique* **43**, 531(1982).
A.T.Boothroyd and R.C.Ball, *Macromolecules* **23**,1729(1990).
131. T.A.Witten and P.Pincus, *Macromolecules* **19**, 2509 (1986).
132. L.Willner, O.Jucknische, D.Richter, L.J.Fetters, and J.S.Huang, *Europhys. Lett.* **19**,297(1992).
133. See for example, K.F.Freed and J.Dudowicz, *Theoretica, Chimica Acta*, **82**, (1992); J. Dudowicz and K.F.Freed, *Macromolecules*, **26**, 213 (1993) and **28**, 6625(1995), and references cited therein

Distribution List

MS-1380	David W. Larson, 4231	3 copies
MS-0339	J. L. Jellison, 1803	1 copy
MS-0342	Kim Mahin	1 copy
MS-1111	Steven J. Plimpton, 1421	1 copy
MS-1111	Grant S. Heffelfinger, 1421	1 copy
MS-1111	Sudip J. Dosanjh, 1421	1 copy
MS-1111	Frank B. Van Swol	1 copy
	Kenneth S. Schweizer Dept. of Materials Sci. & Eng. University of Illinois 1304 W. Green Urbana, Illinois 61801	1 copy
	J. Dana Honeycutt BIOSYM Technologies 9685 Scranton Rd. San Diego, California 92121-3752	1 copy
	Steven Mumby BIOSYM Technologies 9685 Scranton Rd. San Diego, California 92121-3752	1 copy
MS-0335	John G. Curro, 1870	5 copies
MS-9018	Central Tech. Files, 8523-2	1 copy
MS-0899	Technical Library, 4414	5 copies
MS-0619	Print Media, 12615	1 copy
MS-0100	Document Processing, 7613-2 For DOE/OSTI	2 copies